INFORMATION TO USERS

This manuscript has been reproduced from the microfilm master. UMI films the text directly from the original or copy submitted. Thus, some thesis and dissertation copies are in typewriter face, while others may be from any type of computer printer.

The quality of this reproduction is dependent upon the quality of the copy submitted. Broken or indistinct print, colored or poor quality illustrations and photographs, print bleedthrough, substandard margins, and improper alignment can adversely affect reproduction.

In the unlikely event that the author did not send UMI a complete manuscript and there are missing pages, these will be noted. Also, if unauthorized copyright material had to be removed, a note will indicate the deletion.

Oversize materials (e.g., maps, drawings, charts) are reproduced by sectioning the original, beginning at the upper left-hand corner and continuing from left to right in equal sections with small overlaps. Each original is also photographed in one exposure and is included in reduced form at the back of the book.

Photographs included in the original manuscript have been reproduced xerographically in this copy. Higher quality 6" x 9" black and white photographic prints are available for any photographs or illustrations appearing in this copy for an additional charge. Contact UMI directly to order.

UMI®

Bell & Howell Information and Learning
300 North Zeeb Road, Ann Arbor, MI 48106-1346 USA
800-521-0600

The Effects of Sodium Cations on Rabbit Muscle Enolase

— Evidence for the binding of 2PGA to apo-enolase with Na^+

Tong Lin

A Thesis

in

The Department

of

Chemistry and Biochemistry

Presented in Partial Fulfilment of the Requirements

for the Degree of Master of Science at

Concordia University

Montreal, Quebec, Canada

November, 1998

ABSTRACT

The Effects of Sodium Cations on Rabbit Muscle Enolase (ββ)
— Evidence for the Binding of 2PGA to Apo-enolase with Na^+

Tong Lin

Enolase, a dimeric enzyme, in the presence of Mg^{2+} catalyzes the reversible dehydration of 2-phospho-D-glycerate (2PGA) to form phosphoenolpyruvate (PEP) in the glycolytic pathway. Studies in the inactivation of rabbit muscle enolase by $NaClO_4$ show that both Mg^{2+} and 2PGA protect the enzyme from the inactivation. The protection provided by Mg^{2+} and 2PGA is attributed to a series of interactions between the ligands and the active site residues, and to the interactions throughout the side chains of the secondary elements in the two monomers. However, surprisingly, in the absence of Mg^{2+}, 2PGA still protects the apo-enolase from inactivation even at high concentrations of metal chelating reagents such as EDTA and EGTA. This is not supposed to occur because, according to the literature, the substrate binds to the enzyme only when a divalent metal ion is bound in the high affinity site I. Inductively coupled plasma mass spectroscopy was applied to the apo-enolase sample to identify the trace metal ions, but those trace metal ions are not responsible for the protection of the apo-enolase by 2PGA. Apo-enolase incubated in $NaClO_4$ is protected by 2PGA, while apo-enolase incubated in TMA-ClO_4 is not protected by 2PGA, indicating that the presence of Na^+ is necessary for the protection. The protection is enhanced with increasing concentrations of Na^+ and 2PGA. These results suggest that Na^+ permits the binding of 2PGA to the apo-enolase which protects the enzyme from the inactivation.

The binding of 2PGA to the apo-enolase in the presence of Na^+, as monitored by Trp fluorescence and near-UV CD, produces a small but substantial conformational change in the enzyme which is similar to the change upon binding of the substrate to the holo-enzyme. Steady-state kinetics studies indicate that Na^+ significantly increases K_m and K_i for Mg^{2+}, and competes with Mg^{2+} for the inhibitory site III. A combination of the present studies and previous studies on the effects of metal ions implies that the conformational site I and inhibitory site III initially exist in the active site, where Na^+ might bind and permit the binding of the substrate.

The inactivation of apo-enolase by $NaClO_4$ is associated with the dissociation of the dimeric enzyme as indicated by cross-linking plus SDS-PAGE and the fourth derivative spectra. 2PGA protects the apo-enzyme against the dissociation, as well as the inactivation. The binding of 2PGA to apo-enolase decreases K_d and increases ΔG_o of dissociation. $NaClO_4$ changes the quaternary and the tertiary structures of the enzyme, but has little effect on the secondary structure as shown in the far-UV CD spectra.

Moreover, the effects of several inhibitory substrate analogues, phosphoglycolate, phosphonoacetic acid, 3PGA and glycerol 2-phosphate, were characterized. The relationships between the conformational change upon the binding of these inhibitors or other divalent metal ions (Mn^{2+}, Co^{2+}, Zn^{2+} and Ca^{2+}) and the protection of holo-enolase from the inactivation by $NaClO_4$ have also been investigated. The conformational change as monitored by tryptophan fluorescence is not correlated to the protection of enolase from the inactivation.

ACKNOWLEDGMENTS

I would like to thank Dr. Mary Judith Kornblatt for her intensive supervision and financial support of this project. Her thoughtful direction is the source of strength that led to this discovery. I am very grateful to Dr. Joanne Turnbull for her invaluable advice which always put light on this study. I would also like to thank Dr. Peter Banks, Dr. Jack Kornblatt, Dr. Wendy Findlay, Dr. Justin Powlowski, Dr. Paul Joyce, Dr. R. T. Patterson, Dr. Salin, M. Ryback, Isabelle Rajotte, Vincent, Angela and Tania for all their helpful suggestions as well as their generous offers of the use of their instruments. Special thanks are given to Amanda Foster for her nice gift of editing this paper. Finally, I would like to express my gratitude to my dear mother, father, grandmother and sister for their love in all my efforts during the accomplishment of this project.

Contents

Contents

Contents

Abbreviations

EAB = Enolase assay buffer (imidazole, KCl, $Mg(OAc)_2$ and EDTA buffer)

EDTA = Ethylenediaminetetraacetic acid

EGTA = Ethyleneglycol-bis-(ß-amino-ethyl ether)N,N'-tetraacetic acid

ICP = Inductively coupled plasma trace metal analysis

PhAH = Phosphonoacetohydroxamate

O.D. = Optical density

PEG = Poly(ethyleneglycol)

PEP = Phosphoenopyruvate

PG = phosphoglycolate

2PGA = 2-Phospho-D-glycerate

3PGA = 3-Phosphoglycerate

SDS-PAGE = Sodium dodecyl sulphate polyacrylamide gel electrophoresis

MT = Mes and Tris buffer

MTME = Mes, Tris, $Mg(OAc)_2$ and EDTA buffer

TMA^+ = Tetramethylammonium ion

Trp = Tryptophan

TSP = Tartronate semialdehyde phosphate

List of Figures

List of Tables

CHAPTER 1 Introduction

1.1 Introduction to enolase

1.1.1 Role of enolase in metabolism

Enolase (2-phospho-D-glycerate-hydrolase, E.C.4.2.1.11) is a metalloenzyme which catalyzes the dehydration of 2-phospho-D-glycerate (2PGA) to form phosphoenolpyruvate (PEP) in glycolysis, as well as the hydration of PEP to PGA in gluconeogenesis (Brewer, 1981; Wold, 1971).

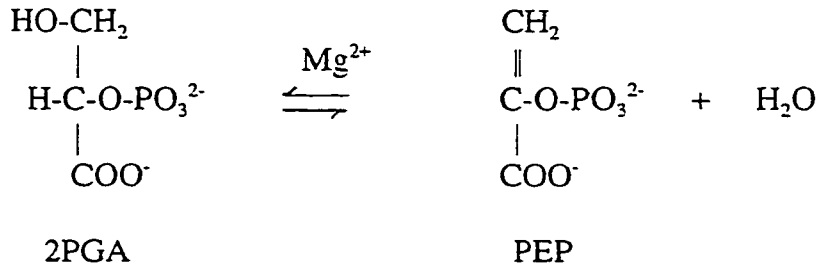

2PGA PEP

1.1.2 General structural characteristics of enolase

All known enolases, except the octameric enolases from thermophilic bacteria, are dimers with two identical subunits of 40 to 50 kDa (Wold, 1971). The amino acid sequences of enolases are highly conserved in different organisms. Two yeast isozymes: enolase A and B show 95% identical sequences (Chin, et al., 1981). Mammalian enolases have at least 80% sequence identity among their isozymes (α, β, and γ homodimers or heterodimers) and have more than 60 % sequence identity with yeast enolase (Lebioda, et al., 1989).

The X-ray crystal structures of enolases from baker's yeast (Lebioda and Stec, 1991; Wedekind, et al.,1994; Larsen, et al., 1996) and from lobster muscle (Duquerroy, et al., 1995) have been resolved so far. Their structures are highly homologous. Each subunit of the enolases consists of two domains as shown in Fig.1.1 (Lebioda, et al., 1989). The smaller N-terminal domain has a three-stranded antiparallel β-meander followed by four α-helices. The larger C-terminal domain is an atypical 8 fold α/β barrel with a topology of $\beta\beta\alpha\alpha(\beta\alpha)_6$. The active site is located at the C-terminal end of the barrel among loops contributed by both domains. Most subunit interactions are between two strands (strand 9 and strand 10) in the N-terminal domain of one monomer and one helix (helix H) in the C-terminal domain of the other monomer. There is a deep cleft between two subunits, which is accessible to the solvent.

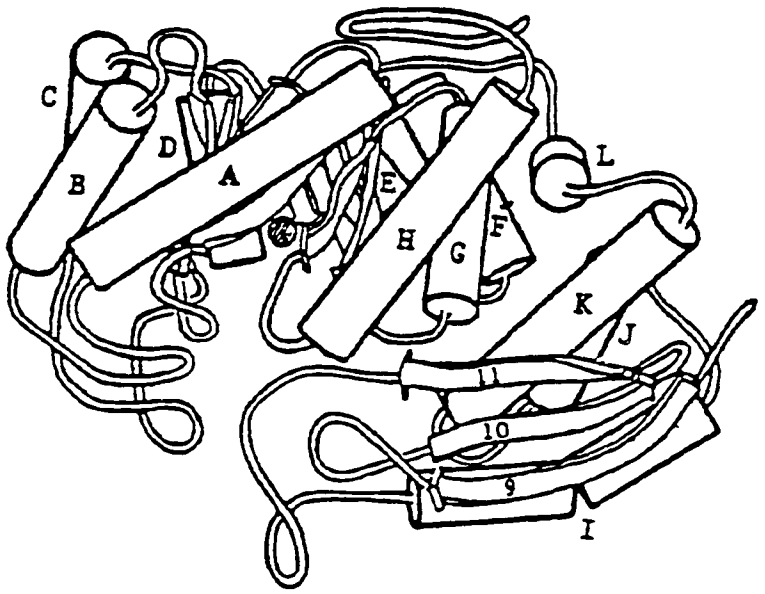

Fig. 1.1 Cartoon representation of a subunit of Baker's yeast enolase Each subunit is organized into two domains. The active site is located in a deep cleft, in which the hatched circle represents the position of the conformational cation (taken from Lebioda, et al., 1989).

1.1.3 Chemical mechanism

To produce catalytic activity, enolases have an absolute requirement for certain divalent metal ions. Three metal ion binding sites per subunit have been found in enolases. The first metal ion, traditionally called "conformational", binds to the high affinity site I and enables the binding of the substrate (Brewer and Weber, 1966). The second metal ion, called "catalytic", binds to the lower affinity site II only when the substrate or a substrate analogue is bound to the enzyme, and then catalysis occurs (Brewer and Collins, 1980). When the concentration of metal ions is high, the third metal ion, called " inhibitory", can bind to site III. Its binding as its name indicates, inhibits enzymatic activity (Faller et al., 1977). Enolase can bind to most of the divalent metal ions, but different metal ions exhibit different binding affinities and activities. The natural cofactor, Mg^{2+} gives the highest activity. The other divalent metal ions such as Zn^{2+}, Mn^{2+}, Co^{2+}, Ni^{2+} and Cu^{2+} produce lower activity than Mg^{2+}, while Ca^{2+} and Sm^{2+} do not activate the enzymes (Brewer, 1985). Activation by various divalent metal ions is not associated with their binding affinities in the conformational site I, for example, Sm^{2+} and Ca^{2+} do not produce activity, but they bind more strongly than the natural cofactor Mg^{2+} (Stec and Lebioda, 1990).

It is suggested by isotope-exchange studies that the enolase-catalyzed reaction proceeds in a stepwise manner (Dinovo and Boyer, 1971; Anderson, et al., 1994). The first step is the abstraction of the proton from C2 of 2PGA by a base in the active site to form an enolate intermediate. The second step is the elimination of hydroxyl group from the intermediate in the form of general-acid catalysis (shown in Fig. 1.2). This stepwise model of the reaction is also confirmed by later mutagenesis studies (Sangadala, et al., 1995; Poyner,

et al., 1996). For this stepwise reaction to be accomplished, a base to remove the C2 proton, a means to stabilize the intermediate and an acid to withdraw the C3 hydroxyl group are required. However, the acidity of the C2 proton is relatively weak. It has a pK_a around 30 (Gerlt and Gassman, 1992; Poyner, et al., 1996), whereas the catalytic turnover of the reaction is high, for example, 80 s^{-1} for yeast enolase. This creates considerable interest in the mechanism by which enolase overcomes this kinetic barrier in the ionization step.

Fig. 1.2 Stepwise model for enolase-catalyzed reaction

A, acid; EB, enzymic base (Taken from Reed, et al., 1996)

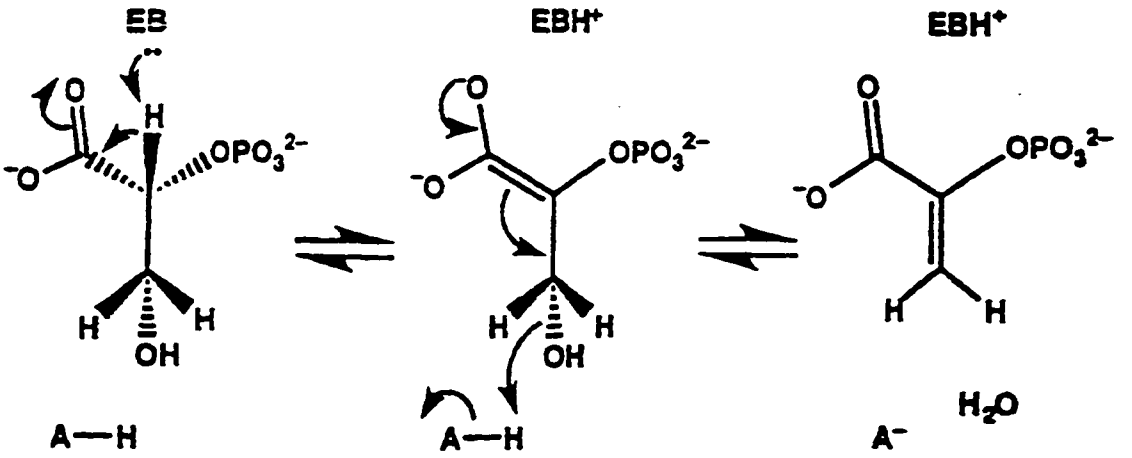

The interdependence of enolase structure, mechanism and catalytic properties has been studied through the combined methods of X-ray crystallography, site-directed mutagenesis, and kinetic analysis.

Three proposals for the acid/base catalysts were suggested based on separate structural studies in the literature before 1996. The first X-ray structure of yeast enolase was solved in 1989, and was followed by a series of extensive investigations of catalytic and

inhibitory complexes. The first proposal called "charge shuttle mechanism", was suggested by Lebioda and Stec (1991). An intervening water molecule which was activated by Glu211 and Glu168 was believed to function as the general base catalyst to abstract the C2 proton.

The second proposal was derived from the structure of the enolase complex with PhAH (a strong competitive inhibitor) and two bound metal ions (Wedekind, et al., 1994). This structure indicated that if the substrate occupied the position of PhAH, the amino side chain of Lys345 would point to the C2 proton of 2PGA. Lys345 would be the potential catalytic base.

The third proposal arose from the structure of the lobster enolase observed by Duquerroy, et al. (1995). They suggested that His157 was the base that removed the C2 proton, while an intervening water molecule assisted to keep the substrate in the carboxylic acid form.

However, the electron densities in these crystal structures were ambiguous with respect to the positions of the hydroxymethyl and carboxylate groups of the substrate. These earlier crystals of enolase and its complexes were grown in the solutions containing 3M $(NH_4)_2SO_4$ at low pH. This crystallization solution is problematic, since the high ionic strength significantly decreased the binding constant of the catalytic metal ions (Larsen et al., 1996). Not surprisingly, the observed structures usually lacked the second metal ion, except those using PhAH, the strongest competitive inhibitor reported, as the substrate analogue (Zhang, et al., 1994; Wedekind, et al., 1994).

Only in 1996 was the bound substrate correctly located in the active site. The recent X-ray structure of yeast enolase with bound 2PGA and both magnesium ions at 1.8 Å

resolution, demonstrated by Larsen and his coworkers (1996), unambiguously shows the positions of the hydroxymethyl and carboxylate groups of the substrate at the active site. This structure was determined using the crystals grown in PEG at pH 8.0. This avoided the negative effect of the high ionic strength caused by $(NH_4)_2SO_4$ in the earlier crystal structures. In this structure, the high affinity Mg^{2+} coordinates to the carboxylate oxygens of the substrate in a bidentate manner and also to the carboxylate side chains of Asp246, Glu295, Asp320, and to a water molecule (Fig. 1.3). The lower affinity Mg^{2+} coordinates to a phosphoryl oxygen and one of the carboxylate oxygens of the substrate, forming a μ-carboxylate bridge. This second metal ion also interacts with the carbonyl and γ-oxygens of Ser39 from the active site loop. The binding of these two metal ions stabilizes the negative charge in the enolate intermediate.

Fig. 1.3 Schematic diagram of the interactions among the enolase active site residues and the $(Mg^{2+})_2$-substrate/product complex The dashed lines indicate the coordination between atoms. The interatomic distances are shown on the dashed lines (taken from Larsen, et al. 1996).

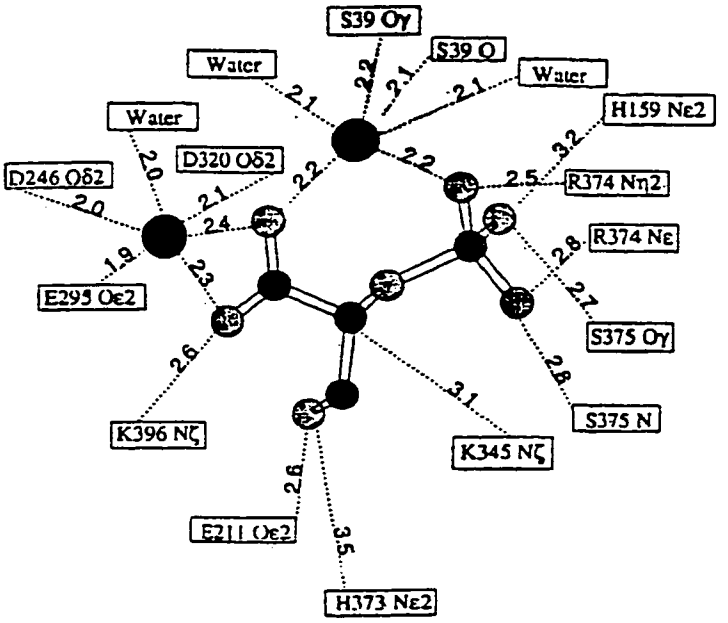

The crystal structures show that many charged and polar residues are distributed in the active site of enolase (Lebioda and Stec, 1991), among which Glu211 and Glu168 are positioned close to the hydroxyl methyl moiety of 2-PGA. Lys345 lies on the opposite surface of the active site from Glu211 and Glu168 with its ε-amino group pointing towards the C2 proton of 2PGA. Based on the active site structure, it is proposed that Lys345 serves as the base abstracting the C2 proton in the first step. Glu211 and Glu168 are involved in the second step of the reaction and function as general acid catalysts. In 1997, Zhang and coworkers reported a crystal structure of asymmetric dimer enolase-2PGA/enolase-PEP. The difference between the two monomers in this crystal structure is that the position of His159 is changed from interacting with the phosphate moiety of the substrate in one subunit to being separated by water molecules from the product in the other subunit. The imidazolium of His159 is suggested to transfer a proton to the phosphate moiety, which provides additional electron withdrawing from carbon-2.

With the continuous refinement of the crystal structures of enolase and its complexes, efforts also have been made in site-directed mutagenesis studies to confirm the conclusions drawn from the X-ray crystal structures. Five of the active site residues (Glu168, Glu211, Lys345, His373 and Lys396) have been substituted (Sangadala, et al., 1995; Poyner, et al., 1996; Reed, et al., 1996; Brewer, et al., 1997). The mutations of Lys345 to Ala, Glu168 to Gln and Glu211 to Gln significantly lower the activity by about 10^5 relative to wild-type enolase (Poyner, et al., 1996). Both mutant proteins Glu168Gln and Glu211Gln are able to catalyze the exchange of the C2 proton of 2PGA with deuterium in D_2O (step 1), but cannot catalyze the ionization of tartronate semialdehyde phosphate (TSP), (mutant that retains the

catalytic base should ionize bound TSP); whereas Lys345Ala fails in the C2 proton exchange but maintains activity in ionization of TSP. These observations support that Lys345 serves as the catalytic base, while Glu168 and Glu221 are crucial in the removal of the C3 hydroxyl group.

Based on the structural and mutagenesis studies, a picture of enolase-catalyzed mechanism at optimum pH was recently drawn by Zhang and his coworkers (1997). When 2PGA binds to the active side, residues Glu167, Lys396 and both Mg^{2+} orientate the substrate and neutralize its negative change through interactions with its carboxylate group. Then three loops: Ser36-His43, Val153-Phe169 and Asp255-Asn266 move to form a closed conformation, so Ser39 coordinates catalytic Mg^{2+} and His159 interacts with the phosphate group of 2PGA through donation of a proton to it. Arg374 and catalytic Mg^{2+}also act to neutralize the negative charge in the phosphate group, which effectively lowers the pk_a of 2PGA of C2. Lys345 whose proton is lost due to the decrease of the pK_a of its ϵ-ammonio group by Arg374, accepts one proton from C2 of 2PGA. The proton shared by Glu168 and Glu211 forms a water molecule with the hydroxyl group of 2PGA, thus PEP is generated. In the reverse reaction, the hydration of PEP, a hydroxyl group formed by the deprotonation of the water molecule held by Glu168, Glu211 and His373, adds to C3, while a proton from the ϵ-ammonio group of Lys345 adds to C2 and produces 2PGA.

The inhibitory site III has not been observed in the X-ray structures so far due to its binding affinity being the weakest among the three metal binding sites. However the studies by EPR and equilibrium dialysis indicate that three metal ion binding sites per subunit exist in the presence of the substrate/product (Hanlon and Westhead, 1969; Lee and Nowak,

1992). In the absence of the substrate/product, two metal ions per subunit were found for Zn^{2+}, Co^{2+} or Cu^{2+} (Elliott and Brewer, 1980; Brewer and Collins, 1980; Rose, et al., 1984; Dickinson, et. al., 1980). As for Mg^{2+} and Mn^{2+}, their binding constants in the inhibitory site III under the experimental conditions seem to be even lower and thus cannot be detected. The existence of the catalytic site II depends on the binding of the substrate/product, whereas the first conformational site I and the third inhibitory site III is independent of the substrate/product binding, though their binding abilities appear to be enhanced by the presence of the substrate (Brewer and Ellis, 1983). The inhibition at high concentration of metal ions in the presence of the substrate/product, is suggested to be attributed to the sequential binding of the metal ions which affects the release of the product (Zhang, et al., 1994). The mechanism of this inhibition has not been well established.

1.1.4 Conformational change

Binding of the substrate or competitive inhibitors usually induces a conformational change in the protein. The conformational change alters the environments of certain aromatic residues, which can be reflected by the spectral methods such as fluorescence, UV and UV CD. As observed earlier in yeast enolase, binding of the first metal ion is associated with the changes in fluorescence and ultraviolet absorption (Brewer and Weber, 1966). The presence of magnesium ions in the protein sample produces a peak at 296 nm in difference absorption spectrum and an increase associated with a hydrophobic (blue) shift in fluorescence emission spectrum, indicating the decreased exposure of the aromatic residues to the solvent. This conformational change maintains the protein in a more compact conformation as indicated by

hydrodynamic property studies. The fluorescence change in yeast enolase produced by substrates and competitive inhibitors in the presence excess Mg^{2+} or other activating divalent metal ions has also been extensively investigated by Brewer (1971). The amount of increase in fluorescence which is attributed to the decrease in quenching of tryptophan residues, varies with inhibitors and divalent ions. For example, phosphoglycolate (PG), a competitive inhibitor, produces a greater increase than the substrate, while another inhibitor, 3-phosphoglycerate (3PGA) causes little change in fluorescence intensity. Mn^{2+} and Zn^{2+} produce increases comparable to that of Mg^{2+}, while Ni^{2+} and Co^{2+} induce much lower increases. Steady-state quenching and dynamic fluorescence were also used by Brewer et al.(1987) to investigate the conformational change in yeast enolase. Subunit association was found to be strengthened by the binding of the conformational metal ion and an increase in average lifetime was observed with the addition of the substrate.

UV CD spectra of yeast enolase with different metal ions, substrates and inhibitors (PG) were studied by Collins and Brewer (1982). Binding of the first metal ion or of the substrate causes a change in tertiary structure but does not affect the secondary structure. A similar increased signal at 283 nm is observed in near-UV CD spectra upon the addition of the activators Mg^{2+}, Ni^{2+} or the nonactivator Ca^{2+}, while a similar decreased signal at 280 nm is produced by the addition of substrates/products to the above holo-enzymes. It was concluded that the activation by certain divalent cations is not attributed to their ability to cause a structural change.

Although the binding of the ligands induces the spectral change in the enzyme, no obvious motion of the two domains or subunits was observed in the crystal structures of both

yeast enolase and lobster enolase (Stec and Lebioda, 1990; Duquerroy, et al., 1995). The major conformational change in response to the binding of substrates or inhibitors in the active site, occurs through the movement of three loops: Ser36-His43, Val153-Phe169 and Asp255-Asn266 (numbered by yeast enolase). Upon binding of substrates or inhibitors, these loops move and approach the active site to form the "closed" conformation as opposed to the "open" conformation of the native enzyme (Zhang, et al., 1997). There are five tryptophans and nine tyrosines in yeast enolase (Chin, et al., 1981). Among the five tryptophans, two (Trp303 and Trp306) lie on an α-helix in the α/β barrel; two (Trp367 and Trp56) on the loops, and one (Trp272) on a β-turn following the mobile loop from residues Asp255-Asn266. Trp56 is positioned in the cleft of the subunit interface. Though none of these aromatic residues is directly located in the three mobile loops, binding of the substrate and inhibitors does result in a series of new interactions dominated at the active site and propagated to more remote regions throughout the structure (Wedekind, et al., 1994; Zhang, et al.,1997), which causes the change in the average microenvironments of the aromatic residues and account for the spectral difference.

Certain salts also have profound effects on the spectral properties of the enzyme. They change the enzyme conformation through their effects on the binding of the ligands to the enzyme or on the tertiary and secondary structure of the enzyme. Brewer (1969) reported that in the presence of excess EDTA or Mg^{2+}, 1M KCl and K(OAc) produce opposite changes in the absorption, fluorescence and fluorescence polarization spectra of yeast enolase. The different effects were interpreted as a result of the difference in solubility of anion-amide group complexes. In another study by Collins and Brewer (1982), 1M KCl slightly decreased

the content of the secondary structure of yeast enolase as observed by far-UV CD spectra. At this concentration of KCl, the enzyme is probably partially denatured.

Kornblatt et al.(1996) used UV, UV CD and fluorescence as tools to explore the effect of $NaClO_4$ on rabbit muscle enolase and applied the derivative UV spectra to monitor the dissociation of the dimeric enzyme. $NaClO_4$ induces the change in the tertiary structure, but does not affect the secondary structure. It has been suggested that the role of $NaClO_4$ on inactivation/dissociation of the enzyme is to increase the flexibility of certain loops, which disrupt the active site structure and the subunit contact. Above all, the interactions between salts and proteins, either direct or indirect, or both, are complex. The mechanisms of the different salt effects are still being investigated.

1.2 Effects of monovalent cations on enolase

Enolase activity has been shown to be influenced by certain monovalent cations. Kornblatt and Klugerman (1988) have reported that Li^+ and Na^+ inhibit both yeast and rabbit enolases, whereas K^+, NH_4^+, Cs^+ and Rb^+ activate the rabbit enolase, but not the yeast enolase. The mechanism of the inhibition of yeast enolase by Li^+ and Na^+ was investigated using steady-state kinetics, kinetic isotope effects and hydrogen exchange measurements by Kornblatt and Musil (1990). Steady-state kinetic studies indicate that Li^+ shows higher inhibition than Na^+, although they exhibit the same inhibition patterns. At pH 7.1, the inhibition shows a hyperbolic mixed pattern; while at pH 9.2, the inhibition becomes competitive with respect to Mg^{2+}. Li^+ decreases the kinetic isotope effect on V_{max}, but does not change the rate of the exchange of the C2 proton. It was concluded that Li^+ binds to the

enzyme and decreases the rate of at least one step in the mechanism and the step that Li^+ inhibits is not the proton abstraction, but may be the release of the product or Mg^{2+}.

Further studies on the effects of Li^+ on rabbit muscle enolase by stop-flow fluorescence methods (Kornblatt, 1996) confirmed that Li^+ does not inhibit the proton abstraction, but affects the catalysis by decreasing the formation of the intermediate (EMSM)*, which originates from a conformational change of EMSM (where E is enolase, M is the metal ion and S is the substrate). It has been proposed that Li^+ may compete with Mg^{2+} for the inhibitory site III and inhibit the enzymatic activity.

Fig. 1.4 Schematic diagram of the interactions among the enolase active site residues and the Mg^{2+}-substrate-Li^+ complex (taken from Zhang, et al., 1997).

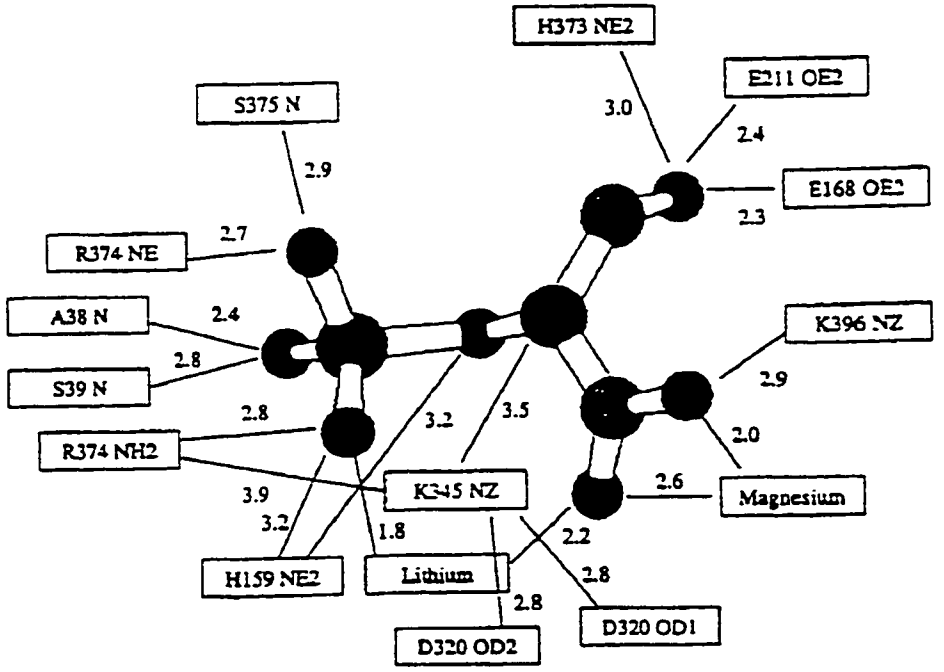

However, the detailed mechanism of the inhibition by monovalent cations has not yet been clearly understood. In the latest crystal structure of yeast enolase (pH 9.3) where an asymmetric dimer was observed by Zhang and coworkers (1997), the weak electron density in the catalytic metal ion binding site II of the 2PGA subunit was suggested to represent a Li^+, as shown in Fig. 1.4. Li^+ may bind to a site which is very close to the catalytic site II and affect the binding of the second metal ion.

1.3 Inactivation/dissociation of enolase

Inactivation of oligomeric proteins by chemical or physical agents is usually accompanied by dissociation (Jaenicke and Rudolph, 1986). Studies of inactivation and dissociation of enolase by different methods have been made to understand the relationship of the enzyme structure and its function. The subunit contacts of enolase are involved in hydrophobic, hydrophilic interactions and hydrogen bonds (Brewer, et al., 1987; Lebioda, et al., 1989; Stec and Lebioda, 1990). There are two ion pairs (Glu20-Arg414 and Arg8-Glu417 in yeast enolase) and a series of hydrogen bonds between the subunits as observed in the crystal structures of yeast enolase. The association of the two subunits is not very strong and in the presence of chemical or physical disruptions the subunits dissociate.

Enolase has been inactivated/dissociated by various salts (Gawronski and Westhead, 1969; Trepanier; et al.,1990; Kornblatt, et al., 1996), hydrostatic pressure (Paladini and Weber, 1981; Kornblatt and Hui Bon Hoa, 1987; Kornblatt, et al., 1995) or by increasing temperature at low enzyme concentrations. Whether the generated monomer is active or inactive mainly depends on the method used, although the active site of enolase appears to

be completely within the monomer. Yeast enolase was found to be dissociated into fully active monomers at a low concentration of 0.7μg/ml and a temperature of about 40°C (Keresztes-Nagy and Orman, 1971; Holleman, 1973). The monomers produced by high concentrations of salts in most cases are inactive. Brewer and Weber (1968) incubated yeast enolase at high concentration of KCl (1 M) with excess EDTA. The resulting monomers as detected by sedimentation equilibrium are inactive. Consistent results were obtained from another study by Gawronski and Westhead (1969), where subunit scrambling, sedimentation equilibrium and gel filtration were used to monitor the dissociation of yeast enolase by KCl and KBr. It seems that the monomer of the enolase could be active, but the dissociating salts may affect the conformation of the monomer and consequently inactivate the monomer.

Mammalian enolases have also been extensively studied. Inactivation of mouse brain enolases by pressure was found to be reversible and involved with dissociation (Kornblatt, et al., 1982). Research on the dissociation of rabbit brain enolases by pressure using subunit scrambling and crosslinking techniques demonstrated that for $\gamma\gamma$ isozymes, the dissociation occurs before the inactivation, whereas, for $\alpha\alpha$ isozymes, the dissociation is correlated to the inactivation (Kornblatt and Hui Bon Hoa, 1987). The different behaviors of these two enzymes under the applied pressure are attributed to their differing stabilities of the α and γ monomers. In 1990, Trepanier et al. reported that $NaClO_4$ induces dissociation of $\gamma\gamma$ isozyme of rabbit enolase. Fluorescence polarization of FITC-$\gamma\gamma$ (fluorescein isothiocyanate) and crosslinking methods were applied to the study. It was found that the inactivation is a two-step process with dissociation preceding inactivation and the active monomers are produced in the first step before further change in resulting partially active monomers. However, the

structural basis of the inactivation and dissociation had not yet been explored in these studies.

Recently, Kornblatt and coworkers (1996,1998) have thoroughly studied the inactivation of yeast enolase by high pressure and rabbit muscle enolase by $NaClO_4$. The loss of enzymatic activity by hydrostatic pressure or $NaClO_4$ is accompanied by the dissociation of the dimeric enzyme. $NaClO_4$ and hydrostatic pressure cause the changes in the tertiary and quaternary structures of the enzyme as shown by spectral methods. Their major effect on enolase structures is suggested to interfere with the movement of certain loops in which some residues are crucial for the interactions in the active site and subunit contacts. The change in the flexibility of these loops alters the environment of certain aromatic residues, disrupts the active site structure and weakens the subunit interactions. In their studies, the derivative UV spectrum was introduced to probe the dissociation since the small change in the original spectrum can be magnified by derivatives. Through the way that the actual spectrum of the inactivated enzyme was simulated by proportional combination of the derivative spectra of the dimeric and monomeric enolases, the degree of dissociation was determined.

1.4 Effects of substrates and metal cations on inactivation/dissociation of enolase

The presence of Mg^{2+} and substrates shifts the monomer-dimer equilibrium toward the formation of the active dimers (Gawronski and Westhead, 1969). Subunit association is affected by the binding of the metal ions and substrates, which is usually accompanied by a conformational change in the enzyme.

The present work is mostly based on the rabbit muscle enolase. The previous studies on this enzyme have shown that the addition of 2PGA significantly protects the holo-enolase

from inactivation by $NaClO_4$ (Kornblatt, et al., 1996), and effectively prevents it from dissociation as indicated by cross-linking and SDS-PAGE methods (Al-Ghanim, 1994). It appears that binding of the ligands stabilizes the enzyme in a "closed" conformation which makes the enzyme less accessible to the salts, and thus protects its activity and dimeric structures.

The starting point of this project is to explore the relationship between the conformational changes upon binding of the substrate, various inhibitors or divalent metal ions and the protection of enolase by these ligands against inactivation/dissociation. For example, 2PGA, PG and phosphonoacetic acid increase fluorescence, but 3PGA and glycerate 2-phospate do not; Mg^{2+}, Mn^{2+}, Zn^{2+} and Co^{2+} increase fluorescence, but Ca^{2+} does not. Is the conformational change reflected by increased fluorescence necessary for the protection of the enzyme from the inactivation by $NaClO_4$?

While preparing the apo-enzyme (enzyme free of divalent metal ions) for the experiments to see the effects of various divalent cations, I found, to my surprise, that apo-enolase is protected by the substrate, which is not supposed to be, since binding of the substrate presumably occurs only when a divalent metal ion binds in the high affinity site I. The project thus turned to the investigation of this striking protection of the apo-enzyme provided by 2PGA, and the role of sodium cations in the protection.

This study indicates that sodium cation is necessary for the substrate to bind to the apo-enolase and give protection. This binding induces a small conformational change in the enzyme as monitored by Trp fluorescence and near-UV CD. This study suggests that sodium cation permits the binding of 2PGA to apo-enolase, which is contrary to traditional ideas

about the binding of the substrate.

CHAPTER 2 Materials and Methods

2.1 Materials

2.1.1 Enolase and buffer

Rabbit muscle enolase (ββ) suspended in ammonium sulfate was purchased from Boehringer Mannheim. Yeast enolase, in the form of lyophilized powder, was purchased from Sigma.

Mes (4-Morpholineethanesulfonic acid) was purchased from Boehringer Mannheim, while Tris (Tris[hydroxymethyl]aminomethane) was obtained from Sigma. Magnesium acetate and glycerol were from Fisher Scientific and EDTA was purchased from Fluka.

2.1.2 Substrate and inhibitors

2PGA (2-phospho-D-glycerate) used in inactivation experiments was purchased from Boehringer Mannheim, while 2PGA used in enzyme activity assays was purchased from Sigma. The inhibitors 3-phosphoglycerate acid (3PGA) was purchased from Sigma, while phosphoglycolate (PG) from Sigma, phosphonoacetic acid and glycerol 2-phosphate from Aldrich.

2.1.3 Salts

NaCl, KCl, $MnCl_2$, $Zn(OAc)_2$ and $CaCl_2$ were purchased from Fisher Scientific (Certified A.C.S. crystal), while Tetramethylammonium chloride (TMA-Cl), LiCl, NH_4Cl and $Co(OAc)_2$ from Fluka, and $NaClO_4$ from Aldrich.

2.1.4 Chelex and chelating reagents

Chelex 100 resin used to prepare metal-free solutions and apo-enolase, was purchased from Bio-Rad. The other chelating reagents used were EDTA from Fluka, EGTA (Ethyleneglycol-bis-(ß-amino-ethyl ether)N,N'-tetraacetic acid) and o-Phenanthroline (1,10-Phenanthroline) from Sigma.

2.1.5 Crosslinking and SDS-PAGE agents

Glutaraldehyde (Grade 1), in a 25% aqueous solution, and $NaBH_4$ were purchased from Sigma. SDS and Glycine were purchased from Fluka, N'N'-Methylenebis-acrylamide from Eastman Kodak Co., Acrylamide (99.9%) and the High MW SDS-PAGE Standards from Bio-Rad.

2.1.6 Others

Perchloric acid and Tetramethylammonium hydroxide was purchased from Fluka.

Agents for preparation of ICP (inductively coupled plasma trace metal analysis) samples include: high quality HNO_3 (trace-metal grade) from Fisher and standard solutions containing Ca^{2+}, Zn^{2+}, Cu^{2+}, Ni^{2+}, Mg^{2+}, Hg^{2+}, Sr^{2+}, Mn^{2+}, Co^{2+}, Cd^{2+}, Cr^{2+}, Ba^{2+}, Be^{2+} and Pb^{2+}, which were kindly provided by Science Industry Research Unit (S.I.R.U.) in Concordia University.

ADP, NADH, pyruvate kinase and lactate dehydrogenase were purchased from Boehringer.

2.2 Methods

2.2.1 Enzyme preparation

One mL of 10 mg/mL rabbit muscle enolase was pelleted by centrifugation at 15000 RPM at 4 °C for 15 min, and dissolved in 1.5 mL of MTME buffer (pH 7.1) containing the following: 25 mM Mes, 25 mM Tris, 1 mM Magnesium acetate, 0.1 mM EDTA.

The enolase solution was dialyzed against 100 mL of MTME buffer for 3-4 hours, then dialyzed overnight against another 100 mL of fresh MTME buffer. The enolase stock was prepared by dialyzing the above fresh enolase against 50% MTME buffer and 50% glycerol followed by storage at -20 °C.

Yeast enolase was dissolved in MTME buffer and then was dialyzed according to the method described above.

2.2.2 Enzyme activity assay

Enolase activity assay was carried out by addition of enzyme to the enolase assay buffer (EAB, pH 7.1) containing the following: 50 mM Imidazole, 250 mM KCl, 1 mM Magnesium acetate, 0.1 mM EDTA and 1 mM 2PGA.

The production of phosphoenolpyruvate (PEP) was measured by UV adsorption at 240 nm. Only the first 30 s of each assay were used to calculate the rates, since $NaClO_4$-inactivated enzyme slowly reactivates under the assay condition (Kornblatt, 1996). Enolase activities were expressed as change of O.D. at 240 nm per minute.

To characterize the apo-enolase sample, metal-free activity assay was performed in an assay buffer (pH 7.1) containing the following: 50 mM Imidazole, 250 mM KCl and 1 mM

2PGA

Prior to use, the above buffer was passed through a chelex 100 column and the cuvetts were treated by 20% nitric acid overnight to be free of divalent cations.

In order to determine the kinetic properties of enolase (such as K_i of inhibitors), ADP, NADH, pyruvate kinase and lactate dehydrogenase (PK/LDH) were added to convert PEP to lactate. The concentrations of NADH, ADP and PK/LDH in the assay were 5 mM, 35 mM and 2.7 U/mL, respectively. The assay was followed spectrophotometrically by the disappearance of NADH at 340 nm.

2.2.3 Protein assay

Protein concentration was determined by the Bio-Rad Protein Assay, using bovine serum albumin as the standard (Bradford, 1976).

2.2.4 Preparation of inactivating salts

TMA-ClO_4 was prepared in MT buffer (containing 25 mM Tris and 25 mM Mes, pH 7.1) by titration of 2 M perchloric acid with 2 M Tetramethylammonium hydroxide giving a pH 7.1. Similarly, Tris-ClO_4 (pH 7.1) was made by titration of 2 M perchloric acid with 2 M Tris. The ionic strength of the inactivating salts in buffer was measured by an osmometer (μOSMETTE). The ionic strength of these salts was not changed after their solutions were passed through the chelex column to be free of divalent metal ions.

2.2.5 Preparation of chelex columns

Chelex 100 resins are styrene divinylbenzene copolymers containing paired iminodiacetate ions which have high affinity for polyvalent metal ions. Commercial chelex 100 has to be regenerated by a two-step process. First, two bed volumes of 1 M HCl are added to convert the resin to the hydrogen form, then five bed volumes of water are used to rinse the resin until the pH is higher than 5. Second, two bed volumes of 1 M Tris are added and convert the resin to the ionic form (exchanger form). Chelex 100 is usually stored in this Tris form in the refrigerator. Prior to use, ultra pure water is used to wash the Tris out until the pH of the solution is close to 7. After that, at least two volumes of sample buffer should be passed through the chelex column to reach an equilibrium before the sample is applied to the column. The used chelex 100 resin can be regenerated according to the same procedure. The chelex column used to prepare apo-enzyme was made in a transfer pipette containing about 2 mg regenerated chelex 100 resin. A bigger chelex column containing 20 mg chelex 100 resin was used to prepare the metal-free buffer and the apo-enolase sample for ICP trace metal analysis.

2.2.6 Preparation of apo-enolase

Prior to use, all the containers were soaked in 20% nitric acid overnight. MT buffer was passed through a chelex100 column to remove the trace divalent cations. Enolase prepared in MTME buffer was first dialyzed against metal-free MT buffer plus 0.1 mM $Mg(OAc)_2$ for 3-4 hours at 4°C so as to lower the concentration of magnesium ion. A second dialysis was performed overnight using fresh MT buffer containing 0.1 mM $Mg(OAc)_2$. The

dialysis buffer was then changed to metal-free MT buffer containing chelex 100 resin, and the enzyme was dialyzed for another 24 hrs. Finally, dialyzed enolase was passed through a chelex 100 column to be free of divalent cations. Fractions of apo-enolase were collected and characterized by metal-free activity assay (referred to section 2.2.1). No activity was detectable at the high concentration of enolase (up to 30 μg/mL).

Additional methods were used for the characterization of the apo-enzyme subjected to ICP trace metal analysis. Trp fluorescence spectra of apo-enzyme were obtained in the absence and presence of 2PGA. No increased fluorescence was observed upon the addition of 1 mM metal-free 2PGA. Incubations of the apo-enolase were also set up in MT with or without 0.1 M $NaClO_4$ in the presence of chelating reagents EDTA, EGTA and o-phenathroline according to the Methods 2.2.7. The degrees of the inactivation/protection found in ICP apo-enolase were similar to those apo-enzyme previously prepared.

2.2.7 Inactivation of enolase

Inactivation of enolase was performed in MTME buffer (except those with additional description) for holo-enolase or in metal-free MT buffer for apo-enolase with varying concentrations of $NaClO_4$ or Tris-ClO_4 at 15°C, or with TMA-ClO_4 at 0°C. After incubation at a constant temperature for 24 hrs, aliquots of incubations were removed for activity assay. Inactivation was determined by an average of triple assays for each sample except those with additional illustrations. The final concentration of enolase was 1.06 μM except for the experiments involved in UV spectra, far-UV CD spectra and cross-linking plus SDS-PAGE, where a concentration of 1.5 μM was used.

2.2.8 Trp fluorescence spectra of apo-enolase

Fluorescence spectra were recorded on an Aminco-Bowman Series 2 spectrofluorometer in a 10 mm path length quartz cell at 25 °C. Emission spectra (310-350 nm) were collected with excitation at 295 nm. The recording parameters were as follows: scan rate, 1 nm/sec; excitation bandwidth, 2 nm; emission bandwidth, 4 nm and high voltage, 765 v (except those described in legend). The enzyme concentration used was 1.06 μM. When substrates or inhibitors were added to the enolase samples, the interacting mixtures were allowed to reach an equilibrium for 3 min before the spectra were recorded. All the emission spectra were smoothed and corrected by subtraction of the spectrum of the buffer

.

2.2.9 Near and Far-UV CD spectra of apo-enolase

UV CD spectra were obtained on a JASCO J-710 spectropolarimeter purged with nitrogen at a flow rate of 3 L/min at ambient temperature. Near-UV CD spectra in the aromatic side-chain region (255-340 nm) were performed in a 1 cm pathlength cell (~800 μL) at a protein concentration of 10.6 μM. Fifteen scans were collected and averaged for each sample. Far-UV CD spectra in the backbone region (200-250 nm) were recorded in a 0.1 cm pathlength cell (~180 μL) at a protein concentration of 1.5 μM. Ten scans were collected and averaged for each sample.

The other recording parameters of UV CD spectra were as follows: bandwidth, 1.0 nm; scan speed, 100 nm/min; response time, 0.25 s and step resolution, 0.2 nm. All the UV CD spectra were corrected by subtraction of the spectrum of the buffer. The observed

ellipticity (mdeg) was divided by (CL/100) to convert to molar ellipticity, where C is the concentration (M) and L is the pathlength (cm) (Sievers, 1978).

2.2.10 UV spectra of apo-enolase and the fourth derivatives

UV spectra of apo-enolase incubated in varying concentrations of $NaClO_4$ were recorded on a Cary 2290 spectrophotometer at 15 °C. The slit bandwidth was 1 nm, the scan rate was 0.1 nm/s and the data interval was 0.1 nm. Ten spectra from 260-305 nm were collected and averaged for each sample, and then corrected by subtraction of the spectrum of the MT buffer. The fourth derivatives were calculated according to Lange et al. (1996). The extent of dissociation was determined by the simulation of the fourth derivative spectra as described by Kornblatt, et al.(1998). Two spectra of apo-enolase in 0 M and 0.5 M $NaClO_4$ used as the spectra of dimeric and monomeric enolase respectively, were proportionally combined until the positions of peaks and troughs, and ratio of the peak to trough distance fit that of the actual spectrum.

2.2.11 Cross-linking and SDS-PAGE

Enolase incubated in varying concentrations of $NaClO_4$ was cross-linked by glutaraldehyde according to the procedures of Burns and Schachman (1982) and Al-Ghanim (1994), with some modifications. Seventy-five μL of each incubation was removed to a microfuge tube and 6 μL of 0.25 M glutaraldehyde (diluted 1:10 with water) was immediately added to it. After one minute of incubation, 10 μL of 1 M $NaBH_4$ (38 mg/ml in 0.1 M of NaOH) was added to terminate the reaction followed by a 20 minute incubation to

eliminate bubbles. Then, 25 μL of sample buffer (2×concentration) was added. The samples were then boiled in a water bath for 4 min prior to use. SDS-PAGE (10% polyacrylamide gel) was performed on 20 μL sample aliquots. The protein on the gel was visualized by the silver stain (Wray, et al., 1981).

2.2.12 ICP-Mass spectrometry of apo-enolase

Ten mg of enolase was used to prepare apo-enolase according to the procedure as described in Methods 2.2.3. Apo-enolase with a final concentration of 3 μM and specific activity 88.5 units/mg, was characterized by an activity assay, an inactivation experiment and Trp fluorescence (referred to Methods 2.2.3).

Apo-enolase was then placed in a porcelain container followed by addition of 1 mL of concentrated H_2SO_4 and heated on a hot plate. When a white smoke appeared, HNO_3 was added dropwise along the edge of the solutions until the solutions became clear again. This process is called ashing. The ashed apo-enolase was diluted to 50 ml by adding 5% high-quality HNO_3. A sample of chelex-treated MT buffer was prepared in the same manner and used as blank. Three standard solutions containing 1 ppb, 10 ppb and 100 ppb each of Ca^{2+}, Zn^{2+}, Cu^{2+}, Ni^{2+}, Mg^{2+}, Hg^{2+}, Sr^{2+}, Mn^{2+}, Co^{2+}, Cd^{2+}, Cr^{2+}, Ba^{2+}, Be^{2+} and Pb^{2+}, were prepared using the same 5% HNO_3 solution. The ICP mass-spectra were obtained from these samples on an Elan 6000 ICP-MS instrument by the generous help of Dr. Salin and M. Ryback of McGill University. The concentration of each trace metal ion in the apo-enolase sample and the percentage of active sites occupied were calculated from the intensities.

2.2.13 Determination of kinetic parameters

To investigate the effect of Na^+ on the kinetic properties of enolase, activity assays were performed at 1 mM 2PGA and varying concentrations of Mg^{2+} in the absence and presence of 20 mM NaCl. V_{max}, K_m and K_i were determined by a program Grafit (Erithacus Software) using an equation for modified substrate inhibition,

$$v = (V_{max} \times [S] + V_{final} \times [S] \times [S] / K_i) / (K_m + [S] + ([S] \times [S] / K_i)) \quad (1)$$

where S is Mg^{2+} and V_{final} is the final velocity at high concentration of Mg^{2+}. The concentration of Mg^{2+} was not corrected by the subtraction of Mg^{2+} that was bound to 2PGA.

To determine the K_i values of the selected inhibitors, activity assays were performed in the presence of NADH, ADP and PK/LDH (referred to methods 2.2.1). Michaelis Menten Equation in a program ENZFITTER (Biosoft) was used to calculate K_i values.

2.2.14 Determination of K_d and ΔG_d of dissociation

Since the degree of dissociation parallels the degree of inactivation, the degree of inactivation at varying [$NaClO_4$] was used to determined K_d and ΔG_d of dissociation.

$$K_d = 4 (1 - f_D)^2 [\text{enolase}]/f_D \quad (2)$$

$$\Delta G_d = - RT \ln K_d \quad (3)$$

where f_D is the fractions of dimeric enzyme (=1-%inactivation) and [enolase] is the concentration of enolase.

CHAPTER 3 Effects of Sodium Cations and the Substrate on Rabbit Muscle Enolase

Rabbit muscle enolase is inactivated and dissociated when incubated in certain concentrations of $NaClO_4$ (Kornblatt, et al., 1996). Addition of substrates has been found to produce a conformational change in the holo-enzyme and protect the enzyme from inactivation/dissociation. Our interest focuses on the effects of the ligands on inactivation/dissociation of the enzyme. This study started with the investigation of the effects of Mg^{2+} and 2PGA on the $NaClO_4$-induced inactivation of rabbit muscle enolase.

3.1 Effects of Mg^{2+} and 2PGA on inactivation of holo-enolase by $NaClO_4$

Enolase was inactivated by 0.3 M $NaClO_4$ in MT buffer containing varying concentrations of $Mg(OAc)_2$. As Fig. 3.1 shows, the inactivation of holo-enolase was decreased with increasing concentrations of Mg^{2+}. Incubating enolase with 0.1 mM $Mg(OAc)_2$ in 0.3 M $NaClO_4$ resulted in 90% inactivation, while only 30% inactivation was achieved when the concentration of $Mg(OAc)_2$ was above 3 mM. At an extremely high concentration of $Mg(OAc)_2$ (above 10 mM), inactivation seems to increase due to the increasing ionic strength. The binding of metal ions protects the enzyme from the inactivation by $NaClO_4$.

Addition of the substrate to the incubations provides further protection of enolase against the inactivation by $NaClO_4$ (Fig. 3.1). Maximum protection was achieved in the presence of 0.4 mM $Mg(OAc)_2$ and 1 mM 2PGA. Fig. 3.2 demonstrates the percentage inactivation as a function of the concentration of 2PGA. Inactivation significantly decreases

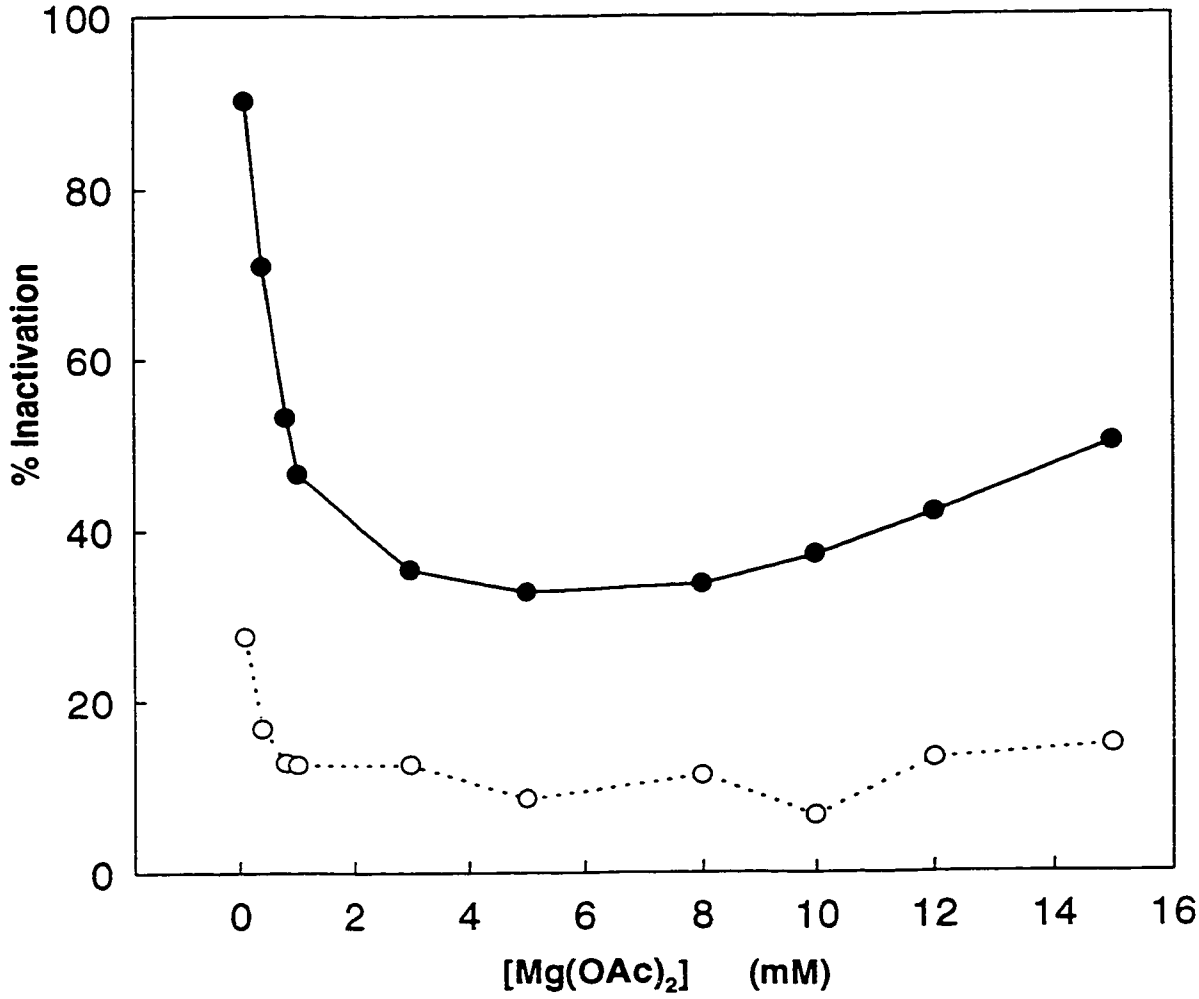

Fig. 3.1 Effect of Magnesium ions on inactivation of enolase by $NaClO_4$. Enolase (1.06 μM) was incubated in 0.3 M $NaClO_4$ with (··o··) or without (—●—) 1 mM 2PGA. Deviations of the average value from the individual values are less than 3.0%.

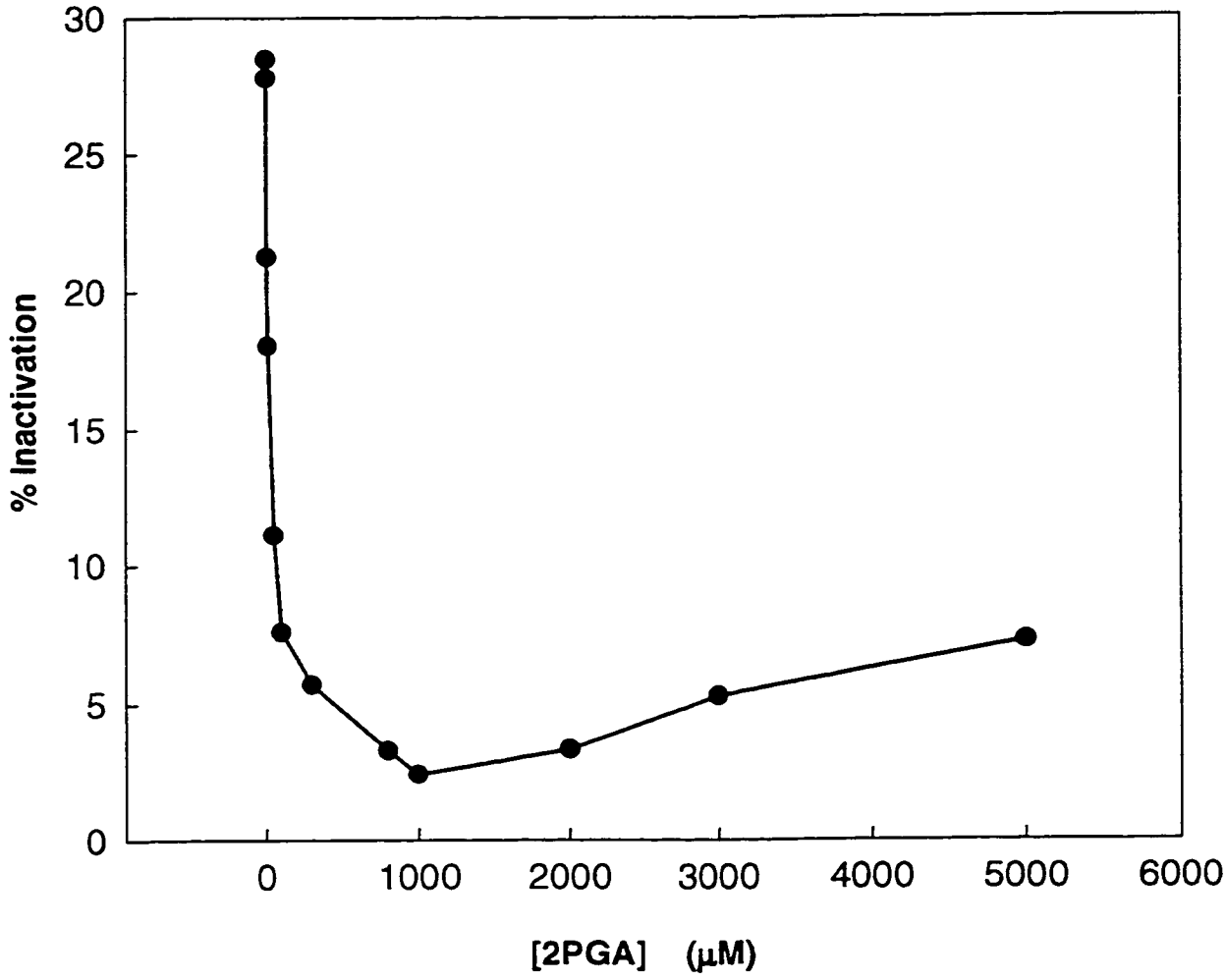

Fig. 3. 2 Effect of the substrate on inactivation of enolase by $NaClO_4$. Enolase (1.06 μM) was incubated in 0.3 M $NaClO_4$ with 5 mM $Mg(OAc)_2$. The deviations of the average value from the individual values are less than 1.5%.

with increasing concentrations of 2PGA and reaches a minimum at about 0.8 M 2PGA. Binding of the substrate not only enhances the interactions among the active site residues, but also promotes the formation of a series of hydrogen bonds between the side chains of the secondary elements (Zhang, et al. 1997). Therefore, the enzyme complex possesses a more compact conformation and exhibits higher ability to resist the inactivation by sodium perchlorate.

3.2 Effects of $NaClO_4$ on inactivation of enolase in the absence and presence of 2PGA

3.2.1 Holo-enolase

Fig.3.3 shows that the inactivation of holo-enolase increases with concentrations of $NaClO_4$. The presence of the substrate efficiently protects the enolase and shifts the curve to the right by around 0.1 M $NaClO_4$. In the absence of 2PGA, the holo-enolase lost 50% activity at 0.32 M $NaClO_4$ and lost all activity at 0.5 M $NaClO_4$. In the presence of 2PGA, about 0.42 M $NaClO_4$ was needed to reach 50% inactivation and 0.6 M $NaClO_4$ was needed to reach 100% inactivation.

3.2.2 Apo-enolase

Apo-enolase is the enzyme free of divalent metal ions. Apo-enzyme was prepared by dialysis and filtration of the enzyme through a chelex100 column according to the procedure described in Methods 2.2.3. Fig. 3.4 shows that a much lower concentration of $NaClO_4$ was

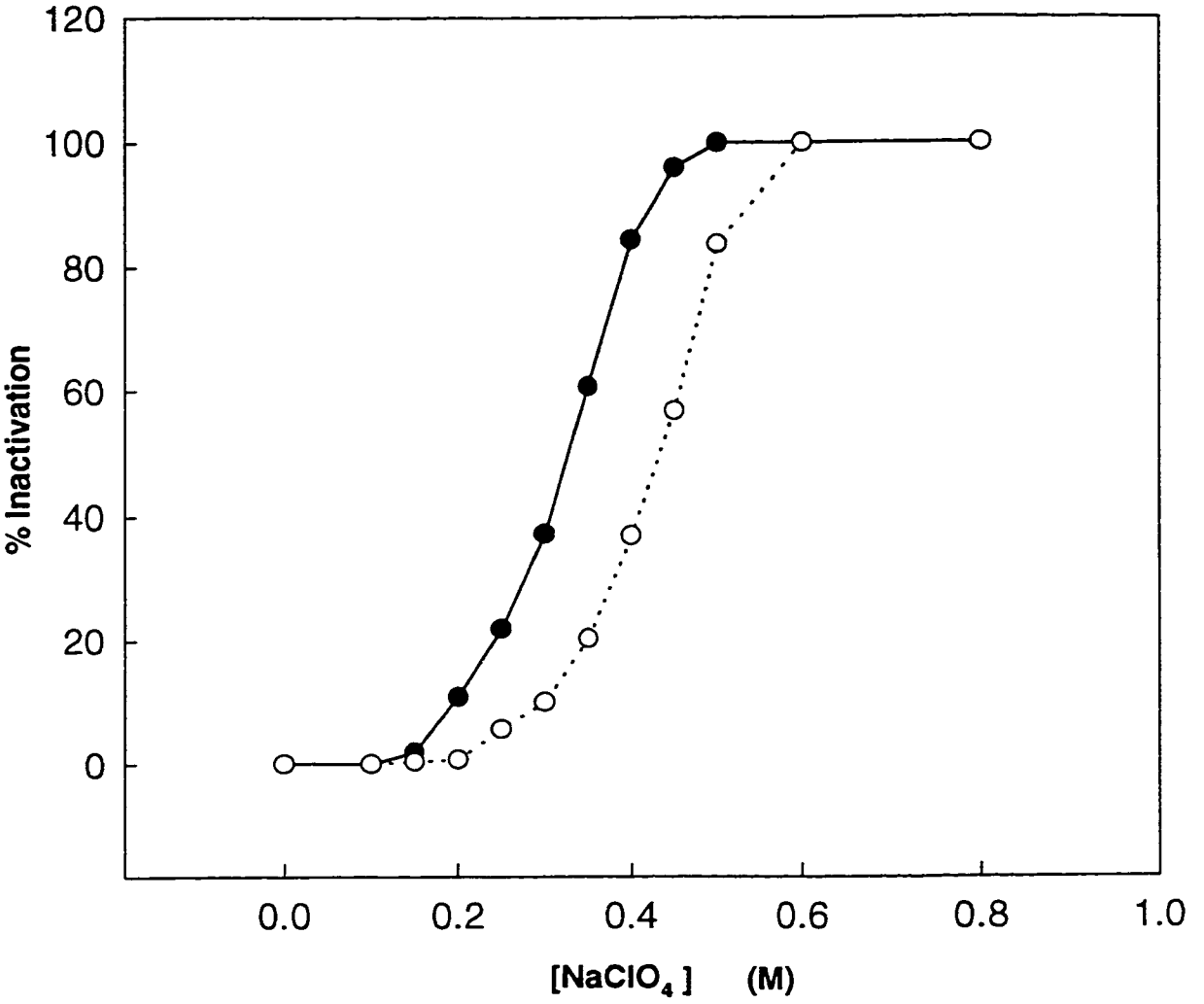

Fig. 3. 3 Effect of [$NaClO_4$] on inactivation of holo-enolase.

1.06 μM enolase was incubated in 5 mM $Mg(OAc)_2$ with (··O·) or without (—●—) 1 mM 2PGA.The deviations of the average value from the individual values are less than 3.0%.

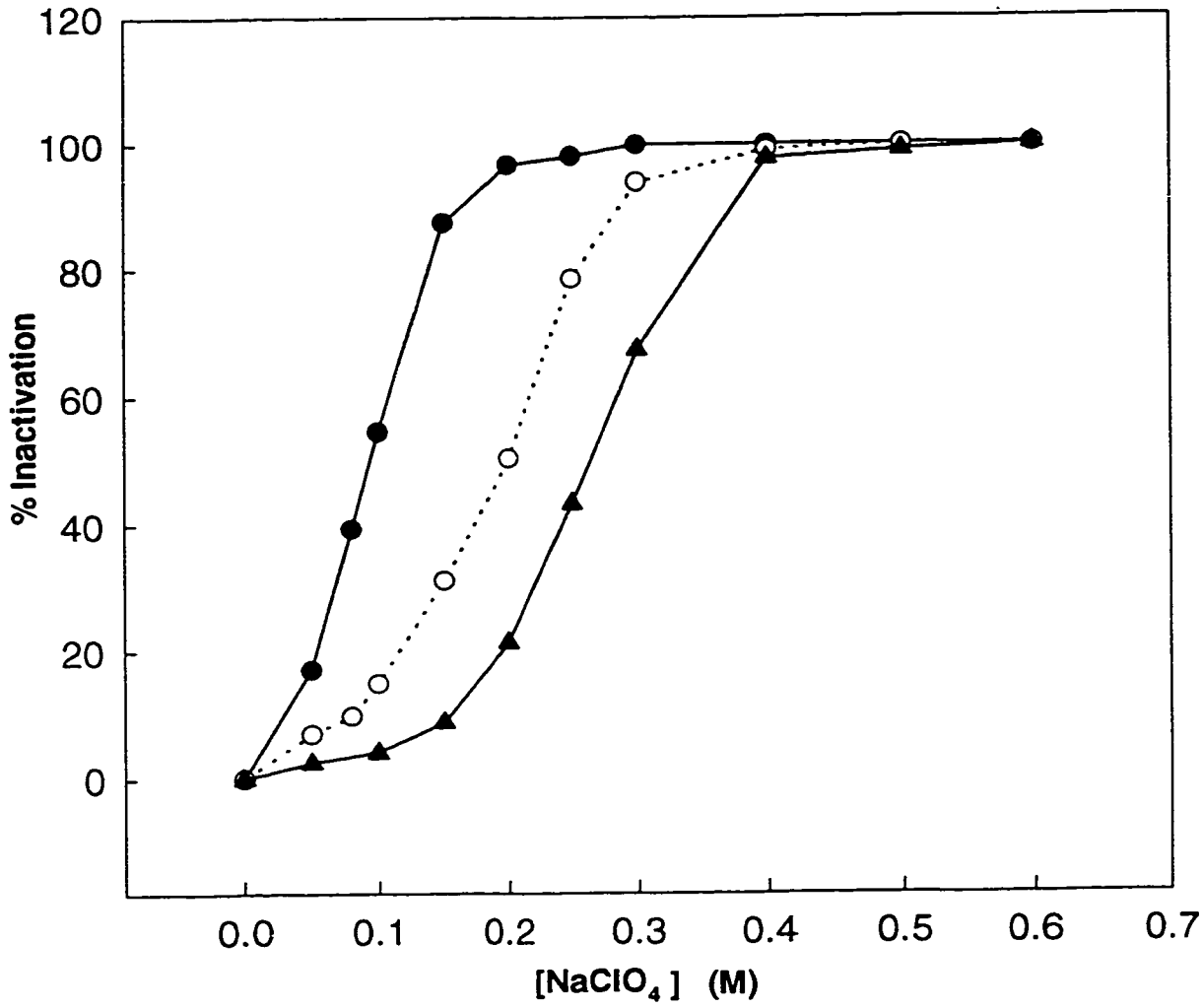

Fig. 3. 4 Effect of [$NaClO_4$] on inactivation of apo-enolase in the absence and presence of 2PGA. 1.06 μM enolase was incubated in 0.1 M $NaClO_4$ in the absence (—●—) and presence (··○··) of 1 mM 2PGA, or in the presence of 5 mM $Mg(OAc)_2$ (—▲—). The deviations of the average value from the individual values are less than 5.0%.

needed to achieve the same extent of inactivation of the apo-enolase as that of the holo-enolase. Inactivation increased to 50% at 0.1 M $NaClO_4$, and 100% at 0.2 M $NaClO_4$. In the absence of divalent metal ions, the conformation of apo-enolase appears to be more exposed to the solvent, and thus, the apo-enzyme exhibits much higher sensitivity to $NaClO_4$.

The apo-enolase is protected by the substrate. This is surprising since the binding of the conformational metal ion is necessary for the binding of the substrate; the substrate cannot bind to the enzymes without the binding of the first divalent metal ion. 2PGA was supposed to have no affect on the apo-enolase. The results in Fig. 3.4 show however, that the apo-enolase with 2PGA is more stable than the apo-enolase alone, though it is less stable than the holo-enolase. To achieve 50% inactivation, the concentration of $NaClO_4$ needed in the incubation is 0.1 M for the apo-enolase, 0.2 M for the apo-enolase with 1 mM 2PGA and 0.26 M for the apo-enolase with 5 mM $Mg(OAc)_2$.

3.2.3 Effect of 2PGA on inactivation of apo-enolase by $NaClO_4$

Fig. 3.5 shows that the percentage inactivation of apo-enolase incubated in a 0.1 M $NaClO_4$ as a function of varying concentrations of 2PGA. With a higher concentration of 2PGA, lower inactivation is achieved by $NaClO_4$. The protection of the apo-enolase from inactivation is significantly increased at the concentrations of 2PGA from 10 μM to 2 mM. 2PGA does interact with the apo-enzyme and provides protection.

There are three possibilities that could contribute to the protection of apo-enzymes by the substrate. The first possibility is that it might be due to contamination from the preparation of apo-enzyme or metal-free solutions. The small amount of trace divalent metal

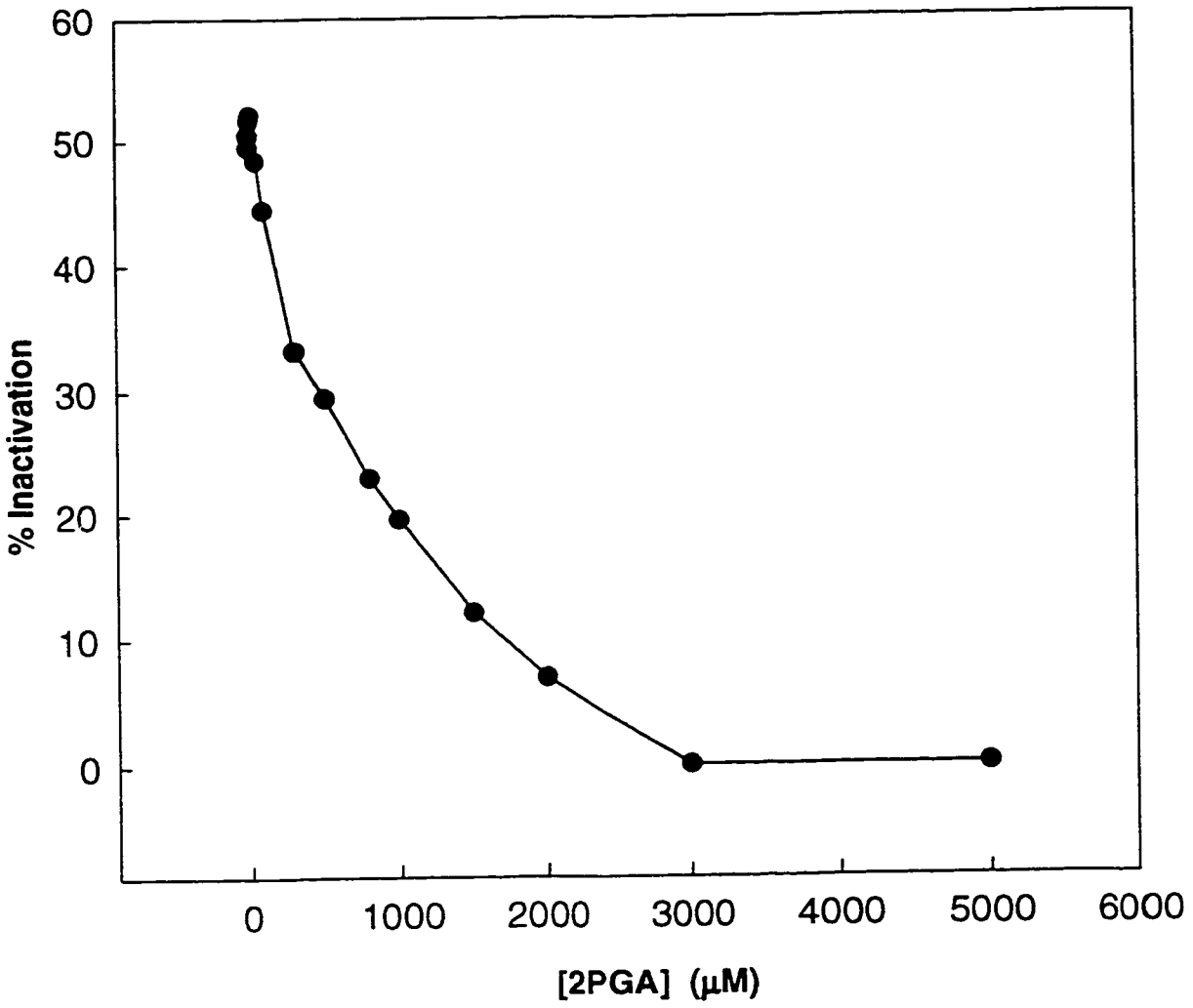

Fig. 3. 5 Effect of [2PGA] on inactivation of apo-enolase by $NaClO_4$. 1.06 μM apo-enolase was incubated in 0.1 M $NaClO_4$ with varying concentrations of 2PGA.The deviations of the average value from the individual values are less than 3.0%.

ions in the incubations permit the binding of the substrate and protect the enzymes from inactivation. The second possibility is that the substrate can directly bind to the enzyme without any ions and provide the protection. The third possibility is that there are metal ions in the incubations that behave as divalent metal ions. They can also bind to the apo-enzyme and promote the binding of the substrate. The metal ion would be Na^+, since sodium perchlorate was used to inactivate the enzyme.

To examine the first possibility, the effects of trace metal ions on the inactivation of the apo-enolase were investigated.

3.3 Effects of trace metal ions on protection of apo-enolase by 2PGA

Enolase can bind to most divalent metal ions. The commercial enolase sources are originally produced with its physiological cofactor, Mg^{2+} and might also contain other divalent metal ions in the conformational site I, which is located in the deep end of the α/β barrel of the C-terminal domain. The presence of the trace metal ions in the apo-protein sample is of concern. In order to eliminate the effects of these trace metal ions, two chelating reagents were chosen to be added into the incubations. ICP-mass spectra were also performed on the apo-enolase and the chelex-treated buffer samples to identify the trace metal ions.

3.3.1 Protection by 2PGA in the presence of selected chelating reagents

EDTA, EGTA and o-phenathroline are chelating reagents which have high affinity for most divalent metal ions. Table 3.1 shows the binding constants of these chelating reagents to certain divalent metal ions. One mM of EDTA, EGTA and o-phenathroline were added to

the incubations of apo-enolase, respectively. The inactivation of apo-enolase by 0.1 M $NaClO_4$ in the absence and presence of 1 mM 2PGA was examined and is shown in Fig.3.6. Addition of EDTA and EGTA to the incubations slightly decreased the protection of apo-enolase provided by 2PGA, but did not eliminate the protection. Substantial protection can still be obtained in the presence of 2PGA. Apo-enolase with 2PGA was inactivated by about 15% less than the apo-enolase without 2PGA. O-phenathroline appears to have other effects on apo-enolase, since it shows higher protection than that apo-enolase with 2PGA alone, which we cannot explain.

3.3.2 ICP- mass spectrometry trace metal analysis

In order to identify the trace metal ions, inductively coupled plasma (ICP) mass spectrometry was applied to the apo-enolase sample and the chelex-treated buffer. ICP is a sensitive and accurate (high resolution) technique that is used to detect small amount of trace metal ions in the solution. In ICP, the atoms are generated and excited by a plasma torch with high temperature, and mass spectra are recorded on the ionized atoms (Robinson, 1996). Results from the ICP analysis are summarized in Table 3.2. The buffer used for the incubations of apo-enolase was metal free, but the protein sample did contain certain trace metal ions. The contamination of the apo-enolase came from the trace metal ions of Zn^{2+}, Cu^{2+} and Ni^{2+}. Mg^{2+} had little effect, since it only existed in less than 2% of the active sites. The signal of Ca^{2+} is overlapped by that of argon ions, thus, the amount of Ca^{2+} could not be estimated. However, the trace of Zn^{2+}, Cu^{2+} and Ni^{2+} was estimated to totally occupy about 25-30% of the active sites, which might contribute to the protection of the apo-enolase from

Table 3.1 Affinity of the Chelating Reagents to Certain Divalent Metal Ions			
Log K values[a] (Equil. : ML/M.L)	EDTA (25 °C , 0.1 [b])	EGTA (25 °C , 0.1)	o-phenanthroline (25°C, 0.1)
Mg^{2+}	8.85	5.28	1.20
Ca^{2+}	10.65	10.86	0.70
Ba^{2+}	7.86	8.30	—[c]
Zn^{2+}	16.50	12.60	6.40
Mn^{2+}	13.88	12.18	4.00
Fe^{2+}	14.30	11.80	5.85
Co^{2+}	16.45	12.35	7.08
Ni^{2+}	18.40	13.50	8.60
Cu^{2+}	18.78	17.57	7.40
Cd^{2+}	16.50	16.50	5.80
Cr^{2+}	13.60	—[c]	—[c]
Sr^{2+}	8.74	8.43	—[c]
Hg^{2+}	21.50	22.90	19.65
Pb^{2+}	18.00	14.54	4.65

a. Smith and Martell, 1989; b. Ionic strength; c. Not obtained.

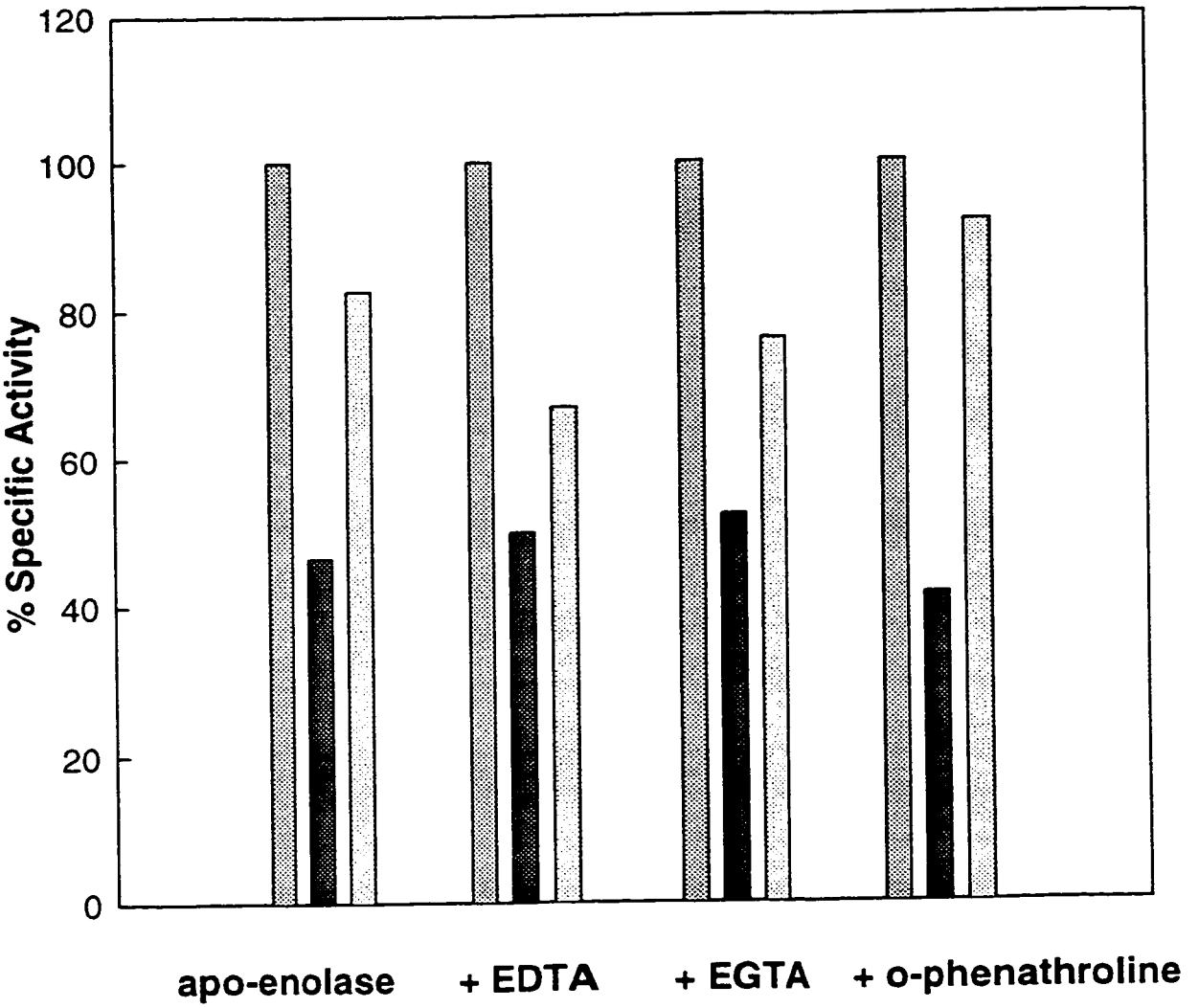

Fig. 3. 6 Protection of apo-enolase by 2PGA in the presence of chelating reagents. 1.06 μM apo-enolase alone ( ), apo-enolase in the 0.1 M $NaClO_4$ without ( ) or with ( ) 1 mM 2PGA were incubated in the absence and presence of 1 mM EDTA, 1 mM o-phenathroline or 1 mM EGTA, respectively. Data are the average values from the triplicate assays.The deviations of the average value from the individual values are less than 2%.

Table 3.2 Inductively Coupled Plasma - Mass Spectrometry Metal Trace Analysis[a]							
Metals	**Intensity** (Standard) 1 ppb	**Intensity** (Stsndard) 10 ppb	**Intensity** (Standard) 100 ppb	**Intensity** of buffer	**Intensity** of enolase	**[Metal]** (ppb)	**% active sites**
Ca	1804	1748	5988	768	1762	—[b]	—[b]
Zn	0	0	14503	363	3013	21[c]	12
Cu	0	6823	99243	0	7773	8-12[c]	5-8
Ni	468	4270	45086	0	2040	5	3
Mg	1181	8305	82035	56	908	1	1.5
Hg	503	2833	25853	354	665	1.6	0.3
Sr	2042	19786	201260	252	459	0.3	0.2
Mn	1989	19964	203640	0	228	0.1	0.1
Co	1823	19177	195490	0	371	0.5	0.1
Cd	216	2192	22366	12	29	0.2	0.1
Cr	1334	13248	138520	0	0	0	0
Ba	2033	20373	206660	0	0	0	0
Be	118	1128	11416	3	5	0	0
Pb	2288	23655	241390	0	0	0	0
Total	—	—	—	—	—	38-42	23-26

a. ICP samples were prepared by ashing 25 mL of apo-enolase (0.26 mg/mL) and 25 mL chelex-treated MT buffer and then diluting them with 5% HNO_3 to 50 mL, respectively; b. Intensity of Ca^{2+} is overlapped by that of argon ions, therefore, the amount of Ca^{2+} could not be estimated; c. Since the intensities of the standards were not linear, the amount of the metal ions was estimated by simply multiplying its intensity to the ratio of the intensity of the standard and the concentration of the standard.

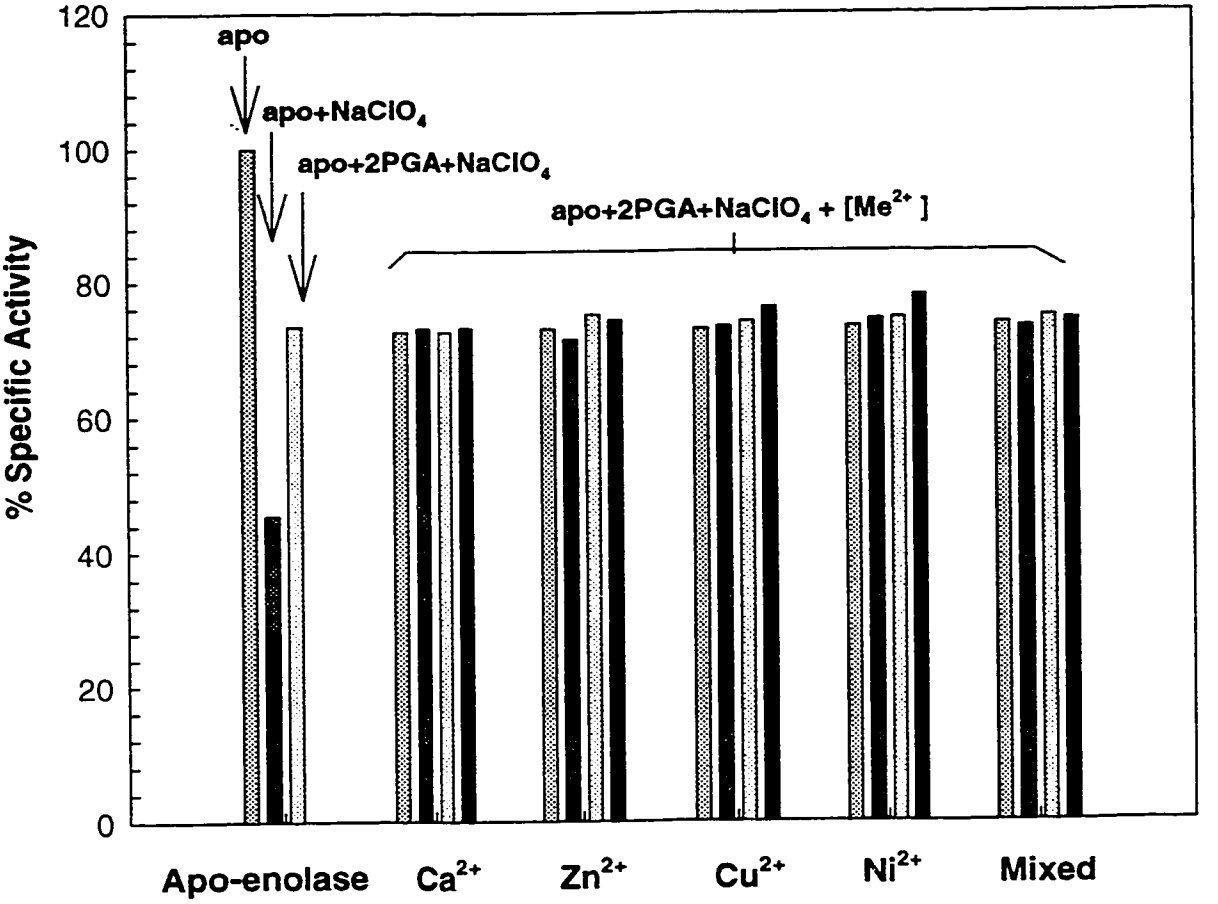

Fig. 3. 7 Effects of trace metal Ions on inactivation of apo-enolase by $NaClO_4$. 1.06 μM enolase was incubated in 0.1 M $NaClO_4$ in the presence of 1 mM 2PGA and 0.1 mM EDTA with varying concentrations of Ca^{2+}, Zn^{2+}, Cu^{2+}, Ni^{2+} and a mixture of these four metal ions, respectively, from 0.5 μM (▨), 1.0 μM (■), 2.0 μM (▭) to 5.0 μM (■). Data are the average values of the triplet assays. The deviations of the average values are less than 3%.

the inactivation by $NaClO_4$.

To estimate the effects of these trace metal ions, varying concentrations of these metal ions and their mixtures of Ca^{2+}, Zn^{2+}, Cu^{2+} and Ni^{2+}, respectively, from 0.5 μM (which was equal to about 50% of the active sites) to 5.0 μM (equal to about 250% of the active sites), were added to the incubations in the presence of 0.1 mM EDTA. Under this concentration of EDTA, the concentration of $EDTA^{4-}$ which chelates the divalent metal ion as the binding constants shows, was around 0.1 μM (Bell, 1977; Martell and Calvin, 1955). Therefore, there were always free divalent metal ions in excess in the incubations where 0.5 - 5.0 μM of trace metal ions were added. No substantially higher protection was observed beyond what was obtained for the apo-enolase with 2PGA alone, even in the presence of 5.0 μM trace metal ions (shown in Fig.3.7). Therefore, these trace metal ions do not account for the protection of apo-enzyme provided by 2PGA. To minimize the effects of the trace metal ions, the following incubation experiments were set up in the presence of 0.1 mM EDTA.

3.4 Effects of Na^+ on the protection of apo-enolase by 2PGA

The trace metal ions do not protect the apo-enolase from inactivation by $NaClO_4$. Therefore, it is crucial to determine whether the sodium cation is necessary for the protection of the apo-enzyme against inactivation, so as to examine the second possibility that the substrate can bind to the enzyme without any metal ion.

3.4.1 Necessity of Na^+ for protection of apo-enolase by 2PGA

TMA-ClO_4 (tetramethylammonium perchlorate) was chosen to replace $NaClO_4$ in the

incubations. TMA^+ would not be expected to bind to the enzyme in the active site, because its size is large compared to that of Na^+. But the solubility of TMA-ClO_4 in MT buffer is rather low, so the temperature of the incubation was decreased to 0°C in order to achieve a particular range of inactivation. (Inactivation is enhanced by a lower temperature). Table.3.3 shows that apo-enolase inactivated by 0.04 M $NaClO_4$ was protected by 1 mM 2PGA, while apo-enolase incubated in the same concentration of TMA-ClO_4 was not protected by the substrate. Thus, the presence of sodium ions is necessary for the protection of the apo-enzyme. 2PGA alone does not show any protection.

Table 3.3 Necessity of Na^+ on protection of apo-enolase from inactivation

Samples [a]	Relative activity (%) [b]
Apo-enolase alone	100
+ 0.04 M $NaClO_4$	33.2
+ 0.04 M $NaClO_4$ + 1 mM 2PGA	56.4
+ 0.04 M TMA-ClO_4	44.7
+ 0.04 M TMA-ClO_4 + 1 mM 2PGA	45.0

a. Apo-enolase was incubated in 0.04 M $NaClO_4$ (or 0.04 M TMA-ClO_4) with 0.1 mM EDTA in the absence and presence of 1 mM 2PGA at 0°C for 24 hrs; b. Data are the average values of triplicate assays. The deviations of the average value from the individual values are less than 3.5%.

3.4.2 [Na^+] dependence of the protection by 2PGA

Apo-enolase was incubated in 0.04 M TMA-ClO_4 with varying concentrations of NaCl (Fig.3.8). Inactivation, in the absence of 2PGA, is independent of the concentration of NaCl. In the presence of 2PGA, protection was dramatically increased by increasing concentrations of NaCl (from 5 mM to 40 mM). The sodium ion is an inhibitor of both yeast and rabbit muscle enolase. It can bind to the enzyme and inhibit at least one step in the mechanism (Kornblatt and Musil, 1990). The interaction between Na^+ and the apo-enzyme might affect the active site structure and facilitate the binding of the substrate. However, the affinity of this binding appears to be very low, since a relatively high concentration of Na^+ is required for the protection of apo-enolase by 2PGA.

The effect of Na^+ was also investigated through the incubation of apo-enolase in 0.1 M Tris-ClO_4. Fig.3.9 shows that higher protection is achieved at a higher concentration of NaCl, which is consistent with the result in section 3.4.2. It is confirmed again that the sodium ion is crucial for the protection of apo-enzyme from the inactivation. Apo-enolase appears to be more sensitive to Tris-ClO_4 than to $NaClO_4$, which might be attributed to the interaction of the apo-enolase with the Tris base (Brewer, et al., 1978; Musil, 1992).

3.5 Spectral characterization of the binding of 2PGA to apo-enolase-Na^+ complex

In order to investigate the structural change of the apo-enolase upon binding of the substrate in the presence of sodium cations, fluorescence and near-UV CD spectroscopies were applied to the apo-enolase samples.

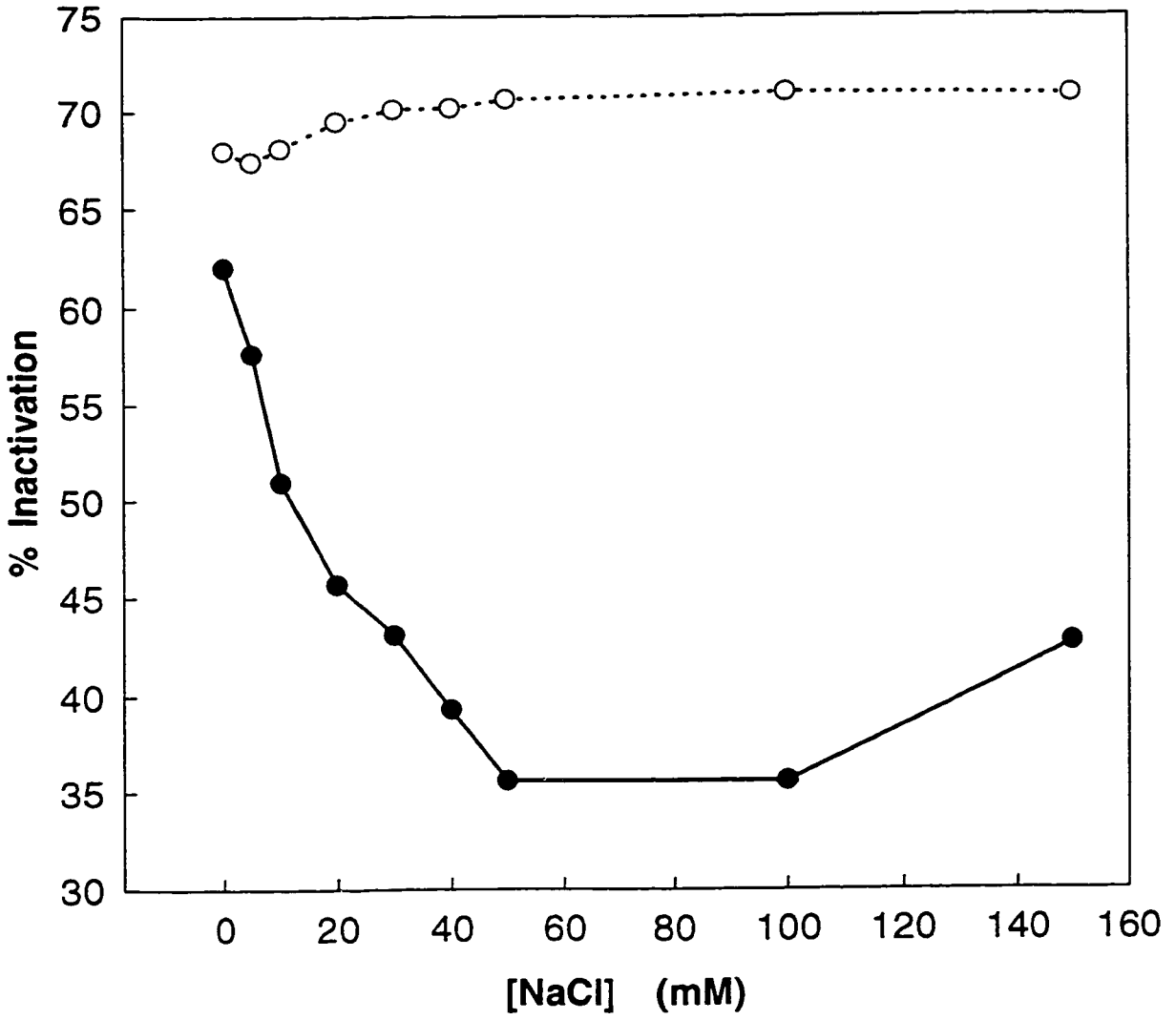

Fig. 3. 8 Effect of sodium ions on inactivation of apo-enolase by TMA-ClO_4. 1.06 μM apo-enolase was incubated in 0.04 M TMA-ClO_4 with 0.1 mM EDTA in the absence (—●—) and presence (-·○·-) of 3 mM 2PGA at 0°C for 24 hrs. The deviations of the average value from the individual values are less than 3.5%.

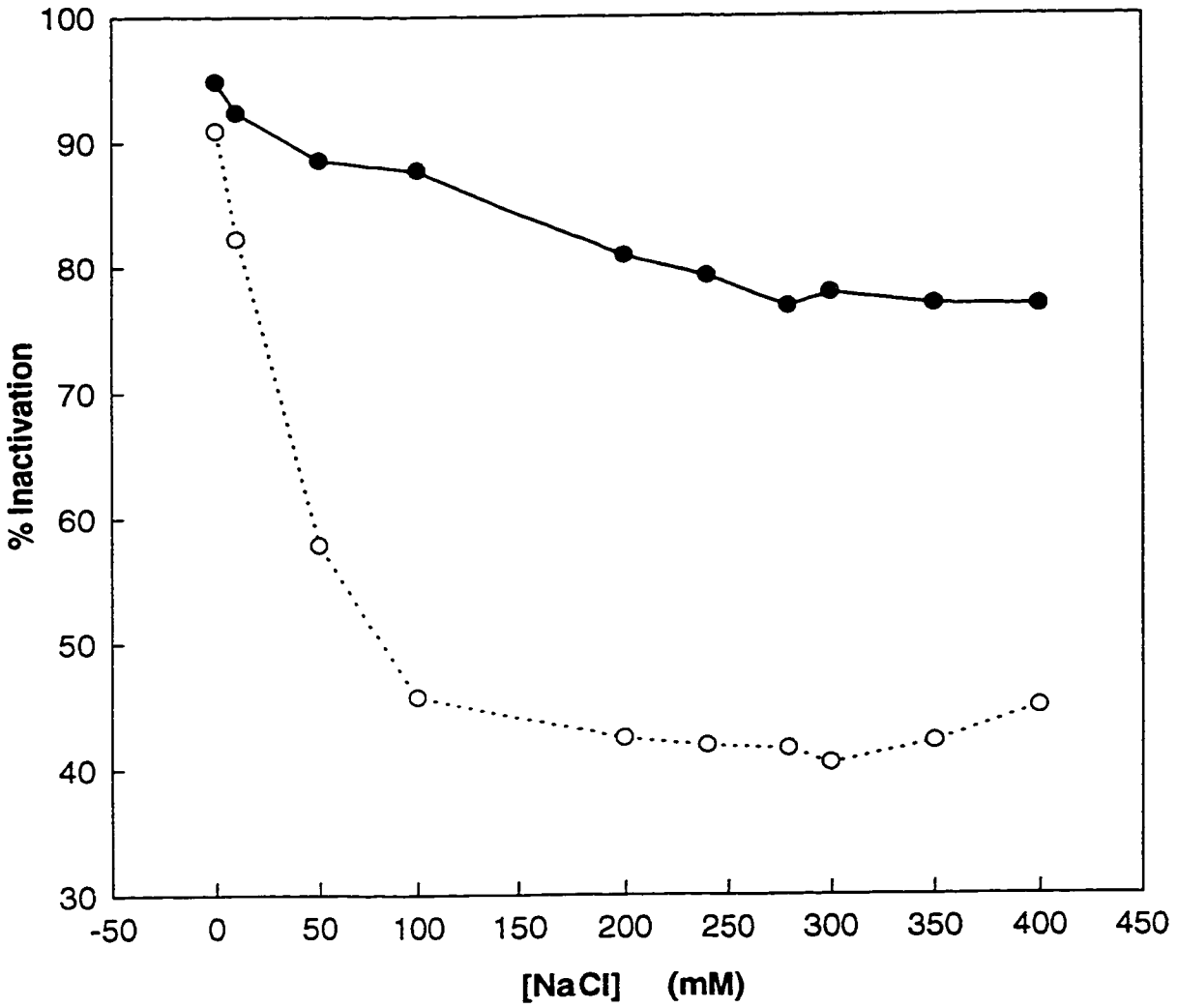

Fig. 3. 9 Effect of sodium ions on inactivation of apo-enolase by Tris-ClO_4. 1.06 μM apo-enolase was incubated in 0.1 M Tris-ClO_4 with 0.1 mM EDTA in the absence (—●—) and presence (··o··) of 3 mM 2PGA. Data are the average values of duplicate assays. The deviations of the average value from the individual values are less than 3.5%.

3.5.1 Trp fluorescence spectroscopy

The emission spectrum at excitation wavelength 295 nm is only attributed to the tryptophan residues (Chen, 1990). The change in the tryptophan fluorescence indicates the differing environments of the tryptophan residues. The tryptophan fluorescence spectrum obtained on 1.06 μM of apo-enolase has a maximum emission at 334 nm as shown in Fig.3.10. No significant change in fluorescence is observed in the apo-enolase upon the addition of 1 mM 2PGA, while in the presence of 0.08 M NaCl, a small but substantial increase occurs upon the addition of the substrate. There is no shift in λ_{max}, but the fluorescence intensity at 334 nm is increased from 280.3 to 294.2 (about 5% increase in I_{max}). The binding of the substrate to the apo-enolase potentiated by sodium ions results in a conformational change that alters the average environment of the tryptophan residues to a less quenching environment. A similar conformational change has also been observed in the holo-enolase upon the binding of the substrate (about 20% increase in I_{max}) (Fig. 3.11).

3.5.2 Near-UV CD spectroscopy

The binding of the substrate to apo-enolase was also investigated by near-UV CD spectra (255-340 nm) which reflects the contributions of aromatic side chains and disulfide bonds (Woody and Dunker, 1996). The difference in near-UV CD spectra provides useful information on the conformational change in the protein. As shown in Fig.3.12, the near-UV CD spectrum of apo-enolase is characterized by two peaks at 290 nm and 297 nm, two troughs at 285 nm and 278 nm, and two small shoulders at 263 nm and 259 nm. The signal above 290 nm is attributed to the tryptophan residues; the signals at 285 nm and 278 nm are

Fig. 3.10 Trp Fluorescence of the binding of 2PGA to apo-enolase in the presence of sodium ions. Fluorescence spectra of 1.06 μM apo-enolase in (A) MT buffer containing 0.08 M NaCl and 0.1 mM EDTA (pH 7.1), and in (B) MT buffer containing 0.1 mM EDTA (pH 7.1), were taken at 25°C with excitation 295 nm, excitation bandwidth 2 nm, emission bandwidth 4 nm and scan rate 1 nm/sec in the absence (▲) and presence (●) of 1 mM 2PGA.

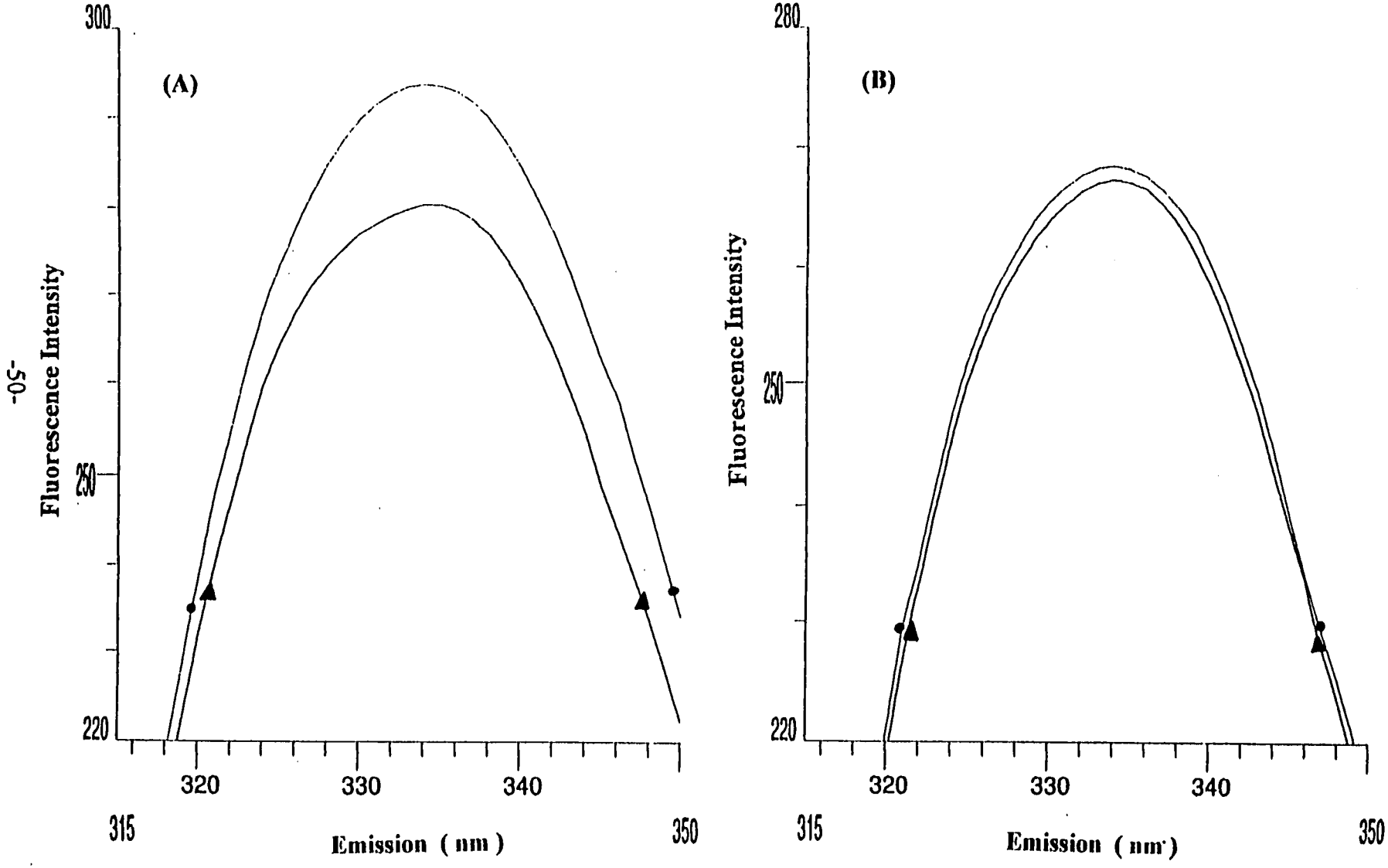
(A)
300
250
220
Fluorescence Intensity
315
320
330
340
350
Emission (nm)
(B)
280
250
220
Fluorescence Intensity
315
320
330
340
350
Emission (nm)

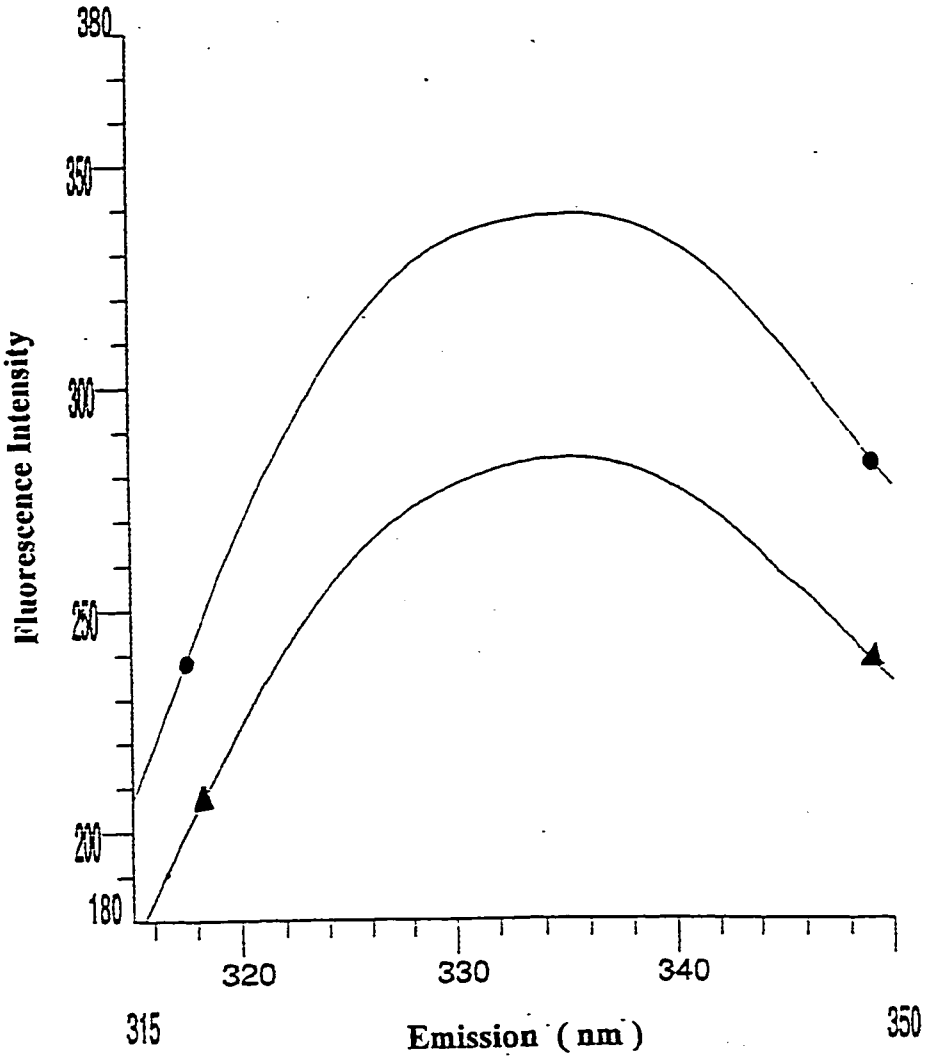

Fig. 3. 11 Trp Fluorescence of the binding of 2PGA to holo-enolase

Spectra of 1.06 μM apo-enolase in MT buffer (pH 7.1) with 0.3 M NaCl were taken at 25°C with excitation 295 nm, excitation bandwidth 2 nm, emission bandwidth 4 nm and scan rate 1 nm/sec in the absence (▲) and presence (●) of 1 mM 2PGA and 1 mM $Mg(OAc)_2$.

Fig. 3.12 Near-UV CD spectra of the binding of 2PGA to apo-enolase in the presence of sodium ions. The near-UV CD spectra of 10.6 μM apo-enolase in (A) MT buffer containing 0.3 M NaCl and 0.1 mM EDTA (pH 7.1), and in (B) MT buffer containing 0.3 M TMA-Cl with 0.1 mM EDTA (pH 7.1), were taken at 25 °C with bandwidth 1.0 nm, scan speed 100 nm/min, response time 0.25 s and step resolution 0.2 nm in the absence (——) and presence (- - - -) of 1 mM 2PGA. Fifteen scans were collected and averaged for each spectrum.

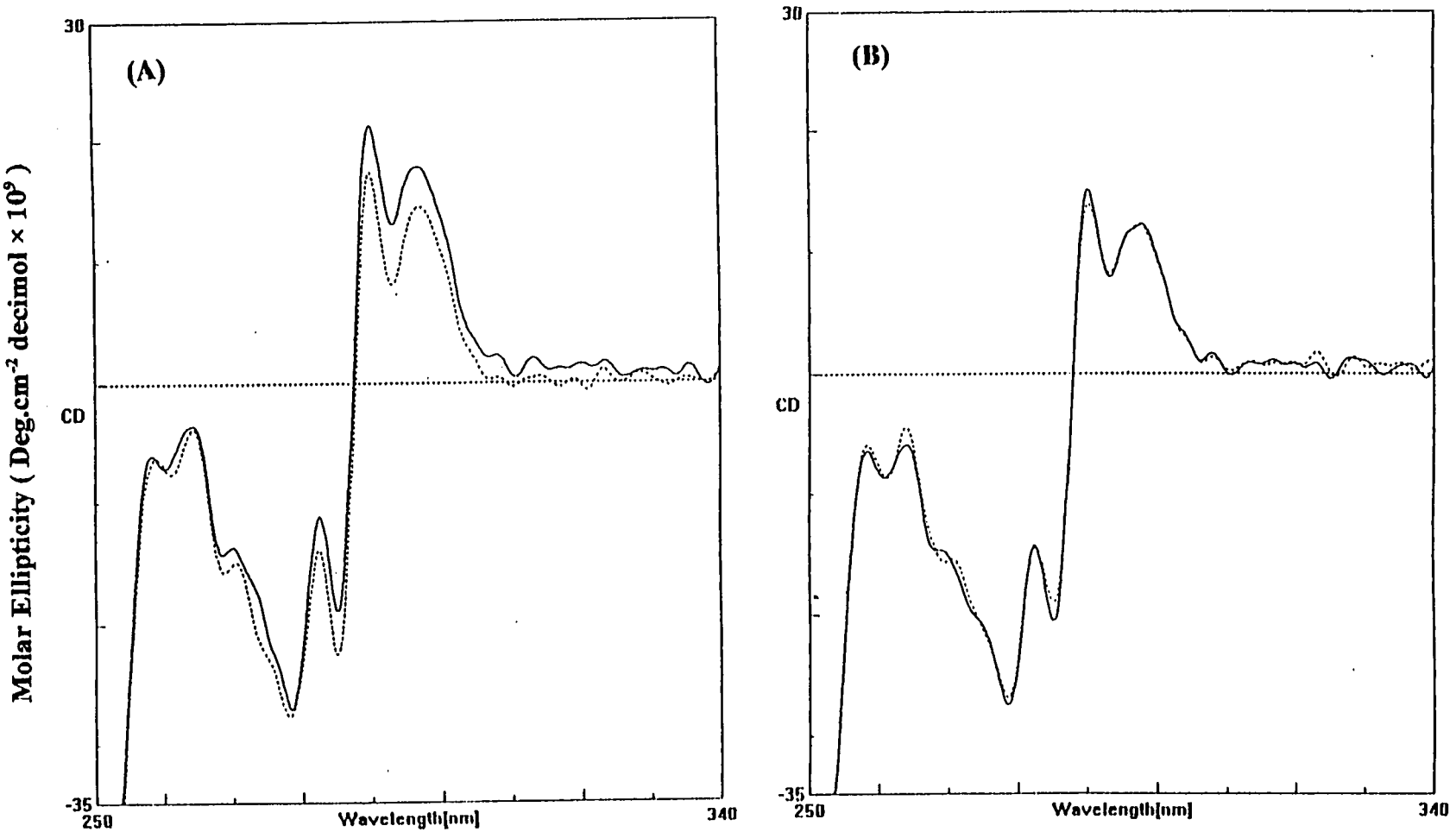
Molar Ellipticity (Deg.cm^{-2} decimol × 10^{9})
(A)
30
CD
-35
250
Wavelength[nm]
340
(B)
30
CD
-35
250
Wavelength[nm]
340

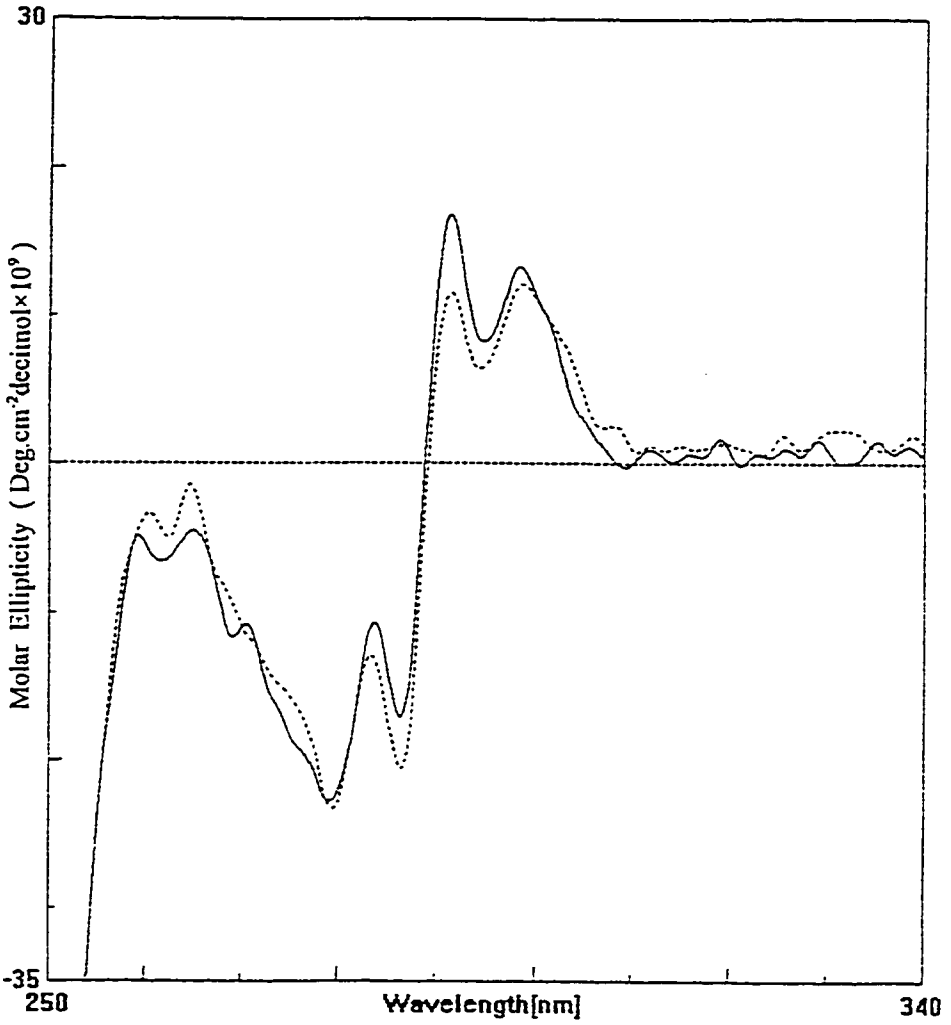

Fig. 3. 13 Near-UV CD spectra of the binding of 2PGA to holo-enolase

The near-UV CD spectra of 10.6 μM enolase in MTME buffer (pH 7.1) were taken at 25 °C with bandwidth 1.0 nm, scan speed 100 nm/min, response time 0.25 s and step resolution 0.2 nm in the absence (——) and presence (- - - -) of 1 mM 2PGA. Fifteen scans were collected and averaged for each spectrum.

generated by both the tryptophan and tyrosine residues; the shoulders at 263 nm and 259 nm are due to the phenylalanine residues. The addition of 1 mM 2PGA results in no substantial change in the spectra of the apo-enolase in 0.3 M TMA-Cl (TMA-Cl was used as an ionic strength control), whereas, an unambiguous change is observed in the spectra of apo-enolase in 0.3 M NaCl. The ellipticity decreases in the region from 282 nm to 297 nm, indicating that the average environment of the tryptophan and tyrosine residues becomes more symmetric. Holo-enolase also undergoes a similar conformational change upon the substrate binding (shown in Fig.3.13).

3.6 Effects of other monovalent cations on inactivation of apo-enolase by TMA-ClO_4

Effects of the other monovalent cations such as K^+ , Li^+ and NH_4^+ on the inactivation of apo-enolase by 0.04 M TMA-ClO_4 with or without 2PGA are shown in Table 3.3. Two concentrations of these monovalent cations (all in the form of chloride salts) were used in the incubations. In the presence of 2PGA, apo-enolase incubated with K^+ or NH_4^+ shows an identical degree of inactivation as the enzyme without monovalent cations. 2PGA does not provide substantial protection to the apo-enolase with K^+ and NH_4^+. Apo-enzyme incubated with Li^+ exhibits a percentage inactivation similar to that of the enzyme incubated with Na^+ when 2PGA is present. Interestingly, the enzyme with Li^+ is less inactivated in the absence of 2PGA than in the presence of 2PGA. Li^+ appears to protect the apo-enolase from the inactivation.

Table 3. 4 Effects of other monovalent ions on inactivation of apo-enolase by TMA-ClO_4 in the absence and presence of 2PGA[a]

Me^+	[Me^+] (mM)	% Inactivation [c] - 2PGA	% Inactivation [c] + 2PGA
no addition	— [b]	68.0	62.0
Na^+	30	70.1	43.1
	100	71.0	35.6
Li^+	30	25.2	37.4
	100	18.3	39.9
K^+	30	63.7	61.0
	100	68.3	62.4
NH_4^+	30	66.2	60.4
	100	65.8	59.1

a. 1.06 μM enolase was incubated in 0.04 M TMA-ClO_4 and 0.1 mM EDTA at 0°C for 24 hrs in the absence (- 2PGA) and presence (+ 2PGA) of 2 mM 2PGA; b. No addition of monovalent ions; c. Data are the average values of triplicate assays. The deviations of the average value from the individual values are less than 3.0%.

3.7 Relationships between inactivation, dissociation and denaturation of apo-enolase incubated in $NaClO_4$

3.7.1. Cross-linking and SDS-PAGE

To determine whether the dissociation occurs when the apo-enolase is inactivated by $NaClO_4$ and whether the dissociation is prevented by 2PGA, gluataraldehyde was used to link the dimeric enzyme through lysine residues in the adjacent monomers. SDS-PAGE was performed on the crosslinked samples. Because SDS will not dissociate the crosslinked enzyme, the crosslinked enzyme can be separated from the uncrosslinked and denatured monomers in the polyacrylamide gel according to their molecular weights. Apo-enolase samples were incubated at different concentrations of $NaClO_4$ in the absence and presence of 2PGA and then were crosslinked by gluataraldehyde. Three major bands were observed in the polyacrylamide gel (shown in Fig.3.12). The upper two bands represent the crosslinked enzyme. The lower band represents a mixture of uncrosslinked enzyme, since not all the dimeric enzyme is efficiently crosslinked by glutaraldehyde. After incubation with $NaClO_4$ (lanes 2 and 4), the bands of crosslinked enzyme became weaker and a diffuse band which migrated more rapidly than the native monomer appeared in the monomer band region, indicating that dissociation occurs during the inactivation. The diffuse band might be due to the internal crosslinking of the dissociated monomers (Al-Ghanim, 1994). The samples with 2PGA (lanes 3 and 5) showed a stronger band of the crosslinked enzyme and a less diffuse band of the monomeric enzyme. These bands appear to be similar to those of the native enzyme. Thus, 2PGA shifts the equilibrium toward association and prevents the enzyme from dissociation.

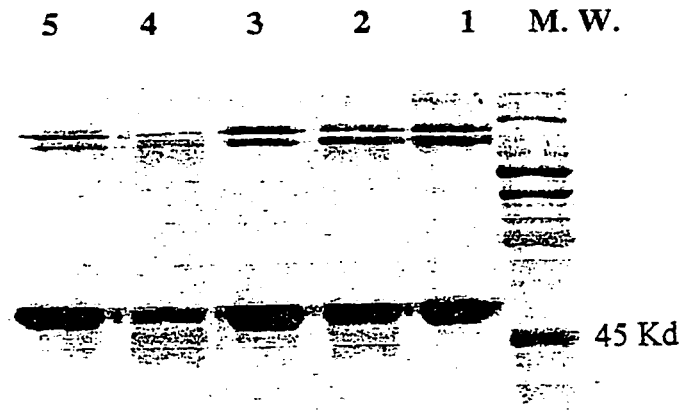

Fig. 3. 14 Crosslinking and SDS-PAGE of apo-enolase incubated in $NaClO_4$ with or without 2PGA. 1.5 μM apo-enolase was incubated in 0.10 M and 0.15 M $NaClO_4$ with 0.1 mM EDTA in the absence and presence of 2 mM 2PGA at 15°C for 24 hrs, followed by crosslinking and SDS-PAGE. Samples: Lane M.W., Molecular Weight Standards (range 45 Kd - 200 Kd); Lane 1, apo-enolase; Lane 2, apo-enolase + 0.10 M $NaClO_4$; Lane 3, apo-enolase + 0.10 M $NaClO_4$ + 2 mM 2PGA; Lane 4, apo-enolase + 0.15 M $NaClO_4$; Lane 5, apo-enolase + 0.15 M $NaClO_4$ + 2 mM 2PGA.

3.7.2 Simulation of the fourth derivative spectra

To determine the degree of dissociation, the fourth derivatives were calculated from the original spectra and the simulation of the actual fourth derivative spectra by proportional combination of the fourth derivative spectra of the dimer and the monomer, were completed according to the method described in section 2.2.7. Fig.3.15 shows the fourth derivative spectra of apo-enolase incubated in varying concentrations of $NaClO_4$ with or without 2PGA. When the concentration of $NaClO_4$ increases from 0 M to 0.5 M, the peaks at 279 nm and 288 nm in the spectrum of apo-enolase decrease to minima, while the troughs at 283 nm and 292 nm shift to maxima, indicating that tyrosine and tryptophan residues are becoming exposed. The presence of 2PGA shifts the positions of the peaks and the troughs toward those of the dimeric enzyme, suggesting the decreased exposure of the aromatic residues. It is confirmed again that the substrate protects the apo-enzyme against dissociation.

The degree of the dissociation was determined by simulation of the actual spectrum. Since no dimers can be observed in the HPLC profile of holo-enolase at 0.5 M $NaClO_4$ (Kornblatt, et al., 1996), it is assume that apo-enolase which is more accessible to $NaClO_4$ than holo-enolase, exists in the monomeric form when incubated in 0.5 M $NaClO_4$. Therefore, the spectra of apo-enolase incubated in 0 M and 0.5 M $NaClO_4$ were used as the spectra of the dimeric and monomeric enolase, respectively. Proportional combination of these two spectra was made to simulate the actual spectrum. Fig.3.16 shows the simulation of the spectra of apo-enolase incubated in 0.18 M $NaClO_4$ with or without 2PGA. It is in good agreement for the actual spectrum of enolase in 0.18 M $NaClO_4$ and the simulated spectrum by a combination of the spectra of 15% dimer and 85% monomer (Fig.3.16 A). The actual

spectrum of enolase with 2PGA in 0.18 M $NaClO_4$ can be simulated for a mixture of 59% dimer and 41% monomer (Fig.3.16 B). The disagreement between this actual spectrum and the simulated one is probably attributed to the conformational change upon the binding of the substrate. A small blue shift and a slight change in intensity have been observed upon the binding of the substrate (data not shown). The degree of the dissociation and the corresponding loss of activity are summarized in Table 3.5. The percentage inactivation of the enzyme is very close to the degree of dissociation, suggesting that the inactivation is highly correlated to the dissociation.

3.7.3 Far-UV CD spectroscopy

Far-UV CD spectra were recorded from the apo-enolase samples incubated in varying concentrations of $NaClO_4$ (Fig.3.17). The far-UV CD spectra of enolase show a double minimum at 209 nm and 222 nm which is characteristic of the α/β protein (Venyaminov and Yang, 1996). At wavelength lower than 208 nm, MT buffer began to significantly contribute to the CD signal. The ellipticity at 222 nm which represents the helical structure of the protein is given in Table 3.5. The enzyme inactivated by $NaClO_4$ (0.10 M - 0.50 M) only slightly decreased the ellipticity at 222 nm compared with the apo-enolase alone, while the enzyme incubated with 2 mM 2PGA maintained a little higher degree of ellipticity. But the difference in the ellipticity at 222 nm of these samples is not significant. It can be concluded that although the enzymatic activity has been dramatically decreased, $NaClO_4$ at the applied concentrations does not affect the secondary structure of the apo-enolase.

Fig. 3.15 The fourth derivative spectra of apo-enolase incubated in varying concentrations of $NaClO_4$. 1.5 μM apo-enolase was incubated in 0.1 mM EDTA plus (A) 0.1 M, (B) 0.15 M, or (C) 0.18 M $NaClO_4$ with (●) or without (▲) 2 mM 2PGA. Apo-enolase alone is represented by a solid line and apo-enolase incubated in 0.5 M $NaClO_4$ is expressed by a dashed line.

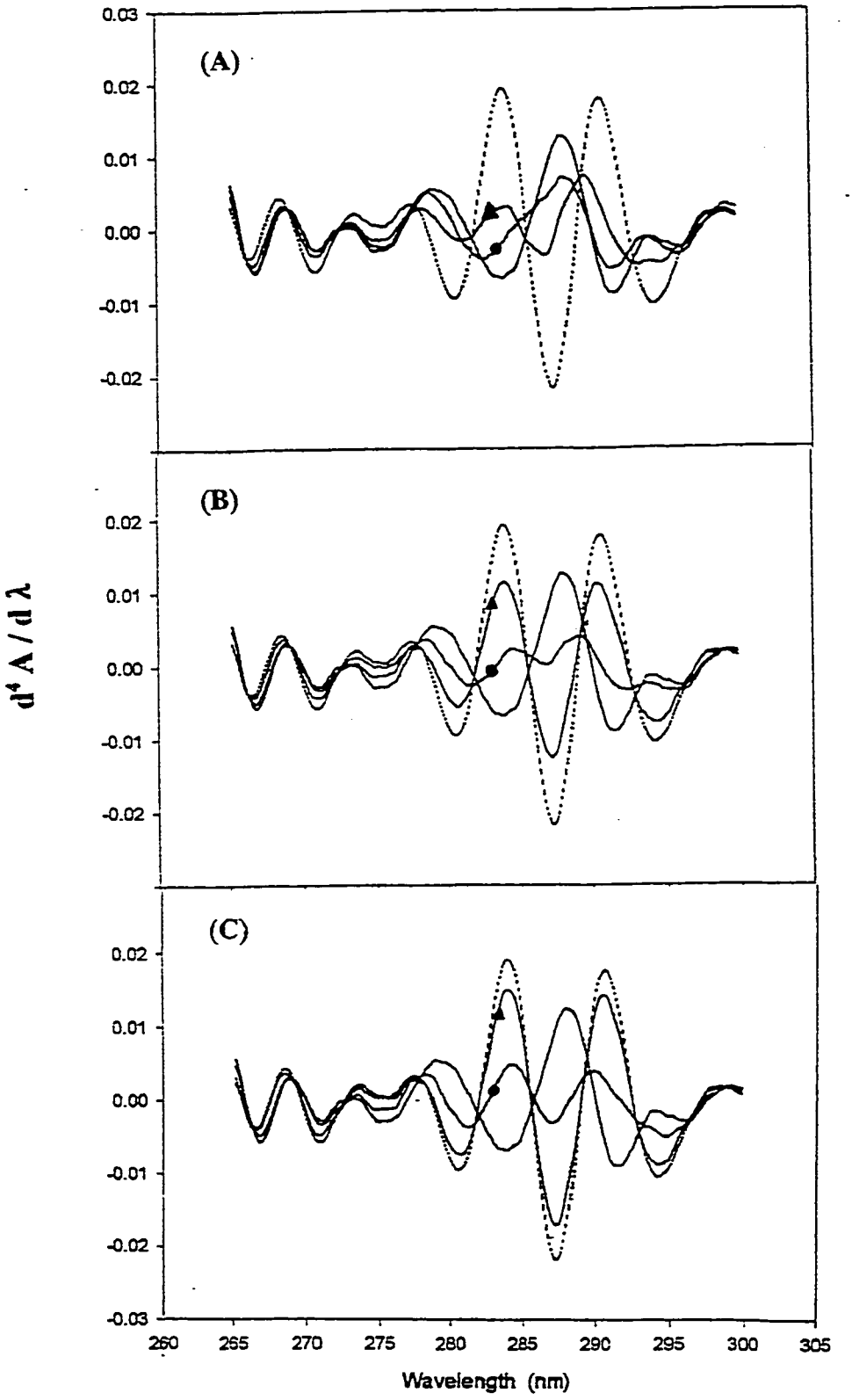
(A)
(B)
(C)
0.03
0.02
0.01
0.00
-0.01
-0.02
-0.03
260
265
270
275
280
285
290
295
300
305
Wavelength (nm)
d⁴ A / d λ

Fig. 3.16 Simulation of the fourth derivative spectra of apo-enolase incubated in 0.18 M $NaClO_4$ with or without 2PGA. (A) the actual spectrum of apo-enolase incubated in 0.18 M $NaClO_4$ (——) and the simulated spectrum by a combination of the spectra of 15% dimer and 85% monomer (- - - -); (B) the actual spectrum of apo-enolase incubated in 0.18 M $NaClO_4$ with 2 mM 2PGA (——) and the simulated spectrum by a combination of the spectra of 59% dimer and 41% monomer (- - - -). The fourth derivative spectra of 1.5 μM apo-enolase and apo-enolase incubated in 0.50 M $NaClO_4$ are used as the spectra of dimer and monomer, respectively.

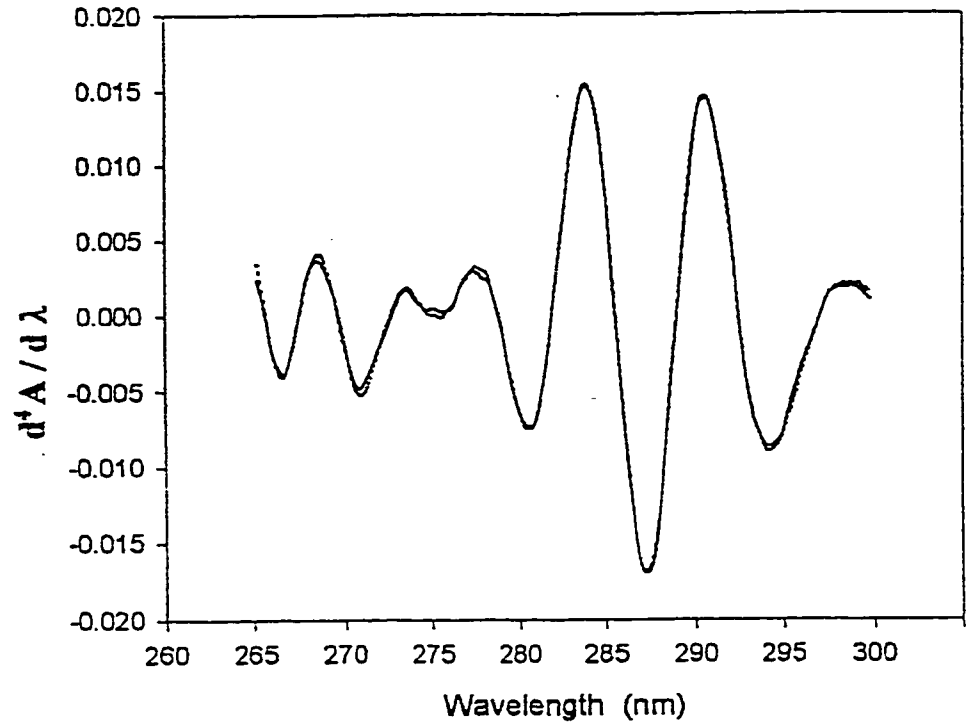
0.020
0.015
0.010
0.005
0.000
-0.005
-0.010
-0.015
-0.020
d¹A / d λ
260
265
270
275
280
285
290
295
300
Wavelength (nm)

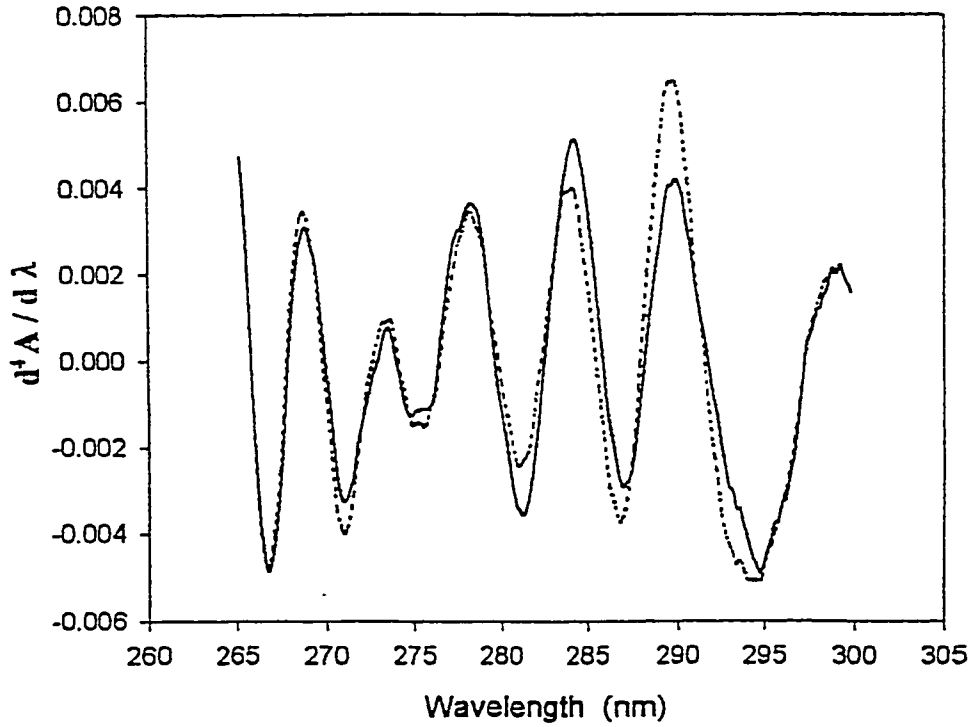
0.008
0.006
0.004
0.002
0.000
-0.002
-0.004
-0.006
d¹A / d λ
260
265
270
275
280
285
290
295
300
305
Wavelength (nm)

Table 3. 5 Comparison of the degrees of inactivation, dissociation and denaturation of apo-enolase incubated in varying concentrations of $NaClO_4$

Samples	Inactivation [a] (%)	Dissociation [b] (% monomer)	Molar Ellipticity (222nm)[c] (Deg.cm^{-2} decimol^{-1}×10^9)
Apo-enolase	0	0	22.8
+0.10 M $NaClO_4$	38.6	39	21.9
+0.15 M $NaClO_4$	73.4	70	21.9
+0.18 M $NaClO_4$	85.7	85	22.1
+0.50 M $NaClO_4$	100	100	21.9
+0.10 M $NaClO_4$ + 2 mM 2PGA	10.5	18	23.3
+0.15 M $NaClO_4$ + 2 mM 2PGA	23.2	33	23.7
+0.18 M $NaClO_4$ + 2 mM 2PGA	37.4	41	23.6

a. The degree of inactivation was measured by activity assay; b. The degree of dissociation was determined by simulation of the fourth derivative spectra; c. Molar ellipticities at 222 nm were obtained by the far-UV CD spectra.

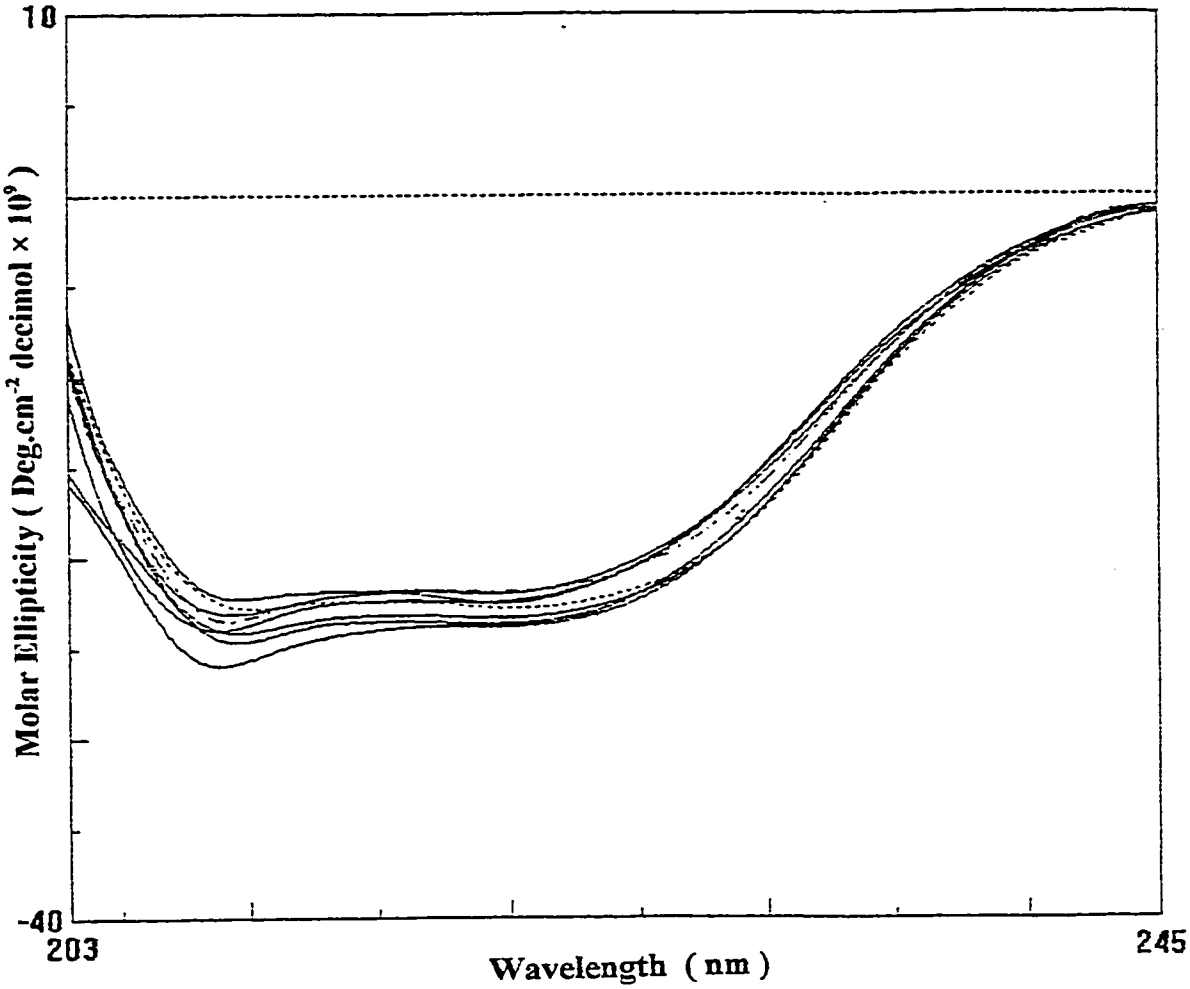

Fig. 3.17 Far-UV CD spectra of apo-enolase incubated in varying concentrations of $NaClO_4$ with or without 2PGA. The spectrum of 1.5 μM apo-enolase alone is shown in a dot line. The spectra of apo-enolase incubated in varying concentrations (0.10 M, 0.15 M, 0.18 M and 0.50 M) of $NaClO_4$ without or with 2 mM 2PGA are located above and below the spectrum of apo-enolase, respectively. The spectra were taken at 25 °C with bandwidth 1.0 nm, scan speed 100 nm/min, response time 0.25 s and step resolution 0.2 nm.

3.7.4 K_d and ΔG_d of the dissociation

Denaturation does not occur during inactivation of apo-enolase by $NaClO_4$. It is assumed that a two-state model exists in the dissociation equilibrium. Since the loss of inactivation parallels to the degree of dissociation (Table 3.5), K_d and ΔG_d of the dissociation can be calculated from the data in Fig.3.4 using the percentage inactivation at varying concentrations of $NaClO_4$ as the degree of the dissociation. Fig.3.18 shows ΔG_d of apo-enolase, apo-enolase with 2PGA and enolase with Mg^{2+} as a function of the concentrations of $NaClO_4$. The dissociation parameters of these enzymes are given in Table 3.6. K_d and ΔG_o of the apo-enolase in the absence of $NaClO_4$ are 23.7 nM and 42 $kJ.mol^{-1}$, respectively. Apo-enolase with 2PGA exhibits a much lower K_d value and a higher ΔG_o value, indicating the stability of the dimer is enhanced by the binding of the substrate. The midpoint of the dissociation for apo-enolase is 0.10 M $NaClO_4$ which is half of that for the apo-enzyme with 2PGA. Holo-enolase is the most stable species among the three; its midpoint of dissociation is 0.26 M $NaClO_4$. The lower values of m for holo-enolase and apo-enolase with 2PGA compared to that of apo-enolase, reflect the smaller solvent-accessible area of these two enzymes in the monomer state (Bianchi, et al., 1994).

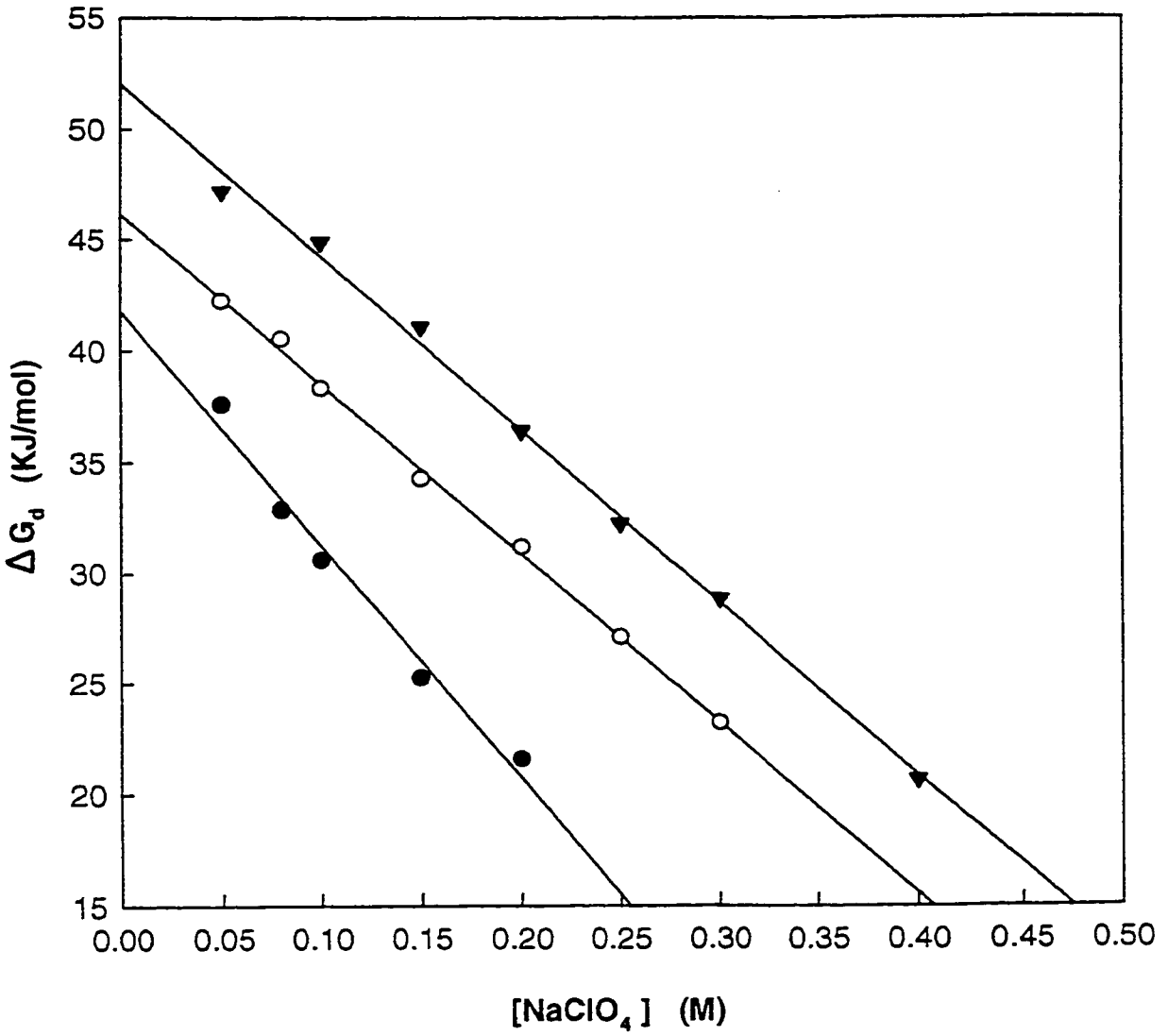

Fig. 3. 18 Effect of [$NaClO_4$] on ΔG_d of dissociation.

1.06 μM enolase was incubated in 0.10 M $NaClO_4$ in the absence of 2PGA (●), in the presence of 1 mM 2PGA (○) and in the presence of 5 mM $Mg(OAc)_2$ (▼).

Table 3. 6 Dissociation parameters of apo-enolase, apo-enolase with 2PGA and enolase with Mg^{2+}

Samples [a]	K_d (nM)	ΔG_o [b] (kJ. mol^{-1})	m [c] (kJ. $mol^{-1}.M^{-1}$)	$[NaClO_4]_{1/2}$ [d] (M)
Apo-enolase	23.7	41.8 ± 1.1	105.0 ± 8.6	0.10
Apo-enolase +1 mM 2PGA	4.45	46.2 ± 0.3	76.4 ± 1.4	0.20
Enolase +1 mM $Mg(OAc)_2$	0.36	52.0 ± 0.5	77.9 ± 2.1	0.26

a. The concentration of apo-enolase was 1.06 μM; b. Values of ΔG_o were extrapolated to 0 M $NaClO_4$; c. Values of m were determined by the slope of the curves (Fig.3.18); d. $[NaClO_4]_{1/2}$ was the concentration of $NaClO_4$ which products 50% dissociated/inactivated.

3.8 Effects of Na^+ on kinetic properties of enolase

Mg^{2+} at a high concentration inhibits the enzymatic activity. When the concentration of 2PGA is held constant at 1 mM with [Mg^{2+}] varying, the kinetic data obtained fit very well to the modified substrate inhibition equation (a Michaelis-Menton equation that includes a term for Mg^{2+} inhibition and a term of the limiting velocity V_{max} approaches) (Fig.3.19). Na^+ also inhibits the rabbit muscle enolase. As Fig.3.19 shown, the presence of 0.02 M NaCl changes the substrate inhibition curves of enolase for Mg^{2+}. Lineweaver-Burke plots (Fig.3.20) indicate that at pH 7.1, the inhibition by Na^+ exhibits a partial competitive character. The effects of Na^+ on the kinetic parameters of rabbit muscle enolase are summarized in Table 3.7. Both K_i and K_m for Mg^{2+} are dramatically increased in the presence of Na^+, while V_{max} is slightly decreased. Na^+ appears to compete with Mg^{2+} for the inhibitory binding site.

Fig. 3.19 Steady-state kinetics of rabbit muscle enolase in the absence and presence of Na^+. Initial velocities were measured at 13.4 nM enolase, 1 mM 2PGA and varying concentrations of $Mg(OAc)_2$ in the absence (▲) and presence (Δ) of 0.02 M NaCl (pH 7.1). Data, determined by triplicate assays, fit to the modified substrate inhibition equation (referred to Methods 2.2.13).

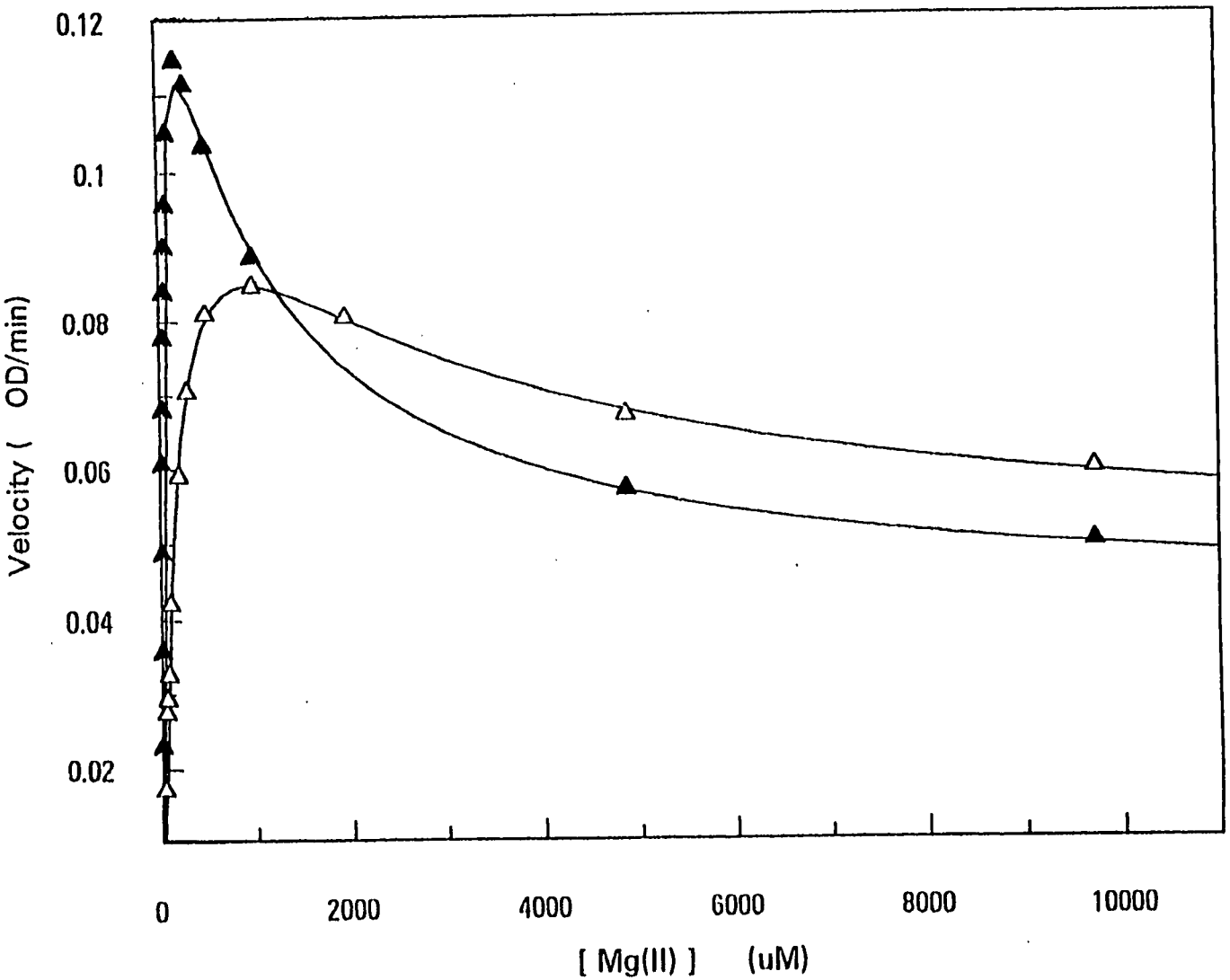
0.12
0.1
0.08
0.06
0.04
0.02
Velocity (OD/min)
0
2000
4000
6000
8000
10000
[Mg(II)] (uM)

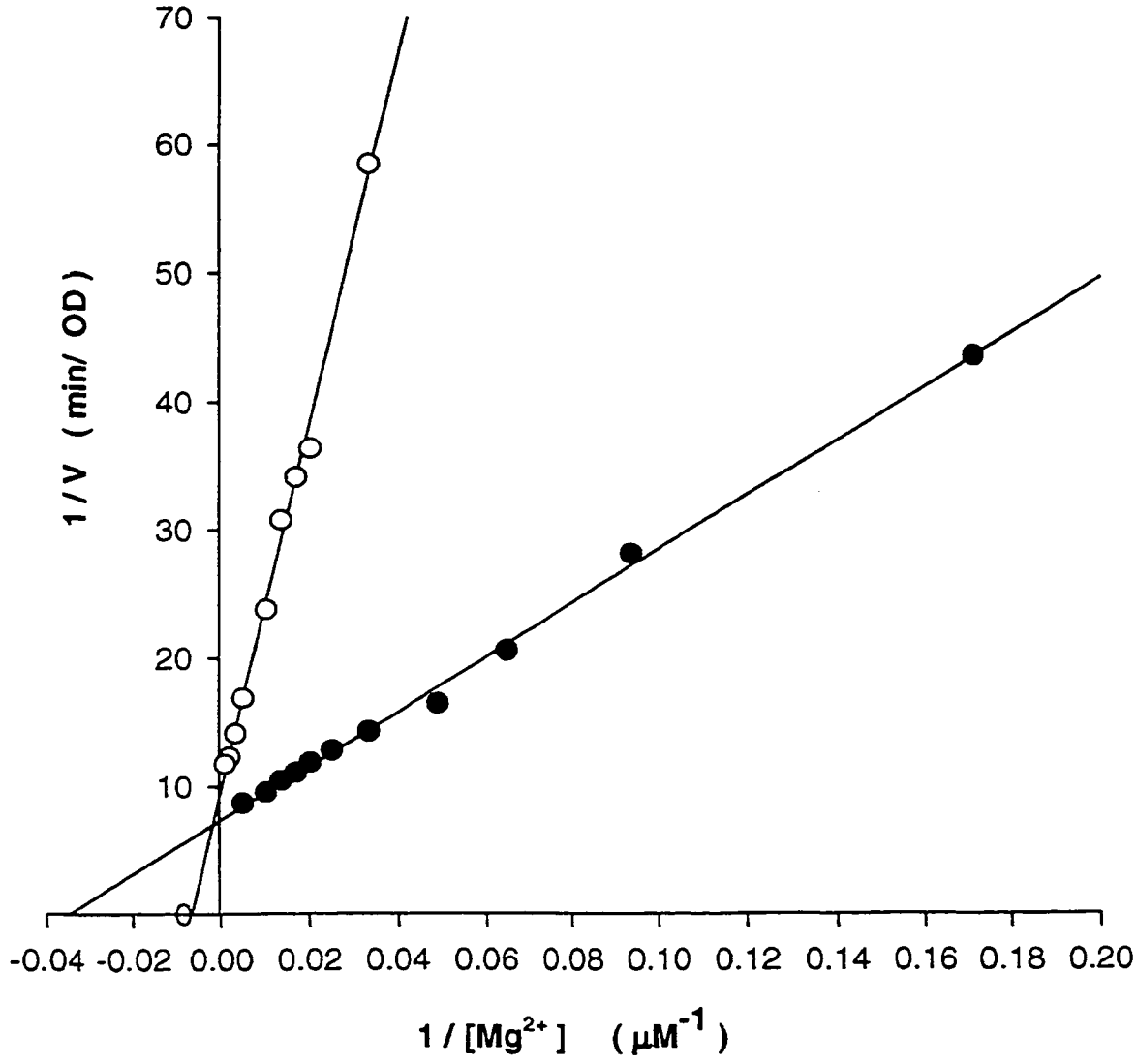

Fig. 3.20 Lineweaver-Burke plots of the inhibition of enolase by Na^+. Data were calculated from Fig. 3.19 in the absence (●) and presence (O) of 0.02 M NaCl.

Table 3. 7 Effects of Na^+ on kinetic properties of rabbit muscle enolase[a]				
Sample	K_m (μM)	K_i (μM)	V_{max} (△OD/min)	V_{final}[b] (△OD/min)
Enolase	32 ± 2	918 ± 141	0.1449 ± 0.004	0.0404 ± 0.003
Enolase + 0.02M NaCl	179 ± 10	2238 ± 459	0.1173 ± 0.003	0.0460 ± 0.003

a. Kinetic parameters of enolase for Mg^{2+} are determined by fitting the data to a modified substrate inhibition equation (referred to Methods 2.2.13); b. V_{final} is the limiting velocity that the enzyme approaches when [Mg^{2+}] is high.

Chapter 4 Relationships Between Increased Trp Fluorescence and Protection of Holo-enolase from Inactivation by $NaClO_4$

Binding of the substrate produces a conformational change in the holo-enolase and protects the enzyme from the inactivation by $NaClO_4$. Various divalent metal ions and inhibitors also can induce different conformational changes in enolase as reflected by the different increase in fluorescence. It is interesting to investigate the relationship between the conformational change and the protection of the enzyme from inactivation by $NaClO_4$.

4.1 Characterizations of the selected inhibitors

Four inhibitors: phosphoglycolate (PG), phosphonoacetic acid, 3PGA and glycerol 2-phosphate were chosen, because their structures are analogous to that of the substrate/product (Fig.4.1). Their kinetic properties were shown in Table 4.1. 3PGA, PG and phosphonoacetic acid are competitive inhibitors of rabbit muscle enolase, while glycerol 2-phosphate exhibits a noncompetitive inhibition. These results support the observation from the recent crystal structures (Larsen, et al., 1996) that the substrate binds to the first metal ion through its carboxylate group, but not through its hydroxyl group as it was thought before. Otherwise, glycerol 2-phosphate would compete with 2PGA , since it imitates the methyl-hydroxyl moiety and the phosphate moiety of the substrate. But this does not occur. The examined competitive inhibitors all contain both the carboxylate and the phosphate moieties. PG and 3PGA show stronger inhibition than 3PGA, which is probably due to the separation of the carboxylate moiety from the phosphate moiety by a C2 in 3PGA.

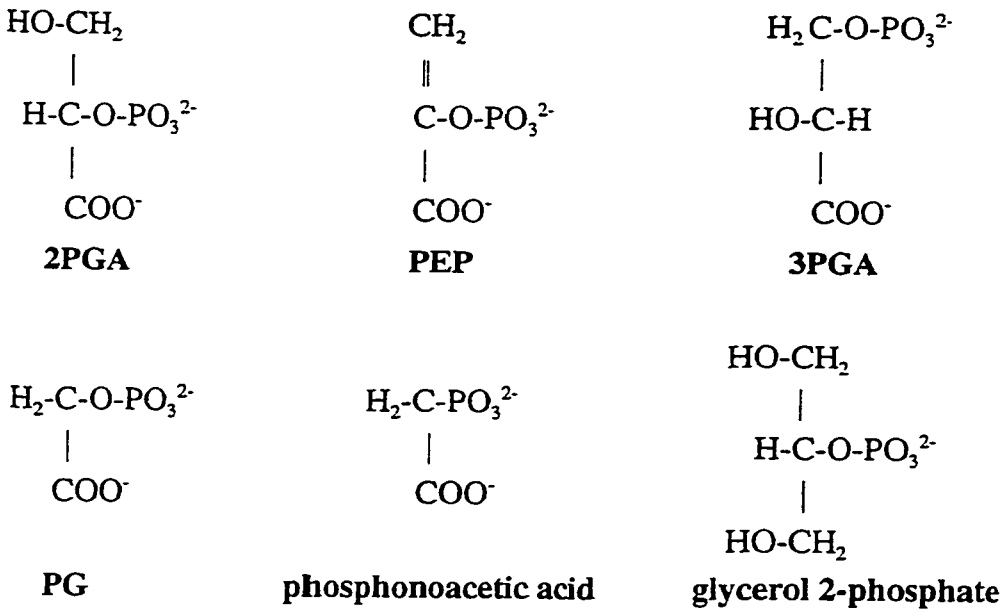

Fig. 4.1 Comparison of the structures of 2PGA, PEP and the selected inhibitors

Table 4. 1 Kinetic properties of the selected inhibitors [a]

Inhibitors	K_i (mM)	$V_{max,\,i}$ / $V_{max,\,2PGA}$	Type of inhibition [b]
phosphoglycolate	0.800 ± 0.065	1.003 ± 0.008	competitive
phosphonoacetic acid	0.822 ± 0.025	0.919 ± 0.014	competitive
3PGA	7.949 ± 0.431	0.903 ± 0.019	competitive
Glycerol 2-phosphate	19.33 ± 1.45	0.833 ± 0.023	noncompetitive

a. Enzyme activity was measured at 10.3 nM enolase, 1 mM $Mg(OAc)_2$ and varying concentrations of 2PGA. NADH, ADP and PK/LDH were used to convert PEP to lactate in the assay (referred to Methods 2.2.1); b. The type of inhibition is also indicated by Lineweaver-Burke plots (not shown) where glycerol 2-phosphate exhibits a curve nearly parallels to that of 2PGA, while the other inhibitors show competitive characteristics.

4.2 Comparison of the increased fluorescence and the protection of enolase upon the binding of 2PGA and the inhibitors

4.2.1 Rabbit muscle enolase

Fig.4.2 shows the increased tryptophan fluorescence upon binding of the substrate and the inhibitors to rabbit muscle enolase. PG and phosphonoacetic acid cause significant increase in fluorescence intensity similar to that observed upon the binding of the substrate, whereas 3PGA and glycerol 2-phosphate induce a very small increase. In Table 4.2, the results from the tryptophan fluorescence are compared to the effects of these inhibitors on the inactivation of rabbit muscle enolase by $NaClO_4$. Phosphonoacetic acid provides protection to enolase comparable to that of the substrate, phosphoglycolate only gives protection when its concentration is high, while 3PGA and glycerol 2-phosphate do not protect the enzyme from inactivation.

4.2.2 Yeast enolase

The effects of the substrate and the inhibitors on tryptophan fluorescence of yeast enolase are shown in Fig.4.3. PG causes a dramatic increase in fluorescence intensity; 2PGA, phosphonoacetic acid and glycerol 2-phosphate also produce significant changes; whereas, 3PGA does not change fluorescence. In the inactivation experiments (Table.4.3), 2PGA and phosphonoacetic acid protect the holo-enolase from inactivation by $NaClO_4$, but PG, 3PGA and glycerol 2-phosphate show little protection.

PG induces a great change in tryptophan fluorescence of both rabbit muscle and yeast enolase, but does not significantly protect the enzymes from the inactivation. Therefore, the

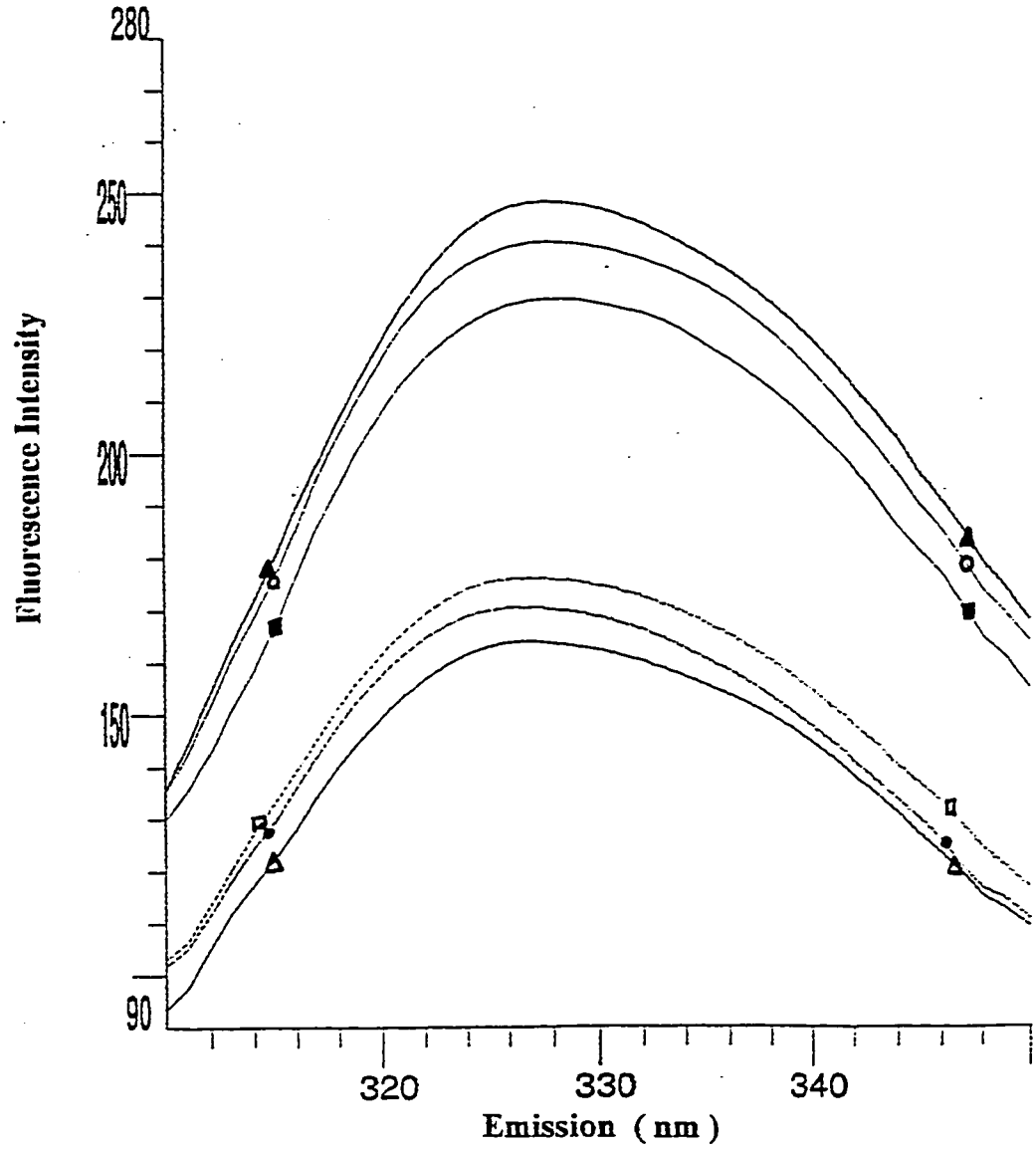

Fig. 4.2 Trp Fluorescence of the binding of 2PGA and the inhibitors to rabbit muscle enolase. The emission spectra of 1.06 μM enolase were taken with excitation 295 nm, bandwidth 2 nm, scan rate 5 nm/sec and voltage 810 v in the addition of 1 mM 2PGA (○), 5 mM PG (▲), 5 mM phosphonoacetic acid (■), 5 mM glycerol 2-phosphate (●) or 10 mM 3PGA (□), respectively. The spectrum of the enzyme with no addition is labeled with (△).

Table 4.2 Effects of 2PGA and the inhibitors on fluorescence and inactivation of rabbit muscle enolase by $NaClO_4$

Substrate or Inhibitors	Concentration (mM)	Inactivation[a] (%)	Protection	(%)Increased Fluorescence[b]
no addition	—	37.7	—	—
2PGA	0.2	14.5	Yes	—[c]
	1.0	9.1	Yes	38.2
	5.0	9.3	Yes	—[c]
Phosphoglycolate (PG)	5.0	33.4	Little	42.8
	10.0	20.0	Yes	—[c]
Phosphonoacetic Acid	1.0	10.0	Yes	—[c]
	5.0	6.6	Yes	33.4
3PGA	5.0	35.3	No	—[c]
	10.0	34.6	No	0.1
Glycerol 2-Phosphate	5.0	41.8	No	3.2
	10.0	40.6	No	—[c]

a. 1.06 μM rabbit muscle nolase was incubated in MTME buffer containing 0.30 M $NaClO_4$ (pH 7.1); b. Trp Fluorescence was excited at 295 nm with bandwidth 2 nm and scan rate 5 nm/sec; c. Data not available.

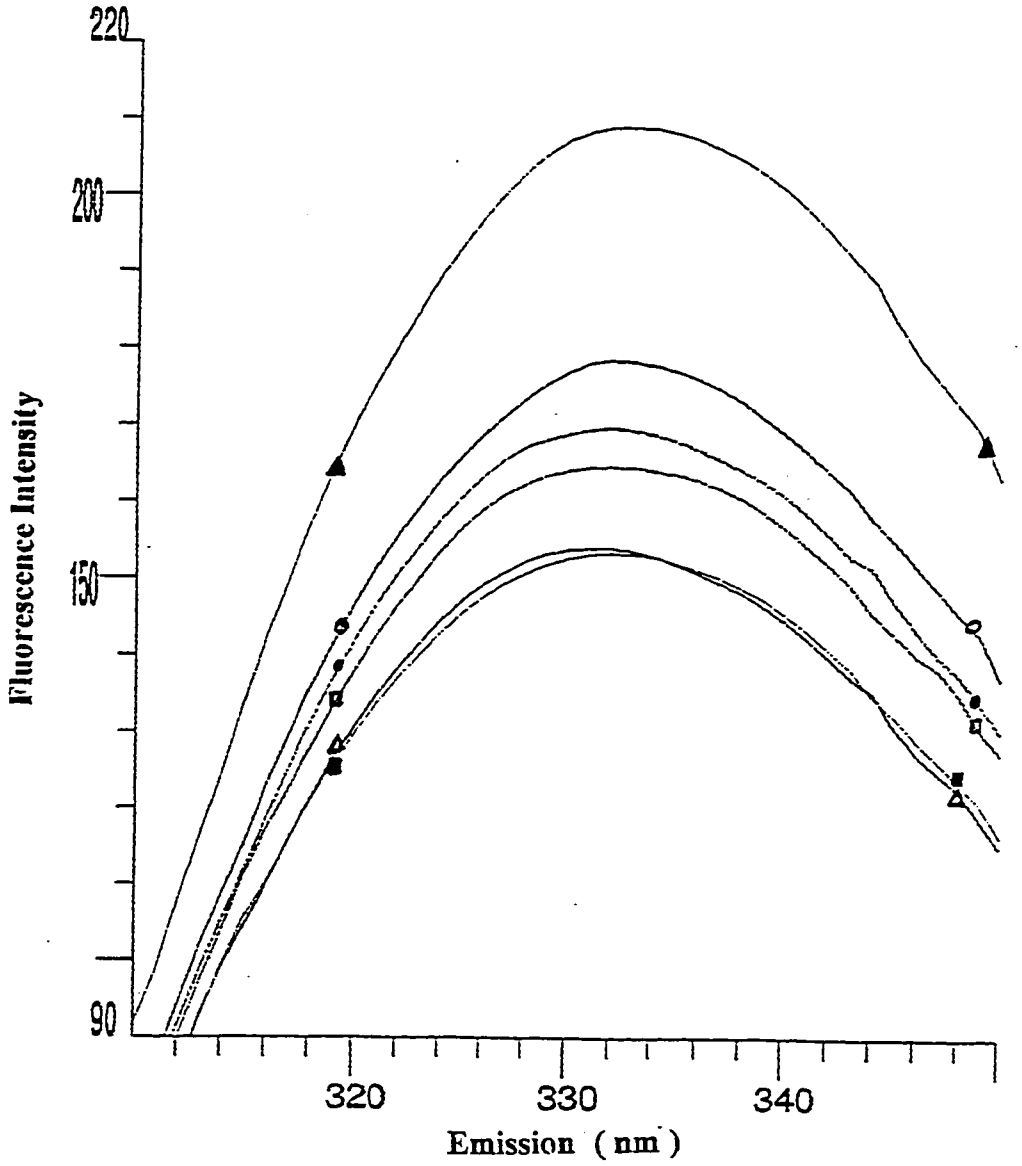

Fig. 4.3 Trp Fluorescence of the binding of 2PGA and the inhibitors to yeast enolase. The emission spectra of 1.06 μM enolase were taken with excitation 295 nm, bandwidth 2 nm, scan rate 5 nm/sec and voltage 730 v in the addition of 1 mM 2PGA (●), 5 mM PG (▲), 5 mM phosphonoacetic acid (○), 5 mM glycerol 2-phosphate (□) or 10 mM 3PGA (■), respectively. The spectrum of the enzyme with no addition is labeled with (△).

Table 4.3 Effects of 2PGA and the inhibitors on fluorescence and inactivation of yeast enolase by $NaClO_4$

Substrate or Inhibitors	Concentration (mM)	Inactivation[a] (%)	Protection	(%)Increased Fluorescence [b]
no addition	—	36.8	—	—
2PGA	0.2	21.6	Yes	—[c]
	1.0	7.0	Yes	9.0
	10.0	6.9	Yes	—[c]
Phosphoglycolate (PG)	1.0	36.7	No	—[c]
	10.0	35.3	No	31.9[d]
Phosphonoacetic Acid	5.0	20.6	Yes	13.8
	10.0	16.2	Yes	—[c]
3PGA	1.0	36.5	No	—[c]
	10.0	27.5	Little	0
Glycerol 2-Phosphate	1.0	31.2	No	—[c]
	10.0	31.5	No	5.2[d]

a. 1.06 μM yease enolase was incubated in MTME buffer containing 0.11 M $NaClO_4$ (pH 7.1); b. Trp Fluorescence was excited at 295 nm with bandwidth 2 nm and scan rate 5 nm/sec; c. Data not available; d. The concentration of the inhibitor added was 5 mM.

increased tryptophan fluorescence is not associated with the protection of holo-enolase from inactivation by $NaClO_4$.

4.3 Comparison of the increased fluorescence and the protection of enolase upon the binding of 2PGA in the presence of varying divalent metal ions

The fluorescence changes upon the binding of 2PGA to rabbit muscle enolase with various divalent metal ions have also been investigated and compared to their effects on the protection of enolase from inactivation (Table.4.4). Mg^{2+}, Mn^{2+} and Co^{2+} produce increased fluorescence upon the substrate binding and protect the enzyme from inactivation. Zn^{2+} also increases fluorescence, but does not protect the enzyme. In contrast, Ca^{2+} does not cause any change in fluorescence, but protects the enzyme.

These results suggest that the increased fluorescence may not provide protection to the enzyme. A change in fluorescence is not necessary for the protection of the holo-enolase Thus, it is confirmed again that the conformational change is not correlated to the protection of the enzyme from inactivation by $NaClO_4$.

Table 4.4 Effects of certain divalent cations on fluorescence and inactivation of rabbit muscle enolase by $NaClO_4$ [a]

Me^{2+}	$[Me^{2+}]$ (mM)	Specific Activity (units/mg)			Protection by 2PGA	Increased Fluorescence [b] (%)
		no $NaClO_4$	+$NaClO_4$	+$NaClO_4$ + 2PGA		
apo-enolase	—	78.6	0	34.3	—	0
$Mg(OAc)_2$	1.0	88.3	10.5	85.4	Yes	32.4
$MnCl_2$	0.5	52.0	13.5	49.4	Yes	25.9
$Zn(OAc)_2$	0.5	20.4	0	0	No	21.3
$Co(OAc)_2$	0.2	43.6	0	43.3	Yes	17.4
$CaCl_2$	0.2	80.5	0	58.5	Yes	0

a. 1.06 μM enolase was incubated in 0.2 M $NaClO_4$ with or without 1 mM 2PGA in the addition of varying metal ions; b. The emission spectra were excited at 295 nm with bandwidth 2 nm, scan rate 5 nm/sec and voltage 840 v.

General Discussion

The reaction enolase catalyzes includes at least the following steps and a series of intermediates exist in the equilibria:

$$E \rightleftharpoons EM \rightleftharpoons EMS \rightleftharpoons EMSM \rightleftharpoons EMPM \rightleftharpoons EMP \rightleftharpoons EM \rightleftharpoons E$$

Where E is enolase, M is Mg^{2+}, EM is the holo-enolase, S is 2PGA and P is PEP. Which species of these intermediates could contribute to the protection of enolase from inactivation by $NaClO_4$?

As Fig. 3.1 and Fig. 3.2 show, the inactivation by $NaClO_4$ is reduced with increasing concentrations of Mg^{2+} and 2PGA. The binding of metal ions and the substrate provides protection of the enzyme from inactivation. It has been observed that a conformational change occurs upon the binding of the first metal ion to the enzyme (Brewer and Weber, 1966). The crystal structure of yeast holo-enolase shows that the metal ion in the conformational binding site I interacts with several active site residues such as Asp246, Glu295, Asp320, Lys396 and water molecules (Wedekind, et al.,1995). The binding of the first metal ion enhances the interactions in the active site and results in a conformational change in the enzyme. These interactions hold the enzyme in a more compact conformation (Brewer and Weber, 1966).

The binding of the conformational metal ion facilitates the substrate binding and allows the second metal ion to bind. Upon the binding of the substrate, three active site loops move and the yeast enolase changes its "open" conformation to a "closed" conformation. The binding of the substrate not only improves the interactions of the residues in the active site, but also produces a series of hydrogen bonds leading to the adjacent subunit. It has been identified that these interactions are responsible for the ordering and stabilization of the conformations of the

subunits (Zhang, et al. 1997). Thus, the enzyme in the presence of the metal ions and the substrate is less accessible to the solvent and more resistant to the inactivation by reagents.

Rabbit muscle enolase has at least 60% sequence identity with yeast enolase, and the charged residues in the active site are highly conserved (Lebioda, et al., 1989). It is assumed that these two enzymes have highly homologous three dimensional structures. The conformational change in rabbit muscle enolase upon binding of the metal ions and the substrate as seen in this study has been observed in yeast enolase (Fig.4.2 and Fig.4.3). The enhanced interactions in the active site and the more compact conformation of the rabbit muscle holo-enolase complex contribute to the protection of the enzyme from inactivation by $NaClO_4$. Therefore, the enzymes bound with the metal ion or with the substrate/product are protected from the inactivation.

However, we found that apo-enolase is protected by the substrate (Fig.3.4). The protection is increased with increasing concentrations of the substrate (Fig.3.5). According to the requisite order of binding of the metal ions and the substrate to the enzyme, 2PGA should not give any protection to the apo-enolase; without the binding of the conformational metal ion in site I, 2PGA cannot bind to the enzyme. Three possibilities might account for the protection as described in the Results 3.2.3. First, it might be due to the contamination of the trace divalent ions in the apo-enzyme sample. Second, the substrate might directly interact with the enzyme in the absence of metal ions. Third, there are metal ions instead of divalent metal ions which can bind to the enzyme and permit the binding of the substrate.

A challenge in this study is to sort out the effects of the trace divalent cations in the apo-enzyme samples. It is very difficult to make the commercial enolase completely free of divalent

metal ions. In order to eliminate the effects of the trace metal ions, three chelating reagents: EDTA, EGTA and o-phenathroline at a concentration of 1 mM which was 500 fold higher than that of the active site, were added to the incubations. As shown in Fig.3.6, substantial protection by 2PGA was still observed in these apo-enzyme samples. To further identify the trace metal ions, ICP MS trace metal analysis was applied to the apo-enolase sample. Results from ICP MS analysis (Table 3.2) reveal that several divalent metal ions such as Zn^{2+}, Cu^{2+}, Ni^{2+}, and possibly Ca^{2+} as well, did remain in the apo-enzyme. The total amount of the trace metal ions was about 30% of the quantity of the active sites. It is a serious concern. The effects of the trace metal ions were estimated by adding these metal ions to the incubations at different concentration levels. The highest concentration (5 μM) applied was equal to 2.5 fold that of the active sites. In the presence of 0.1 mM EDTA, these trace metal ions are in excess, but do not provide significantly higher protection beyond that of apo-enolase with 2PGA alone (Fig. 3.7). It is concluded that the trace metal ions are not responsible for the protection. Therefore, the first possibility is ruled out. The protection of apo-enolase by 2PGA is not attributed to the presence of the trace divalent metal ions.

It is certain that the substrate can interact with the apo-enolase without divalent metal ions. Does the substrate directly bind to the enzyme or through other metal ions rather than the divalent ions? Stec and Lebioda (1990) have reported that a sulfate ion was bound in the active site of yeast apo-enolase. Its position was believed to correspond to the binding site of the phosphate group of the substrate. The sulfate ion coordinates to the side chains of Arg374, Ser375 and Lys345. It has also been shown that nine direct bonds exist between the side chains of the active site residues and the atoms of the substrate in the crystal structure of yeast enolase

(Larsen, et al., 1996). The involved residues include Arg374, Ser375, His159 interacting with the phosphate group of 2PGA (through five bonds), Lys345 coordinating to C2 of 2PGA, Glu211 and His373 interacting with the hydroxyl group of 2PGA, and Lys396 bound to the carboxylate group of 2PGA (Fig.1.3). Hence, the substrate might be able to bind to the active site in the absence of the divalent metal ions.

However, there are metal ions existing in the incubation of the apo-enolase. Because $NaClO_4$ was used to inactivate the enzyme, there are sodium cations present. To examine the second and the third possibilities to account for the protection, TMA-ClO_4 was used to replace $NaClO_4$ in the incubation, since TMA^+ is a much larger cation that would not be expected to bind in the active site. Table 3.3 shows that 2PGA protects the apo-enolase incubated in $NaClO_4$, but does not protect the enzyme incubated in TMA-ClO_4. The data imply that Na^+ is necessary for the binding of 2PGA to the apo-enolase. The protection provided by 2PGA increases with increasing concentrations of Na^+ when the apo-enolase is inactivated by TMA-ClO_4 or Tris-ClO_4 (Fig.3.8 and Fig.3.9).

The binding of the substrate to the apo-enolase in the presence of Na^+ is confirmed by the spectral change in tryptophan fluorescence and near-UV CD (Fig.3.10 and Fig.3.12). The resulting conformational change which is similar to the change observed upon the binding of the substrate to the holo-enolase (Fig.3.11 and Fig.3.13), alters the microenvironments of the tryptophan residues. The increased fluorescence upon binding of the substrate indicates that the average environment of these tryptophan residues becomes less quenching. The symmetry of the average environment of both tryptophan and tyrosine residues is also decreased as implied by the decreased ellipticity in the near-UV CD region. There are three tryptophan residues

(Trp303, Trp306 and Trp367) out of five in yeast enolase which are conserved in rabbit muscle enolase. Although they are located neither in the active site, nor in the subunit interface, the conformational change upon binding of the substrate does affect their microenivronments. The loop movements corresponding to a conformational change from "open" to "closed", occur upon the binding of the substrate as observed in the crystal structures (Wedekind, et al., 1994; Zhang, et al.,1997). A series of new interactions form in the active site and extend to more remote regions throughout the side chains of the secondary elements. The enzyme is in a more compact conformation and less accessible to the solvent. Thus, the apo-enolase with 2PGA is more resistant to the inactivation by $NaClO_4$.

The presence of Na^+ is necessary for the binding of the substrate to the apo-enolase. The effects of Na^+ on the apo-enzyme results from its direct interaction with the protein. Sodium cations are small ions that can penetrate into the inside surface of the protein. They can interact with the residues in the active site and change the equilibrium of the protonization of the charged residues. There are three possible ways in which Na^+ may play a role in the interaction of the substrate with the apo-enzyme. First, sodium ions may not be involved in the direct binding of the substrate, but through their coordination to the active site residues, they may change the microenvironment of the active site or alter the active site conformation which facilitates the binding of the substrate. Second, sodium ions may bind to certain specific site(s) and permit the substrate binding. Third, sodium ions may work in both of the aforementioned ways. We cannot prove which possibility is the most accurate interpretation, but there is evidence which appears to support the second or the third possibility.

It has been shown that Na^+ inhibits the enzymatic activity of both yeast and rabbit

enolases (Kornblatt and Klugerman, 1988). Steady-state kinetic studies on the inhibition of yeast enolase by Na^+ indicate that Na^+ causes a large decrease in K_m for Mg^{2+}, but only a small decrease in K_m for 2PGA (Kornblatt and Musil, 1990). Na^+ mainly affects K_m for Mg^{2+} of yeast enolase. The effects of Na^+ on the kinetic properties of rabbit muscle enolase are shown in Table 3.7. Na^+ significantly increases the K_m and K_i for Mg^{2+}. The change in K_m is difficult to interpret, since K_m encompasses rate constants for many steps in the mechanism. K_i represents the dissociation constant for the binding of the third Mg^{2+} to the enzyme. The large increase in K_i is probably caused by the fact that Na^+ competes with Mg^{2+} for the inhibitory site III. In another experiment, fluorescence titration of rabbit muscle enolase with 2PGA shows that Na^+ only slightly influences the interaction of 2PGA with rabbit muscle enolase (data not shown). It appears that Na^+ binds to a site that significantly affects the binding of Mg^{2+}, but not the binding of 2PGA,

There are three metal binding sites per subunit that have been found in the presence of the substrate/product, the conformational site I, the catalytic site II, and the inhibitory site III. In the absence of the substrate/product, two metal ions per subunit were found for Zn^{2+}, $Co^{2+}$and Cu^{2+} (Elliott and Brewer, 1980; Brewer and Collins, 1980; Rose, et al., 1984; Dickinson, et. al., 1980). It is believed that these two metal ions bind to the conformational site I and the inhibitory site III, respectively. The existence of the catalytic site II depends on the binding of the substrate, while the conformational site I and the inhibitory site III are independent of the substrate binding (Brewer and Ellis, 1983). It appears that the inhibitory site III initially exists in the active site. Since Na^+ competes with Mg^{2+} for the same inhibitory site, Na^+ might bind to this site in the apo-enolase. Is it possible that Na^+ can also bind to the

conformational site I? It seems that even if Na^+ can coordinate to site I, its binding must be very weak compared to that of Mg^{2+}. Because the binding of the first divalent ion in the conformational site I is crucial for the binding of the substrate, the binding of 2PGA would be greatly influenced if Na^+ strongly competes with Mg^{2+} for site I. However, this does not occur to the holo-enolase.

The similarity of the pH effect on the inhibition by Na^+ and on the inhibition by divalent ions provides evidence that Na^+ may bind in the same inhibitory site as divalent ions. Studies on the inhibition of yeast enolase by Na^+ show that the inhibition pattern is changed from the hyperbolic mixed type to the competitive type when the pH is increased from 7.1 to 9.2 (Kornblatt and Musil, 1990). Na^+ appears to be more competitive with respect to Mg^{2+} at a higher pH value. The influence of pH on the Mn^{2+} activation/inhibition of yeast enolase has been extensively studied by Lee and Nowak (1992). The inhibition by Mn^{2+} increases as the pH is increased. The increase in its inhibition parallels the increase in its binding. The binding of Mn^{2+} to the site III becomes very weak at pH values lower 6.6. In contrast with the binding of Mn^{2+} to site III favored by a higher pH, the binding of Mn^{2+} to site I is independent of pH and the binding of Mn^{2+} to site II is only slightly increased over the pH range from 5.2 to 7.5. Since the inhibitory site III appears to has a pK_a about 6.5-7.0, Lee and Nowak proposed that this site may be positioned at the phosphate group of the substrate and may involve histidine(s).

As discussed earlier about the possibility of the direct binding of the substrate to the apo-enolase, the phosphate group of the substrate forms five direct bonds with selected active site residues (Fig.1.3). This region represents the site where the substrate may bind to the apo-enolase. In the latest crystal structure of yeast enolase (Zhang, et al.,1997), it was suggested

that a Li^+ is located in the catalytic site II and coordinates to the phosphate group of the substrate (Fig.1.4). His159 is located close to the Li^+ in this structure. Li^+ has been reported having the same inhibition pattern as that of Na^+ (Kornblatt and Musil, 1990). Studies on the effect of Li^+ on proton abstraction (Kornblatt and Musil, 1990) show that Li^+ does not affect the rate of the C2 hydrogen exchange at a saturating concentration of Mg^{2+}. This might be due to Li^+ (and Na^+) competing with Mg^{2+} for the same site.

This study suggests that the binding of the substrate to the apo-enolase may be through a Na^+ binding in site III. The inhibitory site III may be very close to the catalytic site II. Therefore, the metal ion in site III might shift to the catalytic site II upon the binding of the substrate. At a high concentration of the divalent metal ions, 2PGA-Me^{2+} complex will be formed (Musil, 1992). The metal ion bound to the inhibitory site III might influence the correct coordination of the substrate and the catalytic metal ion to the active site, thus inhibit the enzymatic activity.

The effects of the other monovalent metal ions on the protection of apo-enolase from inactivation are shown in Table 3.4. K^+ and NH_4^+ do not protect the apo-enolase. Li^+ shows protection similar to that of Na^+ in the presence of 2PGA, but Li^+ alone show higher protection of apo-enolase in the absence of 2PGA. Both Na^+ and Li^+ are inhibitors of yeast and rabbit muscle enolase, while NH_4^+ and K^+ are activators to rabbit muscle enolase, but are inhibitors of yeast enolase (Kornblatt and Klugerman, 1988). Li^+ and Na^+ exhibit the same inhibition pattern (Kornblatt and Musil, 1990). Both of them appear to be competitive with Mg^{2+} for the inhibitory site III. They might bind to the apo-enzyme in similar site(s) in the presence of the substrate and provide protection of the apo-enzyme from inactivation. But Li^+ shows higher

inhibition than Na^+. Li^+ may have more complex interactions with the enzyme. It may bind to the charged residues in the active site or in the subunit contact and change the conformation of the enzyme. This conformation may be altered upon binding of 2PGA and become more sensitive to TMA-ClO_4. This may account for that Li^+ alone shows higher protection of apo-enolase in the absence of 2PGA.

K^+ and NH_4^+ appear to interact with the rabbit muscle enolase in a way different from that of Na^+ and Li^+ and do not show protection of the apo-enolase with 2PGA. There are many charged residues in the active site of enolase. Monovalent ions can interact with these charged residues and consequently, modify the environment of the active site. The changes in the microenvironment of the active site may facilitate or may slow down the catalysis. This may explain the fact that K^+ and NH_4^+ activate the rabbit muscle enolases, but inhibit the yeast enolase. The different effects of these monovalent ions on the enzyme are attributed to the difference in their sizes and electronic distributions.

$NaClO_4$, as a chaotropic salt, can inactivate the enzymes by altering their conformations through both direct and indirect interactions with the enzymes. In fact, the major inactivating agent is ClO_4^-. Studies on inactivation/dissociation of two isozymes of rabbit enolase ($\beta\beta$ enolase and $\gamma\gamma$enolase) show that NaCl, contrary to $NaClO_4$, does not cause inactivation/dissociation (Al-Ghanim, 1994; Trepanier, et al., 1990). It is believed that chaotropic reagents such as NaSCN, NaI or NaBr, can disrupt the water structure and promote the hydration of buried surfaces of the proteins (Collins and Washabaugh, 1985). In addition, they may bind to the proteins and therefore select the form of the proteins with larger surface area (Arakawa and Timasheff, 1982). They decrease the structural stability of the proteins and

inactivate the native enzymes.

Inactivation of oligomeric proteins is usually accompanied by dissociation (Jaenicke and Rudolph, 1986). Kornblatt et al. (1996) have proven that the dissociation of rabbit muscle enolase by $NaClO_4$ is a two-state equilibrium of monomers and dimers using HPLC. A spectral simulation method has been applied to determine the degree of dissociation in their studies. In this study, results from the crosslinking and SDS-PAGE experiment show that the amount of the crosslinked enzyme in the apo-enolase sample incubated in 0.15 M $NaClO_4$ is apparently decreased (Fig.3.14), indicating the occurrence of the dissociation. The degree of dissociation is determined by the simulation of the fourth derivative spectra as described by Kornblatt et al.(1998). The fourth derivative spectra is a useful tool to monitor the change in the environment of the aromatic residues during inactivation/dissociation. The small difference in the original spectra can be magnified through the fourth derivatives. As shown in Fig.3.15, the changes in the positions of peaks and troughs in the fourth derivative spectra imply that the exposure of the tyrosine and tryptophan residues increases with increasing concentrations of $NaClO_4$. The average environment of the tyrosine and tryptophan residues are more polar in the monomer than that in the dimer. The degree of dissociation is parallel to the degree of inactivation of the apo-enolase (Table 3.5). This is also true for the holo-enolase as reported by Kornblatt, et al.(1996). $NaClO_4$ dissociates the active dimer into two inactive monomers.

The effect of $NaClO_4$ on the secondary structure of apo-enolase is investigated by the far-UV CD spectra. Little change in the ellipticity at 222 nm was observed. It can be concluded that the inactivation is not due to the loss of the secondary structure. $NaClO_4$ at the concentration used (0 M-0.5 M) only changes the tertiary structure of the apo-enolase, but does

not affect its secondary structure. This result agrees with the finding of Kornblatt, et al.(1996) in the studies of the inactivation/dissociation of rabbit muscle holo-enolase by $NaClO_4$. It has been suggested that the major structural effect of $NaClO_4$ is on the movement of the certain loops which are important to the catalytic activity.

2PGA protects the apo-enolase against dissociation as well as inactivation. The apo-enolase with 2PGA is more resistant to the $NaClO_4$-induced inactivation as indicated in Fig. 3.4. It is also confirmed by both crosslinking and SDS-PAGE and the fourth derivative spectra that the presence of 2PGA shifts the equilibrium toward association. The protection provided by 2PGA is attributed to its binding to the apo-enzyme in the presence of Na^+. The conformational change produced by this binding is similar to which has been observed upon binding of 2PGA to the holo-enolase. The binding of 2PGA to the apo-enzyme promotes the subunit association and generate a more compact conformation in the apo-enzyme as found in the holo-enzyme. The higher value of ΔG_o and lower value of K_d of dissociation for the apo-enolase with 2PGA indicate the higher stability of this complex with respect to the apo-enolase (Table 3.6). The interactions between the substrate and the apo-enzyme stabilize the enzyme, thus protect it from inactivation/dissociation. But the binding of 2PGA to the apo-enolase is probably much weaker than that to the holo-enolase, since even the binding of the first Mg^{2+} to the enzyme provides higher protection (Fig.3.4).

The binding of 2PGA to either apo-enolase or holo-enolase produces a conformational change in the enzyme and protects the enzyme from inactivation/dissociation. The relationship between the conformational change and the protection was investigated using several inhibitors and various divalent metal ions. These ligands cause different conformational changes in the

enzyme. Their effects on the inactivation are shown in Tables 4.2, 4.3 and 4.4. The conformational change characterized by the binding of various metal ions or inhibitors is found not to be correlated to the protection of the enzyme from inactivation. The conformational change in the enzyme may not result in protection, for example, PG and Zn^{2+} which produce a significant change in Trp fluorescence, but do not protect the enzyme from inactivation. In the case of Ca^{2+}, the enzyme is protected though no conformational change is observed upon the addition of the substrate. Hence, it is not necessary for the enzyme to change its conformation in order to obtain the protection.

The lack of correlation between the conformational change and protection of the enzyme from inactivation could be attributed to a series of complex factors. Tryptophan fluorescence reflects the average environment of all the tryptophan residues in the protein. The same increased fluorescence upon binding of different inhibitors or metal ions does not mean that the same conformational change occurs. Effects of these ligands on the tertiary structure of the enzyme vary with their identity. For example, PG and phosphonoacetic acid exhibit similar competitive inhibition constants (K_i) for rabbit muscle enolase and both induce increased fluorescence, but they have different effects on inactivation due to the difference in their structures. The interactions between the active site residues and the ligand depend on the identity of the ligand and cause differing accessibility of the enzyme to the salts. Zn^{2+} produces a large increase in fluorescence similar to that of Mg^{2+}, but it does not protect the enzyme. On the contrary, Ca^{2+} does not change fluorescence, but protects the enzyme. In the crystal structure of yeast enolase-Ca^{2+}-2PGA complex, it was found that the substrate binds in an orthonormal conformation and the Ca^{2+} site (site I) is outward about 0.3Å from the Zn^{2+} site

(Lebioda, et al., 1991). Though this binding does not change fluorescence, it protects the enzyme from inactivation by perchlorate anions. In addition, the distribution of the tryptophan residues is not in the active site, nor in the active site mobile loops. The change in fluorescence may not exactly correspond to the change in the active site. It has been found that the conformational change caused by various divalent ions is not related to the degree of enzymatic activity produced (Brewer, et al., 1985). The conformational change differs by the identity of the metal ions. The differences in size, strength of charge and magmatic field result in the variation of their interactions with the active site residues, and thus cause different movement of the tertiary structure.

Conclusions

1. The binding of Mg^{2+} and 2PGA protects the rabbit muscle enolase from inactivation by $NaClO_4$. The protection increases with increasing concentrations of Mg^{2+} and 2PGA. The protection provided by Mg^{2+} and 2PGA is attributed to the more compact conformation of the enzyme complex with metal ions and the substrate.

2. The apo-enolase inactivated by $NaClO_4$ is protected by 2PGA. The presence of Na^+ is necessary for the protection of apo-enolase by 2PGA. The protection increases with increasing concentrations of Na^+ and 2PGA. The addition of the substrate to the apo-enolase in the presence of Na^+ causes a small increase in tryptophan fluorescence and a decrease in ellipticity in the near-UV CD region. These changes are similar to those observed in the holo-enolase upon binding of the substrate. It is concluded that Na^+ permits the binding of the substrate to the apo-enolase. This binding improves the ability of the apo-enzyme to resist the inactivation by $NaClO_4$.

3. Steady-state studies show that at pH 7.1, Na^+ significantly increases K_m and K_i for Mg^{2+} and slightly decreases V_{max} . It is implied that Na^+ competes with Mg^{2+} for the inhibitory site III.

4. The other monovalent cations, K^+ and NH_4^+ do not protect the apo-enolase from inactivation by TMA-ClO_4, while Li^+ provides protection similar to that of Na^+ in the presence of 2PGA, but Li^+ alone also shows protection in the absence of the substrate.

5. Dissociation occurs during the inactivation of apo-enolase by $NaClO_4$ as indicated by cross-linking using glutaraldehyde plus SDS-PAGE. The degree of dissociation determined by the simulation of the fourth derivative UV spectra is highly correlated to the degree of inactivation, suggesting that the inactivation is associated with the dissociation. $NaClO_4$ dissociates the active dimer into two inactive monomers. The presence of 2PGA shifts the equilibrium toward the association and protects the enzyme from dissociation/inactivation.

6. Results from far-UV CD spectra show that $NaClO_4$ at the applied concentration (0M-0.5M) has little effect on the secondary structure of the apo-enolase. It can be concluded that the structural effect of $NaClO_4$ is on the tertiary and quandary structure of the enzyme as indicated in the fourth derivative UV spectra.

7. For apo-enolase, apo-enolase with 2PGA and holo-enolase, the K_d values of dissociation are 23.7 nM, 4.45 nM and 0.36 nM, and the values of ΔG_o of dissociation in the absence of $NaClO_4$ are 41.8 kJ/mol, 46.2 kJ/mol and 52.0 kJ/mol, respectively. The binding of ligand enhances the subunit interaction and stabilizes the dimeric enzyme.

8. Studies on steady-state kinetics show that phosphoglycolate, phosphonoacetic acid and 3PGA are competitive inhibitors and glycerol 2-phosphate is a noncompetitive inhibitor. 2PGA, phosphoglycolate and phosphonoacetic acid induce increased tryptophan fluorescence of both rabbit muscle and yeast enolases, while 3PGA and glycerol 2-phosphate do not change fluorescence. 2PGA and phosphonoacetic acid protect both the rabbit muscle and yeast enolases

from inactivation by $NaClO_4$, 3PGA and glycerol 2-phosphate do not protect the enolases, while phosphoglycolate does not protect yeast enolase, but protects rabbit muscle enolase only at a high concentration. Therefore, the conformational change upon binding of the substrate or inhibitors is not correlated to the protection of enolase from inactivation.

9. Upon binding of the substrate to rabbit muscle enolase, Mn^{2+} and Zn^{2+} cause a large increase in tryptophan fluorescence similar to that of Mg^{2+}, Co^{2+} induces a small increase, whereas Ca^{2+} does not increase fluorescence. When enolase is inactivated by $NaClO_4$, Mn^{2+}, Co^{2+} and Ca^{2+} protect the enzyme from inactivation, but Zn^{2+} does not. It is confirmed that the conformational change observed by tryptophan fluorescence does not correspond to the protection of enolase from inactivation.

Suggestions for future work

The substrate can bind to the rabbit muscle apo-enolase ($\beta\beta$) in the presence of the sodium ion and protect the enzyme from inactivation by $NaClO_4$. It would be interesting to investigate whether this phenomenon occur to the other apo-enolases, such as yeast enolase, the $\alpha\alpha$ isozyme or $\gamma\gamma$ isozyme of rabbit enolases. Further experiments on yeast apo-enolase would be recommended to explore the binding site(s) of the monovalent ion, since yeast enolase has been extensively studied.

The sodium ion competes with Mg^{2+} for the same site(s). To examine whether Na^+ can bind to the conformational site I, the effect of Na^+ on the exchange rate of the C2 proton under varying concentrations of Mg^{2+} would be probed. Since the divalent metal ion in site I facilitates the binding and orientating the substrate to the precatalytic position and stabilizes the enolate intermediate (Zheng, et al.,1997), the abstraction of the C2 proton would be affected if Na^+ competes for site I when the concentration of Mg^{2+} is low.

It would be interesting to prove that the sodium ion binds to the inhibitory site III. It has been reported that the binding constant of the inhibitory divalent ion is pH dependent (Lee and Nowak, 1992). Studies on the pH influence on the protection of apo-enolase by 2PGA when apo-enolase achieves the same extent of inactivation by $NaClO_4$ at different pH (6.0-9.0), would be performed and compared with the pH effect on the inhibition by divalent ions.

In addition, various competitive inhibitors such as PhAH, phosphonoacetic acid, PG and 3PGA, can be used to examine whether they also provide protection of the apo-enolase. This may provide more information on the relationship between the structures of the substrate/inhibitors and the binding of 2PGA to the apo-enzyme.

Site-directed mutagenesis is a useful tool for the studies on the catalytic mechanism. In the recent X-ray crystal structure (Zhang, et al.,1997), His159 on the active site loop Val153-Phe169 is positioned close to the suggested Li^+. We propose that the inhibitory site III might be close to the catalytic site II. His159 might be involved in the inhibitory function. Mutation of His159 would be helpful to understand the inhibitory mechanisms.

Investigation of the inactivation/dissociation of apo-enolase by $NaClO_4$ through activity assay, fluorescence, crosslinking and SDS-PAGE, would provide information on the way by which the enzyme undergoes the inactivation/dissociation process. Al-Ghanim (1994) has shown that the rabbit muscle holo-enolase is first inactivated by $NaClO_4$, then dissociated into two inactive monomer. It would be of interest to compare the inactivation/dissociation process of the holo-enolase and apo-enolase.

References

Al-Ghanim, A. A. (1994) *Sodium perchlorate-induced inactivation of rabbit muscle enolase: partial inactivation of dimeric enzyme and dissociation into inactive monomers.* (M.Sc. thesis). Concordia University.

Anderson, S. R, Anderson, V. E. and Knowles, J. R. (1994) *Biochemistry 33*, 10545-10555.

Arakawa, T. and Timasheff, S. N. (1982) *Biochemistry 21*, 6545-6552.

Bell, C. F., (1977) *Principles and applications of metal chelation* (Holliday, A. K., Atkins, P. W. and Holker, J. S. E., ed.), pp 75-85, Clarendon Press, Oxford.

Bianchi, E., Venturini, S., Pessi, A., Tramontano, A. and Sollazzo, M. (1994) *J. Mol. Biol. 236*, 649-659.

Braford, M. (1976) *Anal. Biochem. 72*, 248-254.

Brewer, J. M. and Weber, G. (1966) *J. Biol. Chem. , 241*, 2550-2557.

Brewer, J. M. and Weber, G. (1968) *Proc. Natl. Acad. Sci. U.S.A. 59*, 216-223.

Brewer, J. M. (1969) *Arch. Biochem. Biophys. 134*, 59-66.

Brewer, J. M. (1971) *Biochim. Biophys. Acta, 250*, 251-257.

Brewer, J. M., Faini, G. J., Wu, C. A., Goss, L. P. , Carreira, L. A. and Wojclk, R. (1978) in *Physical aspects of protein interactions* (Catsimpoolas, N., ed.), pp 57-78, Elsevier/North-Holland, Amsterdam.

Brewer, J. M. and Collins, K. M. (1980) *J. Inorg. Biochem. 13*, 151-164.

Brewer, J. M. (1981) *Crit. Rev. Biochem. 11*, 209-254.

Brewer, J. M. and Ellis, P. D. (1983) *J. Inorg. Biochem. 18*, 71-82.

Brewer, J. M. (1985) *FEBS Lett. 182*, 8-14.

Brewer, J. M., Bastiaens, P. and Lee, J. (1987) *Biochem. Biophys. Res. Comm. 147(1)*, 329-334.

Brewer, J. M., Glover, C. V. C., Holland, M. J. and Lebioda, L. (1997) *Biochim. Biophys. Acta. 1340*, 88-96.

Burns, D. L., and Schachman, H. K. (1982) *J. Biol. Chem. 257*, 8638-8647.

Chin, C. C. Q., Brewer, J. M. and Wold, F. (1981) *J. Biol. Chem. 236*, 1377-1384.

Chen, R. F. (1990) in *Practical fluorescence. 2nd ed.*, (Guilbeault, G. G., ed.), pp 575-682, Marcel Dekker, Inc., New York.

Collins, K. D. and Washabaugh, M. W. (1985) *Q. Rev. Biophys. 18*, 323-422.

Collins, K. M. and Brewer, J. M. (1982) *J. Inorg. Biochem. 17*, 15-28.

Dickinson, L. C., Rose, S. L. and Westhead, E. W. (1980) *J. Inorg. Biochem. 13*, 353-366.

Dinovo, E. C. and Boyer, P. D. (1971) *J. Biol. Chem. 246*, 4586-4593.

Duquerroy, S., Camus, C. and Janin, J. (1995) *Biochemistry 34*, 12513-12523.

Elliott, J. I. and Brewer, J. M. (1980) *J. Inorg. Biochem. 12*, 323-334.

Faller, L. D., Baroudy, B. M., Johnson, A. M. and Ewall, R. X. (1977) *Biochemistry 16*, 3863-3869.

Gawronski, T. H. and Westhead, E. W. (1969) *Biochemistry 8*, 4261-4270.

Gerlt, J. A. and Gassman, P. G. (1992) *J. Am. Chem. Soc. 114*, 5928-5934.

Hanlon, D. and Westhead, E. W. (1969) *Biochemistry 11*, 4247-4255.

Holleman, W.H. (1973) *Biochim. Biophys. Acta. 327*, 176-185.

Keresztes-Nagy, S. and Orman, R. (1971) *Biochemistry 10*, 2506-2508.

Kornblatt, J. A. , Kornblatt, M. J. and Hui Bon Hoa, G. (1995) *Biochemistry 34*, 1218-1223.

Kornblatt, M. J., Kornblatt, J. A. and Hui Bon Hoa, G. (1982) *Eur. J. Biochem. 128*, 577-581.

Kornblatt, M. J. and Hui Bon Hoa, G. (1987) *Arch. Biochem. Biophys. 252*, 277-283.

Kornblatt, M. J. and Klugerman, A. (1988) *Biochem. Cell Biol. 67*, 103-107.

Kornblatt, M. J. and Musil, R. (1990) *Arch. Biochem. Biophys. 277*, 301-305.

Kornblatt, M. J. (1996) *Arch. Biochem. Biophys. 330*, 12-18.

Kornblatt, M. J., Al-Ghanim, A. and Kornblatt, J. A. (1996) *Eur. J. Biochem. 236*, 78-84.

Kornblatt, M. J., Lange, R. and Balny, C. (1998) *Eur. J. Biochem. 251*, 775-780.

Jaenicke, R. and Rudolph, R. (1986) *Methods in enzymology. 131*, (Hirs, C. H. W. and Timasheff, S. N., ed.), pp 218-249. Academic Press, New York.

Lange, R., Frank, J., Saldana, J. L. and Balny, C. (1996) *Eur. Biophys. J. 24*, 277-283.

Larsen, T. M., Wedekind, J. E., Rayment, I. and Reed, G. H. (1996) *Biochemistry 35*, 4349-4358.

Lebioda, L., Stec, B. and Brewer, J. M., (1989) *J. Biol. Chem. 264*, 3685-3693.

Lebioda, L. and Stec, B. (1991) *Biochemistry 30*, 2817-2822.

Lee, B. H. and Nowak, T. (1992) *Biochemistry 31*, 2165-2171.

Martell, A. E. and Calvin, M. (1955) *Chemistry of the metal chelate compounds* (Latimer, W. M., ed.), pp2-450, Prentice-Hall, Inc., New York.

Musil, R. (1992) *The effects of monovalent cations on yeast enolase.* (M.Sc. thesis). Concordia University.

Paladini, A. A. and Weber, G. (1981) *Biochemistry, 20*, 2587-2593.

Poyner, R. R., Laughlin, L.T., Sowa, G. A. and Reed, G. H. (1996) *Biochemistry, 35*, 1692-

1699.

Reed, G.H., Poyner, R.R., Larsen, T.M., Wededind, J.E. and Rayment, I. (1996) *Current Opinion in Structural Biology 6*, 736-743.

Robinson, J. W. (1996) *Atomic spectroscopy. 2nd ed.*, pp 277-329, Marcel Dekker, Inc., New York.

Rose, S.L., Dickinson, L.C. and Westhead, E.W. (1984) *J. Biol. Chem. 259*, 4405-4413.

Sangadala, V.S., Glover, C.V.C., Robson, R.L., Holland, M.J., Lebioda, L. and Brewer, J. M. (1995) *Biochim. Biophys. Acta. 1251*, 23-31.

Sievers, G. (1978) *Biochem. Biophys. Acta. 536*, 212-220.

Smith, R.M. and Martell, A. (1989) in *Critical stability constants. Vol.6*, pp 96-120, Plenum Press, New York.

Stec, B. and Lebioda, L. (1990) *J. Mol. Biol. 211*, 235-248.

Trepanier, D., Wong, C. and Kornblatt, M. J. (1990) *Arch. Biochem. Biophys. 283*, 271-277.

Venyaminov, S. Y. and Yang, J. T. (1996) in *Circular dichroism and the conformational analysis of biomolecules.* (Fasman, G.D., ed.), pp 69-108, Plenum Press, New York.

Wray, W., Boulikas, T., Wray, V.P., and Hancock, R. (1981) *Anal. Biochem. 118*, 197-203.

Wedekind, J.E., Poyner, R.R., Reed, G. H. and Lebioda, L. (1994) *Biochemistry 33*, 9333-9342.

Wedekind, J.E., Reed, G.H. and Rayment, I. (1995) *Biochemistry 34*, 4325-4330.

Wold, F.(1970) in *The enzymes. 3rd ed., Vol. 5* (Boyer, P.D., ed.), pp 499-538, Academic Press, New York.

Woody, R. W. and Dunker, A. K. (1996) in *Circular dichroism and the conformational*

analysis of biomolecules. (Fasman, G.D., ed.), pp 109-158, Plenum Press, New York.

Zhang, E., Hatada, M., Brewer, J. M. and Lebioda, L. (1994) *Biochemistry 33*, 6295-6300.

Zhang, E., Brewer, J. M., Minor, W., Carreira, L.A. and Lebioda, L. (1997) *Biochemistry 36*, 12526-12534.